EVALUATION OF VISCOUS DRAG REDUCTION
SCHEMES FOR SUBSONIC TRANSPORTS

By

A. Marino, C. Economos
and F. G. Howard

ADVANCED TECHNOLOGY LABORATORIES, INC.

Prepared for

NATIONAL AERONAUTICS AND SPACE ADMINISTRATION

NOV 1975
RECEIVED
NASA STI FACILITY
INPUT BRANCH

NOVEMBER 1975

TABLE OF CONTENTS

LIST OF FIGURES

Page

Page

LIST OF FIGURES (Continued)

Page

APPENDIX A

SUMMARY

This report describes the results of a theoretical study of viscous drag reduction schemes for potential application to the fuselage of a long-haul subsonic transport aircraft. The schemes which were examined included tangential slot injection on the fuselage and various synergetic combinations of tangential slot injection and distributed suction applied to wing and fuselage surfaces. Both passive and mechanical (i.e., utilizing turbo-machinery) systems were examined.

Overall performance of the selected systems was determined at a fixed subsonic cruise condition corresponding to a flight Mach number of $M_\infty = 0.8$ and an altitude of 11,000 m. The nominal aircraft to which most of the performance data was referenced was a wide-body transport of the Boeing 747 category. Some of the performance results obtained with wing suction are referenced to a Lockheed C-141 Star Lifter wing section.

The results of this study show that very substantial reductions in fuselage viscous drag are achievable with tangential slot injection. However, the drag penalties attributable to the components of the baseline design, viz., the turbomachinery and ducts, largely offset the reduction in fuselage viscous drag. In some cases, a net increase in drag accrues to the system. The drag penalties are incurred in the process of reducing the momentum of the captured air used for injection and in pumping this air through the ducts. Perturbations in the baseline design, which involved use of ten (10) slots distributed at equally spaced intervals over the length of the fuselage, did not indicate that any significant improvement in the performance of the baseline design was possible through minor parametric variations. However, it is clear that if alternate designs which avoid the system penalties associated with capturing and pumping high weight flow rates of air can be devised, slot injection, per se, can produce significant viscous drag reductions (i.e., as large as 50%) with minimal complexity and impact on the basic fuselage configuration.

Alternate designs investigated in the present study involved combinations of boundary layer suction on the wing surfaces and injection on the fuselage, and suction and injection combinations applied to the fuselage only.

Overall system performance for these designs is found to be superior to the baseline injection scheme, due primarily to reduction of the requisite flow rates. The latter are based on theoretical estimates of the suction required to maintain a laminar condition in two-dimensional incompressible boundary layer flow. Whether these theoretical estimates will prove valid under actual flight conditions is not known. Nevertheless, with this caveat in mind, it is shown that the considered alternate designs offer significant improvements in fuel consumption and/or range characteristics. Fuel load decreases of the order of 5 to 17% and range increases of 8 to 32% are obtained.

I. INTRODUCTION

The objective of the present study was to evaluate quantitatively a fuselage viscous drag reduction system for a representative subsonic aircraft. At its inception, this study was structured around a baseline scheme which involved tangential slot injection through ten (10) slots at equally spaced intervals along the fuselage. The study was to include theoretical calculations for all system components, including rotating machinery performance and efficiency and duct losses.

In the course of this investigation it was found that the baseline scheme was incapable of providing the anticipated overall system drag reduction and, in some cases, resulted in increased overall system drag. Accordingly, with the agreement of NASA, alternate schemes were examined. These involved the use of boundary layer suction on both fuselage and wing surfaces in various combinations with slot injection. These schemes have been found to provide significant improvement in overall performance.

The efficacy of boundary layer suction in reducing viscous drag resides in the generally recognized principle that suction can stabilize a laminar boundary layer. As a result, the skin friction on a surface through which suction is applied can be reduced to a small fraction of its value for the naturally turbulent boundary layer on the same surface.

Experimental evidence exists demonstrating the ability of suction to maintaining a laminar flow for the conditions of interest in the present investigation under ideal conditions. For the subsonic case the results of References (1) and (2) may be cited. The results of Pfenninger (Reference 3) indicate that similar results can be achieved for supersonic flow for a length Reynolds number up to 5×10^7. The feasibility of suppressing separation and maintaining laminar flow in and downstream of interactions with weak incident shock waves has been demonstrated by the experiments of Groth et al (Reference 4). On the other hand, experience shows that there are formidable problems associated with utilizing laminar flow control when nonuniformities in the suction distribution and/or surface geometry are present. As will be seen later, the schemes which are examined here inherently involve such nonuniformities.

In addition, the fabrication, operation and maintenance problems associated with a suitable porous surface have not been addressed in this study. Accordingly, while the results presented here delineate the potential of these schemes, they should be considered provisional in terms of application.

In the present study the potential benefit in performance due to suction techniques was examined in two distinct ways. In the first of these, suction was applied to essentially constant pressure surfaces (fuselage) to stabilize a laminar boundary layer so as to prevent transition and the associated increases in viscous shear stress on the surface. In the second approach, suction was applied to wing surfaces experiencing adverse pressure gradients with the aim of preventing separation. In these circumstances, improvement in aircraft aerodynamic performance would accrue both from reduction in viscous shear as well as from improved L/D characteristics of the wing.

Theoretical estimates of viscous drag reduction due to tangential slot injection were provided by the NASA Langley Research Center in accordance with contractual agreement. Corresponding estimates of laminar boundary layer behavior with suction were generated by ATL employing various approximate schemes which are described in subsequent sections of this report.

The overall performance of the selected systems was determined at a fixed subsonic cruise condition corresponding to a nominal flight Mach number of $M_\infty = 0.8$ and an altitude of 11,000 m. The aircraft configuration to which most of the performance data was referenced was the Boeing 747. Some of the performance results obtained with wing suction are referenced to a Lockheed C-141 Star Lifter wing section. In this connection it must be emphasized that no optimization in terms of aircraft configuration was attempted in the present study. Accordingly, the results obtained can probably be improved by appropriate changes in configuration. Recommendations in this regard are presented in the last section of this report.

2

II. LIST OF SYMBOLS

a	$(L/D)/(L/D)'$
A	flow area
b	slot width
B	$\Delta W/W_o$
c	chord length
C_f	local skin friction coefficient with suction or injection
C_F	average skin friction coefficient with suction or injection
C_{f_i}	local baseline skin friction coefficient
C_{F_i}	average baseline skin friction coefficient
C_p	pressure coefficient
C_s	suction flow coefficient $- \rho_s v_s / \rho_\infty V_\infty$
d	fuselage diameter
D	net drag with suction or injection
D_F	friction drag on surface affected by suction or injection
D_o	baseline total drag
D_{F_o}	baseline fuselage drag
F	baseline fuel load
F'	fuel load with drag reduction
h	slot height
I	turbo-machine drag per unit flow rate (see page 37)
k_1	line loss recovery factor
L	length of suction or injection interval
L_i	streamwise distance to first slot
L_o	overall length of fuselage
L/D	baseline maximum lift-to-drag ratio
$(L/D)'$	maximum lift-to-drag ratio with drag reduction

3

M	Mach number
N	mass flow function (see page 66)
P	pressure
q	dynamic pressure
r	fuselage radius
$\bar{r}$	r/c
R	baseline range
R'	range with drag reduction
Re_f	Reynolds number based on fuselage length and free stream conditions
v_s	suction velocity
V	axial velocity
w	aircraft weight increment per unit surface area
W	mass flow rate
W_e	$W_o - F$
W_o	gross weight of aircraft
x	streamwise coordinate
$\bar{x}$	x/L_o
X	skin friction reduction parameter (see page 43)
y	normal coordinate
γ	specific heat ratio
δ	boundary layer thickness
δ^*	displacement thickness
η_c	compressor efficiency
η_t	turbine efficiency
θ	momentum thickness
λ	slot injection parameter - $\rho_j V_j / \rho_\infty V_\infty$

μ viscosity

ξ suction parameter - $C_S \rho_\infty V_\infty y / \mu_\infty$

ρ density

Subscripts

c   compressor conditions

j   slot injection conditions

s   suction conditions

1   turbine entrance conditions

2   turbine exit conditions

3   compressor exit conditions

4   compressor entrance conditions

∞ free stream conditions

Superscripts

$(\bar{})$ average values

*   sonic conditions

III. PRELIMINARY CONSIDERATIONS

A. <u>Baseline Aircraft Drag</u> - This study was conducted for typical CTOL cruise flight conditions and a fuselage shape representative of current long-haul subsonic transports. Most of the results of this study are presented in terms of net drag reduction for the various schemes as a percent of a reference total drag D_o corresponding to the selected baseline aircraft. For the present purpose D_o has been taken to correspond to the total drag of a wide body transport (viz., a Boeing 747) cruising at an altitude of 11,000 m and $M_\infty = 0.82$. In order to estimate this parameter the following approximations were employed.

For the cited flight conditions the unit free stream Reynolds number is approximately 6.2 million/m so that, based on a fuselage length of approximately 67 meters[*], a fuselage Reynolds number, Re_F, on the order of 4×10^8 prevails. An average skin friction coefficient based on this Reynolds number can be obtained from the Prandtl-Schlichting correlation (Reference 6) yielding[**]

$$C_{F_i} = 0.455 \ (\log Re_F)^{-2.58} = .00175$$

Taking the diameter of the fuselage to be 6.7 meters the total wetted area is approximately 1400 m^2. Accordingly, D_F, the fuselage drag in the absence of any drag reduction effects is approximately 27,000 newtons.

An average skin friction coefficient for the wing is estimated to be given by the above skin friction law but for a length Reynolds number based

---

[*]Characteristic dimensions of the various aircraft considered here are taken from Reference (5).

[**]Compressibility effects would reduce this value by approximately 10% for the adiabatic wall case. However, this value is considered sufficiently accurate for the present purpose.

on an average chord length of 90 meters. This value (.00231) is applied to an exposed surface area of around 840 m^2. The skin friction drag of the wing is, therefore, 21,000 newtons. Adding 10% to account for skin friction on the empennage and engine pods and profile drag the total zero lift drag of the baseline aircraft is estimated to be 53,000 newtons.

The airplane cruises at maximum (L/D). The drag corresponding to this condition is twice the zero lift drag. Thus, the cruise drag of the baseline aircraft, D_o, is estimated to be 106,000 newtons.

B. <u>Fuselage Geometry and Pressure Distribution</u> - As indicated earlier, calculations of the turbulent shear distribution on the fuselage in the presence of tangential slot injection were carried out at the NASA Langley Research Center. The numerical finite difference technique due to Beckwith and Bushnell (Reference 7) was employed for this purpose.

In order to implement this methodology a body geometry and corresponding pressure distribution were needed. The fuselage was approximated by the quasi-ellipsoid of revolution depicted in Figure (1). In the absence of experimental data an estimate of the pressure distribution was made using the method of Reference (8). This is depicted by the solid line shown in the lower portion of Figure (1). Note that this distribution indicated the existence of sub-ambient static pressures over much of the fuselage surface as well as singularities at the fore and aft stagnation points.

To simplify the numerical procedures, the alternate pressure distribution shown by the dashed line was substituted with the agreement of the contract technical monitor.

C. <u>Wing Geometry and Pressure Distribution</u> - Accurate calculation of the potential benefit of wing suction requires both three-dimensional transonic inviscid analysis and three-dimensional laminar boundary layer analysis. The latter should include the simultaneous effects of suction and rapid streamwise variations in pressure as well as, possibly, stability considerations. Clearly, such a detailed approach would be beyond the scope of the present design study.

$$\bar{r} = \frac{3}{55} \sqrt{1 - (11\bar{x} - 2)^2/2} \; ; \; 0 \leq \bar{x} \leq \frac{2}{11}$$

$$\bar{r} = \frac{3}{55} \; ; \; \frac{2}{11} < \bar{x} < \frac{9}{11}$$

$$\bar{r} = \frac{3}{55} \sqrt{1 - (11\bar{x} - 9)^2/2} \; ; \; \frac{9}{11} \leq \bar{x} \leq 1$$
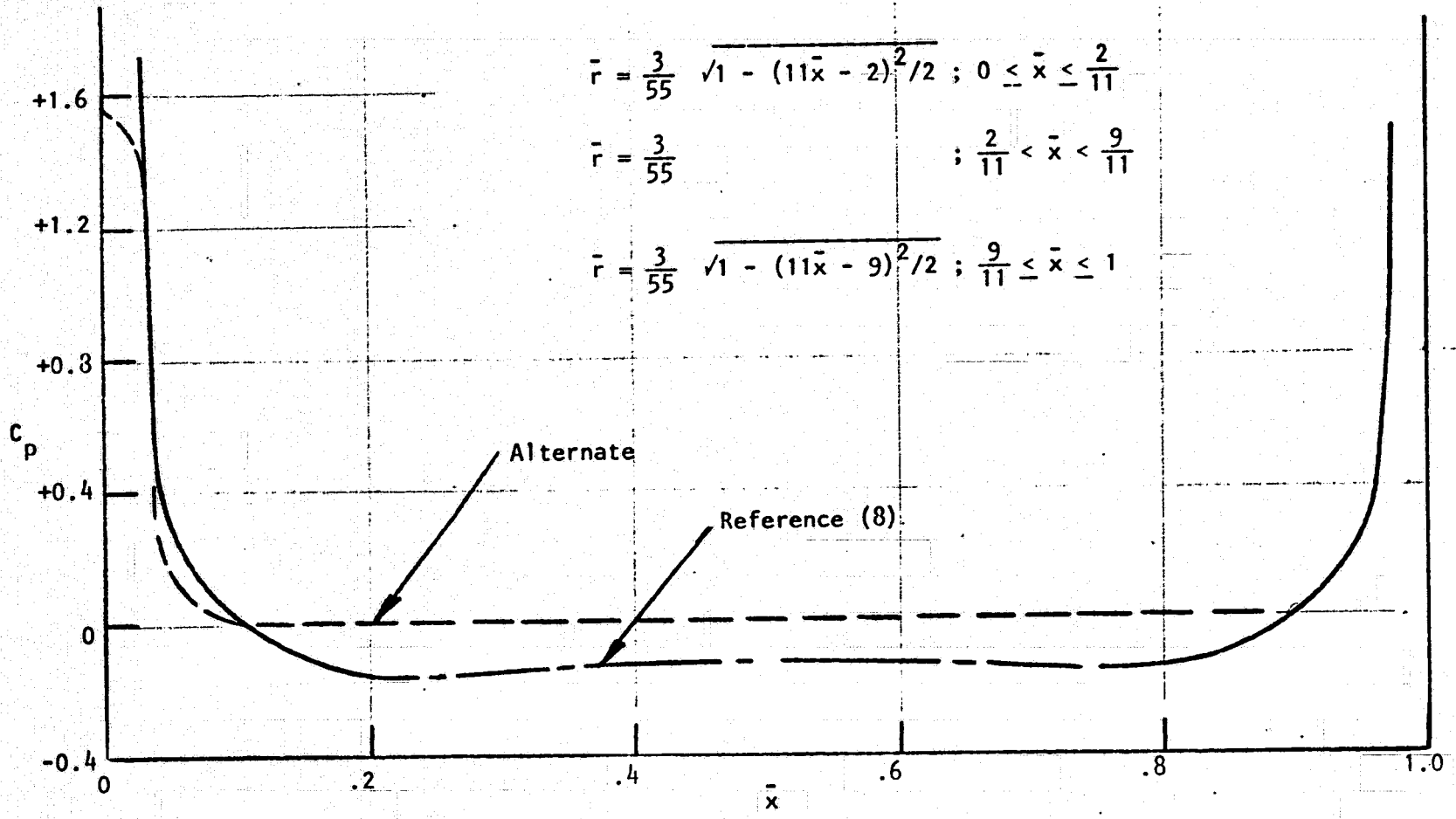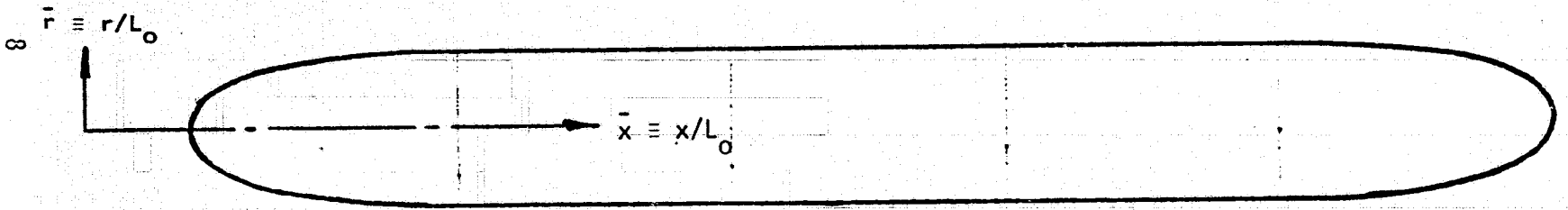
FIGURE 1. FUSELAGE GEOMETRY AND PRESSURE DISTRIBUTION

To provide at least a rough estimate of the effect of suction on the baseline configuration a two-dimensional approach was adopted. Within this idealized framework the essential feature of a super-critical airfoil with the attendant weak shock was retained. In the absence of any direct information on the 747 airfoil the inviscid pressure distribution over a C-141 airfoil section, as obtained from Reference (9), was employed. This pressure distribution for both upper and lower surfaces is shown in Figure (2). It corresponds to flow at M_∞ = 0.76 and an angle of attack of 0.95°. These values are not precisely those of the baseline configuration, particularly the angle of attack. Nevertheless, the resulting pressure variation should be representative in terms of the presence of a normal shock on the upper surface.

The airfoil section geometry is shown in Figure (3).
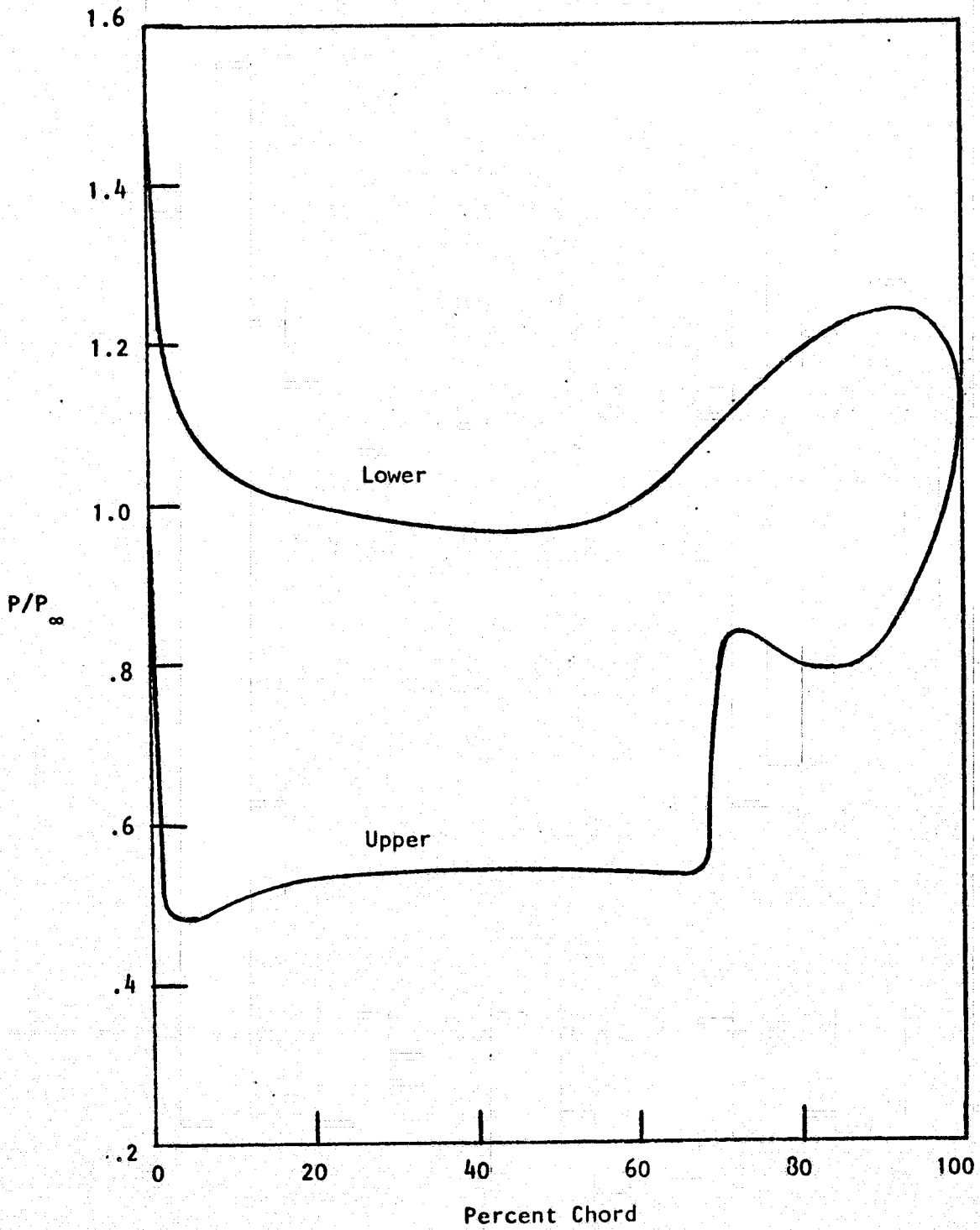
FIGURE 2. PRESSURE DISTRIBUTION ON WING

Upper Surface		Lower Surface	
x/c	y/c	x/c	y/c
0.0003	0.0042	0.0005	-0.0029
.0008	.0059	.0009	-.0041
.0013	.0073	.0017	-.0058
.0018	.0084	.0031	-.0080
.0053	.0131	.0059	-.0109
.0076	.0154	.0099	-.0141
.0112	.0182	.0165	-.0178
.0160	.0213	.0217	-.0201
.0233	.0252	.0373	-.0250
.0480	.0343	.0681	-.0311
.0728	.0408	.0936	-.0345
.0978	.0458	.1038	-.0356
.1178	.0492	.1242	-.0375
.1478	.0534	.1547	-.0398
.1979	.0589	.1750	-.0410
.2480	.0630	.2053	-.0424
.2980	.0659	.2557	-.0441
.3480	.0678	.3059	-.0451
.3979	.0688	.3560	-.0453
.4477	.0688	.4058	-.0449
.4974	.0678	.4554	-.0438
.5470	.0659	.5048	-.0421
.5965	.0630	.5541	-.0399
.6461	.0591	.6025	-.0369
.6962	.0543	.6521	-.0334
.7465	.0485	.6845	-.0307
.7967	.0414	.7247	-.0278
.8472	.0329	.7846	-.0225
.8976	.0235	.8341	-.0180
.9986	.0017	.8670	-.0148
		.8999	-.0114
		.9164	-.0096
		.9651	-.0039
		.9822	-.0019

FIGURE 3. WING GEOMETRY

IV. BOUNDARY LAYER CALCULATIONS

A. **Constant Pressure Laminar Results** - Skin friction reduction due to uniform suction at constant pressure was estimated directly from the incompressible results given by Schlichting (Reference 6). These results are summarized in Figure (4). For the present application the parameter of interest is the net reduction in average skin friction coefficient, C_F, relative to the baseline turbulent value, C_{F_i}. The dependence of this ratio on the relative suction rate C_s has been deduced from the results shown in Figure (4) and are presented in Figure (5) with the length Reynolds number as a parameter.

Indicated in Figure (5) is a "cutoff" value of $C_s = .00012$. This value corresponds to the minimum needed to insure the maintenance of laminar flow as established by the stability considerations outlined in Chapter XVII of Reference (6).

Finally, we note that these incompressible results should be reasonably accurate for the present high speed application since only the ratio of skin friction levels is involved.

B. **Laminar Results with Pressure Gradient** - The analytical method utilized for these calculations is described in detail in Appendix A. It employs the momentum integral technique due to Torda (Reference 10) in conjunction with Thwaites method (Reference 11) to permit initiation of the calculation at a stagnation point.

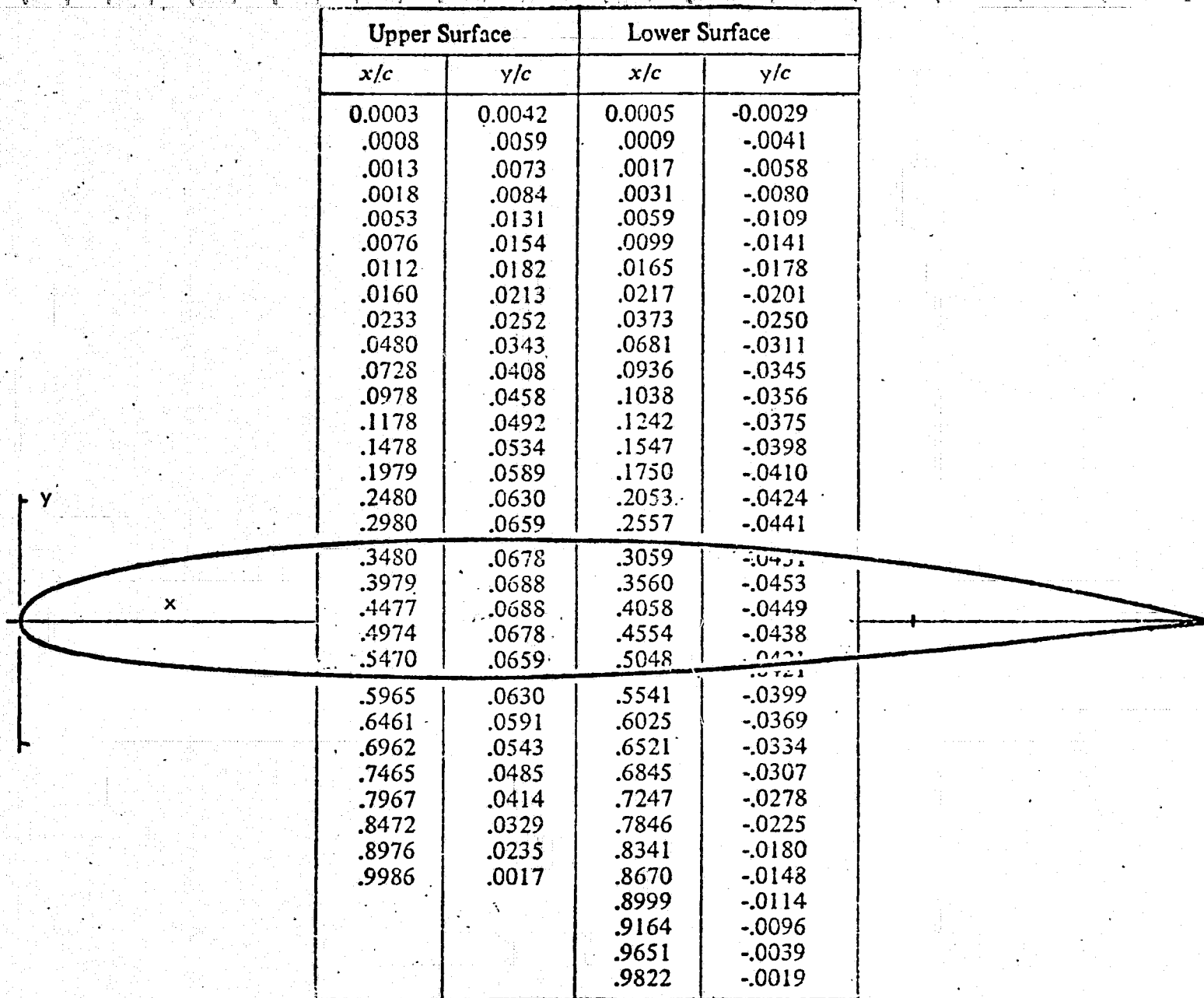The numerical computation scheme based on this method can be exercised in two distinct ways. The more general option accepts arbitrary distributions of suction (or blowing) and pressure gradient and determines all boundary layer characteristics. The alternate option imposes the condition that the boundary layer thickness is constant. In this case, for an arbitrary variation of external pressure, the computation yields the requisite suction distribution as well as the corresponding variation of all other boundary layer properties. The latter option is useful in terms of providing a mechanism by which, in an approximate sense, the preservation of a laminar flow can be assured.
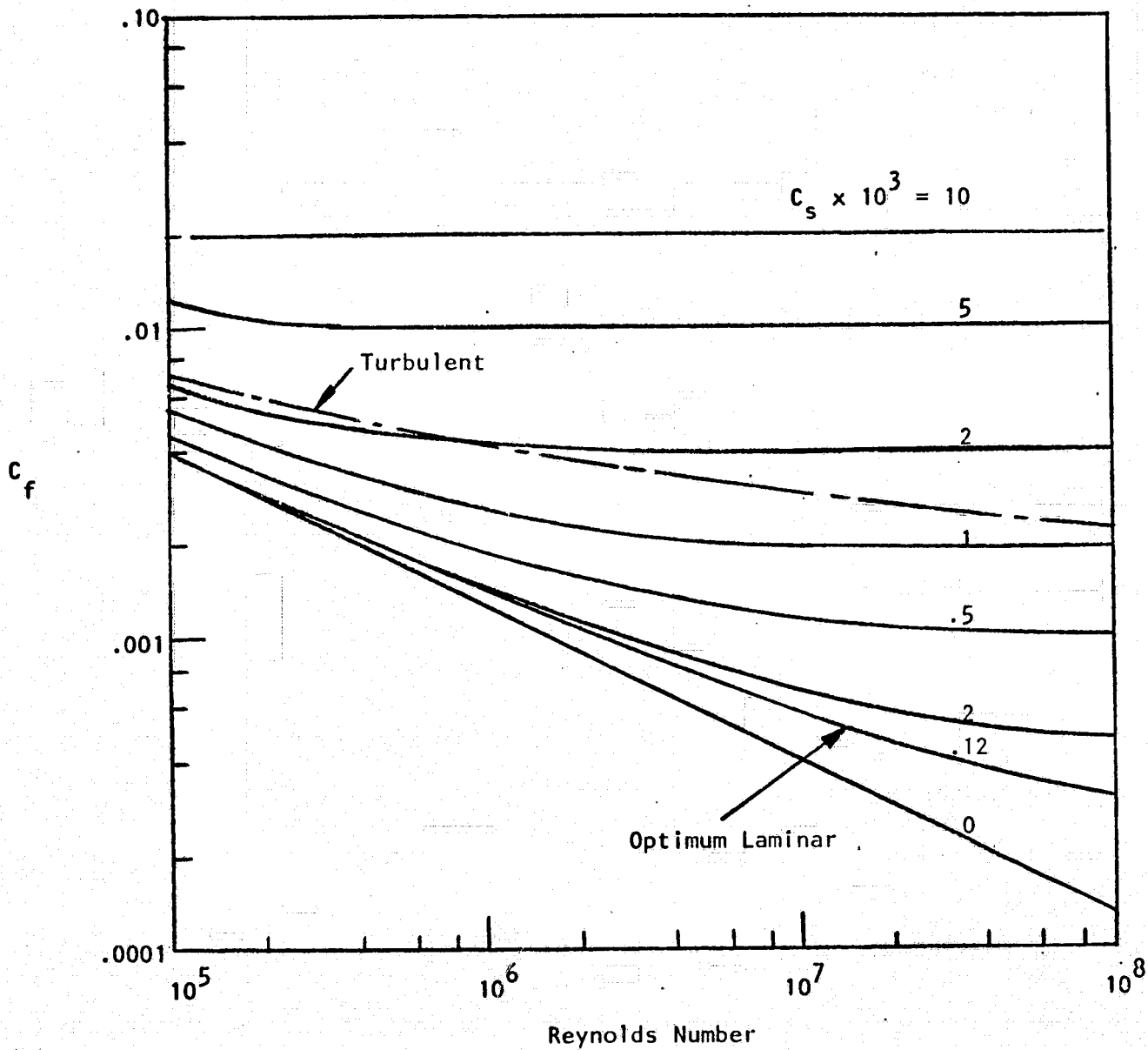
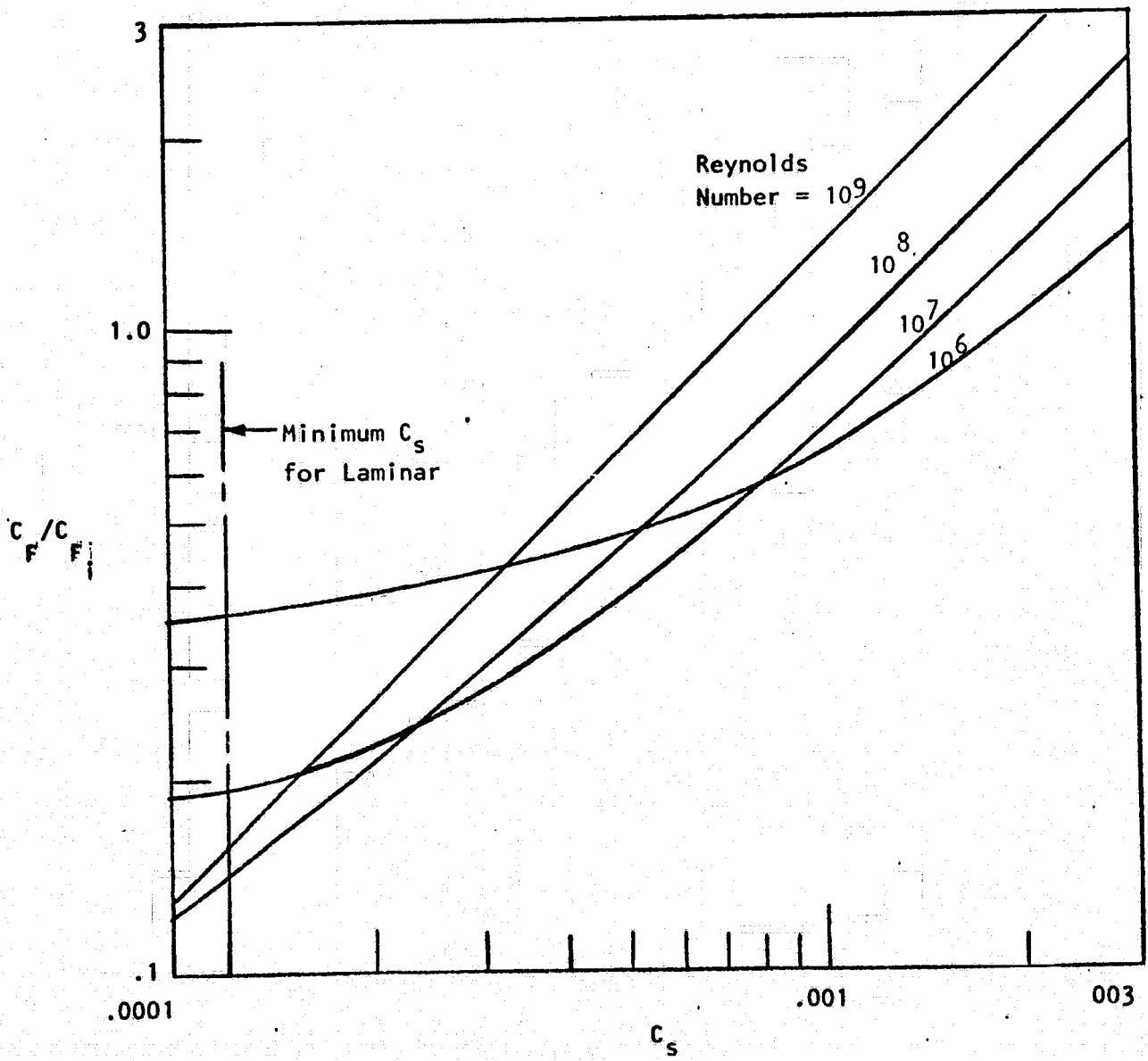FIGURE 4. DRAG COEFFICIENT FOR FLAT PLATE WITH UNIFORM SUCTION

13

FIGURE 5. REDUCED SKIN FRICTION COEFFICIENT WITH SUCTION

In applying this analysis to the baseline wing configuration the following objectives prevailed; the suction distribution should insure that the state of the boundary layer remain laminar; the suction distribution should prevent separation under the influence of the inviscid pressure distribution associated with the baseline configuration; the suction distribution should yield the minimum skin friction consistent with the previous requirements. Toward this end the suction distributions on the wing were determined as follows.

In regions of constant pressure and in regions of favorable pressure gradient (which tends to suppress the rate of growth of the boundary layer), the relative suction rate was maintained constant at the optimum value C_s = .00012. In principle, this can be expected to preserve the laminar boundary layer state. In regions of adverse pressure gradient the variation of C_s was computed by requiring that the boundary layer thickness remain constant at the value associated with the start of the pressure rise. The corresponding momentum thickness is found to decrease through this region so that, here again, it can be anticipated that the laminar state will prevail.

The results of these calculations are shown in Figures (6) and (7). As can be seen, very modest increases of suction over the optimum value are required to prevent separation on the lower surface of the wing. On the upper surface, of course, a very large "spike" of suction intensity is needed at the 70% chord station and at the trailing edge to maintain an attached laminar flow. Note, however, that although the maximum value of C_s is on the order of 40 times the optimum rate it is still less than .1% of the unit free stream flow rate.

The corresponding distribution of skin friction is shown in Figure (7). These laminar distributions have been compared with turbulent estimates made using the method described in Reference (12). Note that for the upper surface, separation is predicted at the 70% station and that the turbulent shear is assumed to be vanishingly small thereafter.

The pertinent results needed for the performance calculations are the net reduction in average shear for the entire wing and the average suction rate.
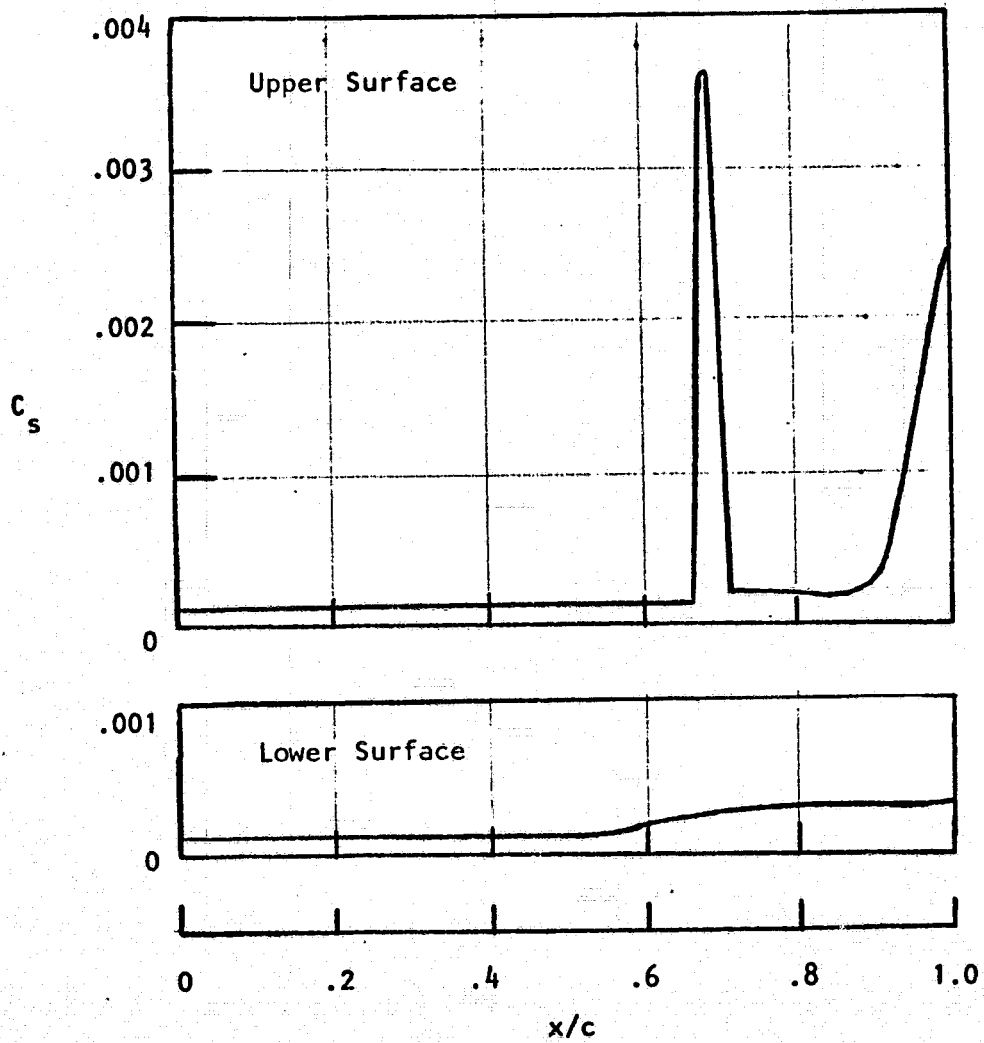
FIGURE 6. CHORDWISE VARIATION OF SUCTION PARAMETER ON WING SURFACES
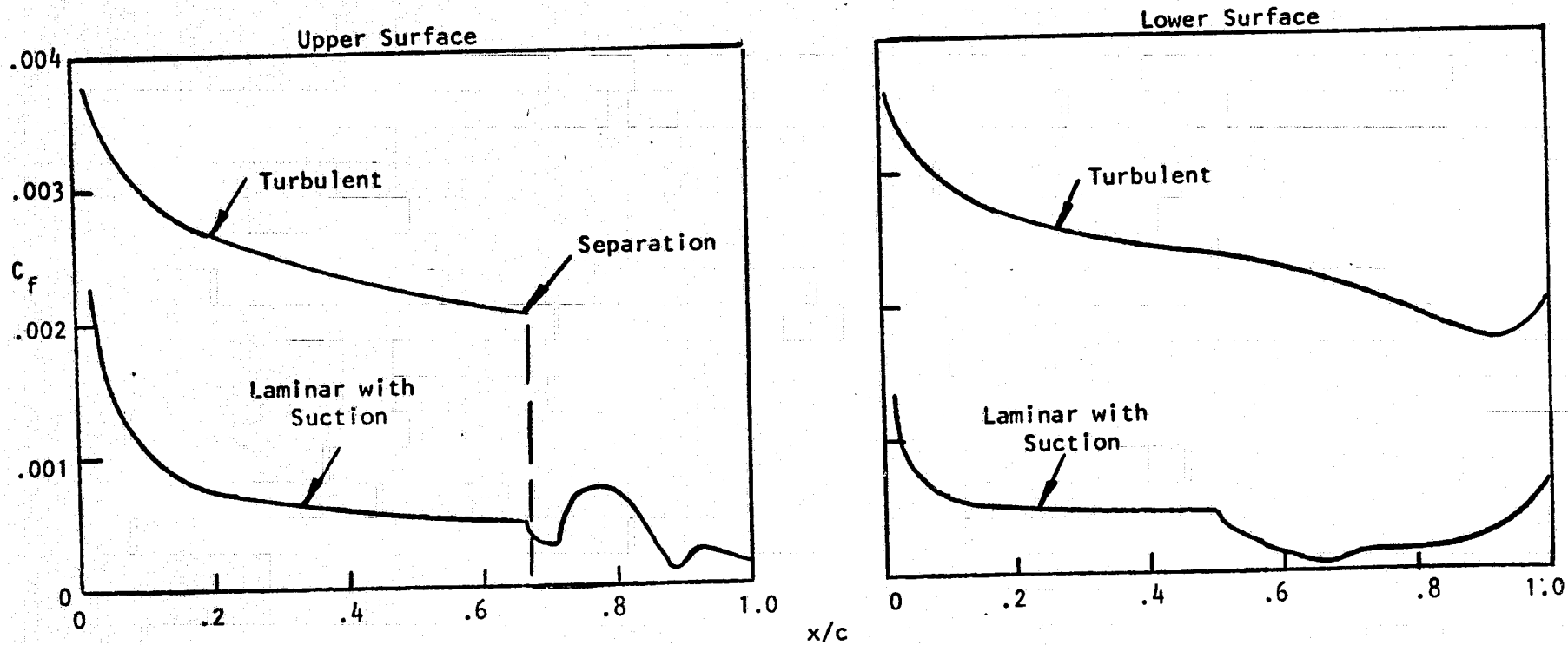
FIGURE 7. CHORDWISE VARIATION OF LOCAL SKIN FRICTION ON WING SURFACES

These data have been computed from the above results and are summarized below in Table I. The results indicate that the wall shear is reduced to approximately 25% of the turbulent values by application of suction at a rate on the order of twice the optimum value for a flat plate.

TABLE I
SUMMARY OF VISCOUS DRAG REDUCTION RESULTS ON WING

	Upper Surface	Lower Surface	Total Wing
Average turbulent shear C_{F_i}	.00175	.00283	.00229
Average laminar shear C_F	.000575	.000375	.000475
C_F/C_{F_i}	.343	.133	.238
Average suction parameter C_s	.000375	.000185	.00028

C. <u>Turbulent Results With Slot Injection</u> - Turbulent boundary layer solutions with tangential slot injection were obtained by F. G. Howard at the NASA Langley Research Center[*]. These were carried out for the fuselage configurations previously shown in Figure (1). The first slot is located at $x/L_o = 1/11$ and subsequent slots are placed at intervals of $\Delta x/L_o = 1/11$, u, to a maximum of 10 slots.

The assumed surface pressure distribution up to the first slot is shown in Figure (8); from the first slot to the end of the fuselage the pressure coefficient was assumed constant and equal to zero. The numerical method of Reference (14) was used to calculate the boundary layer characteristics up to the first slot, assuming a fully developed turbulent boundary layer from the

---

[*]A more complete presentation of these results may be found in Reference (13).

18

FIGURE 8.   INITIAL VELOCITY PROFILE AT FIRST SLOT AND PRESSURE
VARIATION TO FIRST SLOT
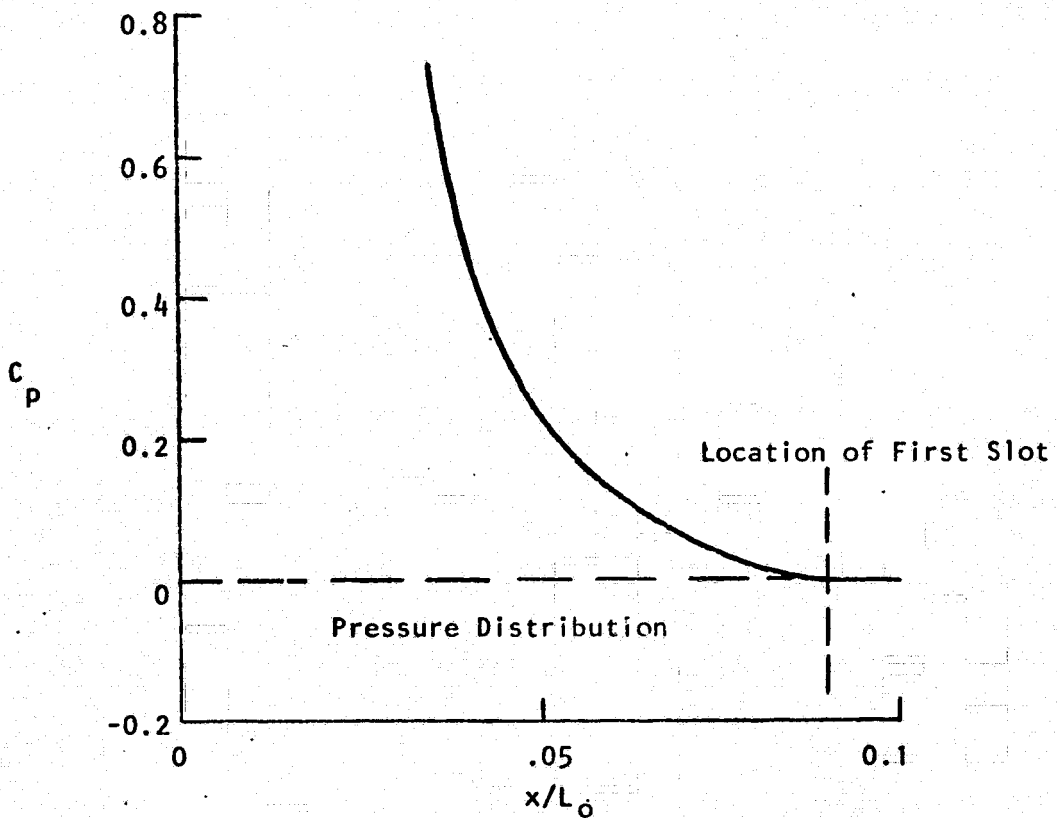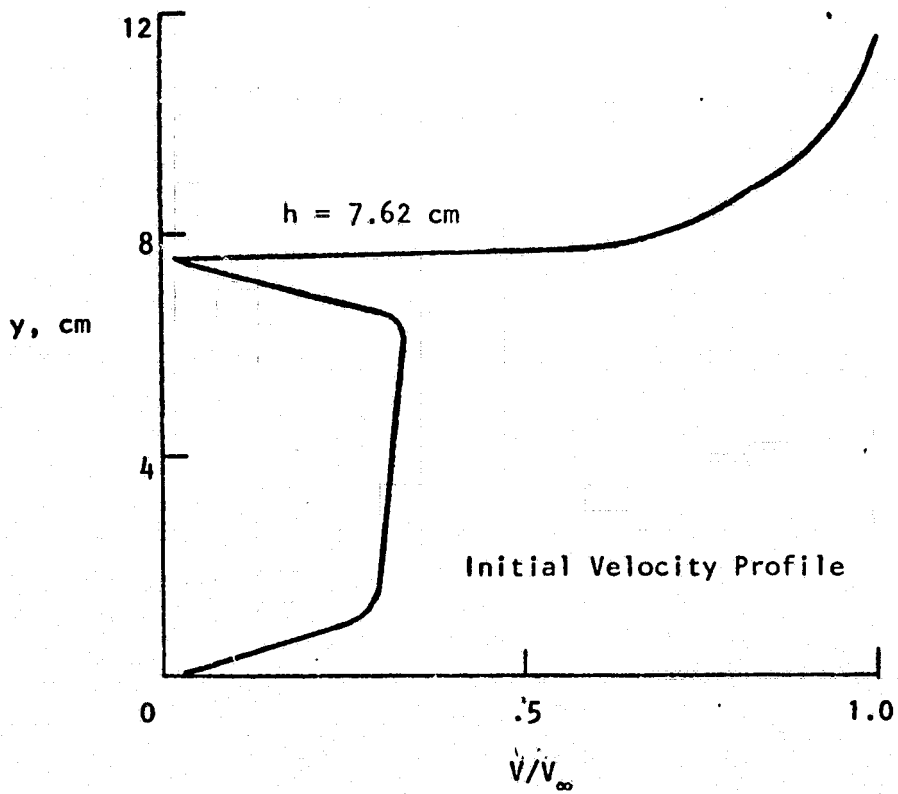
19

nose. The boundary layer thickness just upstream of the first slot is δ = 3.6 cm, the displacement thickness is δ^{*} = .57 cm, and the momentum thickness is θ = .35 cm. The boundary layer velocity profile was then combined with estimated slot exit velocity profiles having a shape similar to those measured in Reference (15), and an average Mach number of M_{j} = 0.2. The resultant complete velocity profile was used as input for the slot injection code of Reference (7). The resultant velocity profile at the first slot (for h = 7.62 cm) is shown in Figure (8). The slot to free stream total temperature ratio was assumed constant and equal to 0.9895. The variation of skin friction and velocity profiles downstream of a single slot is indicated in Figure (9).

The numerical finite-difference solution of Reference (7) was modified so that the effect of multiple slot injection on the fuselage skin friction could be determined. The local skin friction coefficients (C_{f}) obtained downstream of one, three, five and ten slots (slot height (h) of 7.62 cm) are compared with the local skin friction coefficient on the fuselage without slots in Figure (10). The local skin friction reduction with only one slot is significant when compared to that without slot injection. The beneficial effect of the slot injection is most pronounced immediately downstream of the slot exit and diminishes with increasing distance downstream from the slot; this occurs because in the near slot region the wall friction is influenced only by the slot flow while further downstream mixing between the high momentum boundary layer flow and the relatively low momentum slot flow increases the wall shear. The effect of slot height on skin friction variations with downstream distance is demonstrated in Figure (11) for the ten slot case. For these calculations the slot velocity profiles were scaled by the slot height so that the slot mass flow varied in proportion to slot height.

As in the case of the laminar results, the net reduction in average skin friction relative to the baseline value, $C_{F}/C_{F_{i}}$, is needed for the performance calculations. For this purpose the average wall shear of the fuselage was estimated from the data shown in Figures (10) and (11) and normalized with respect to the corresponding average for the no slot case. The resulting variation with number of slots and slot height is presented in Figure (12).
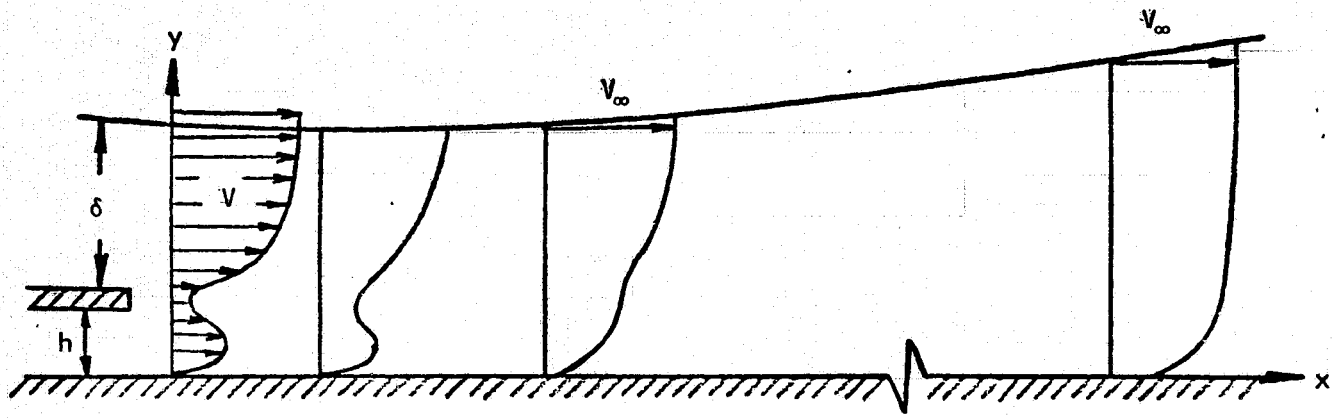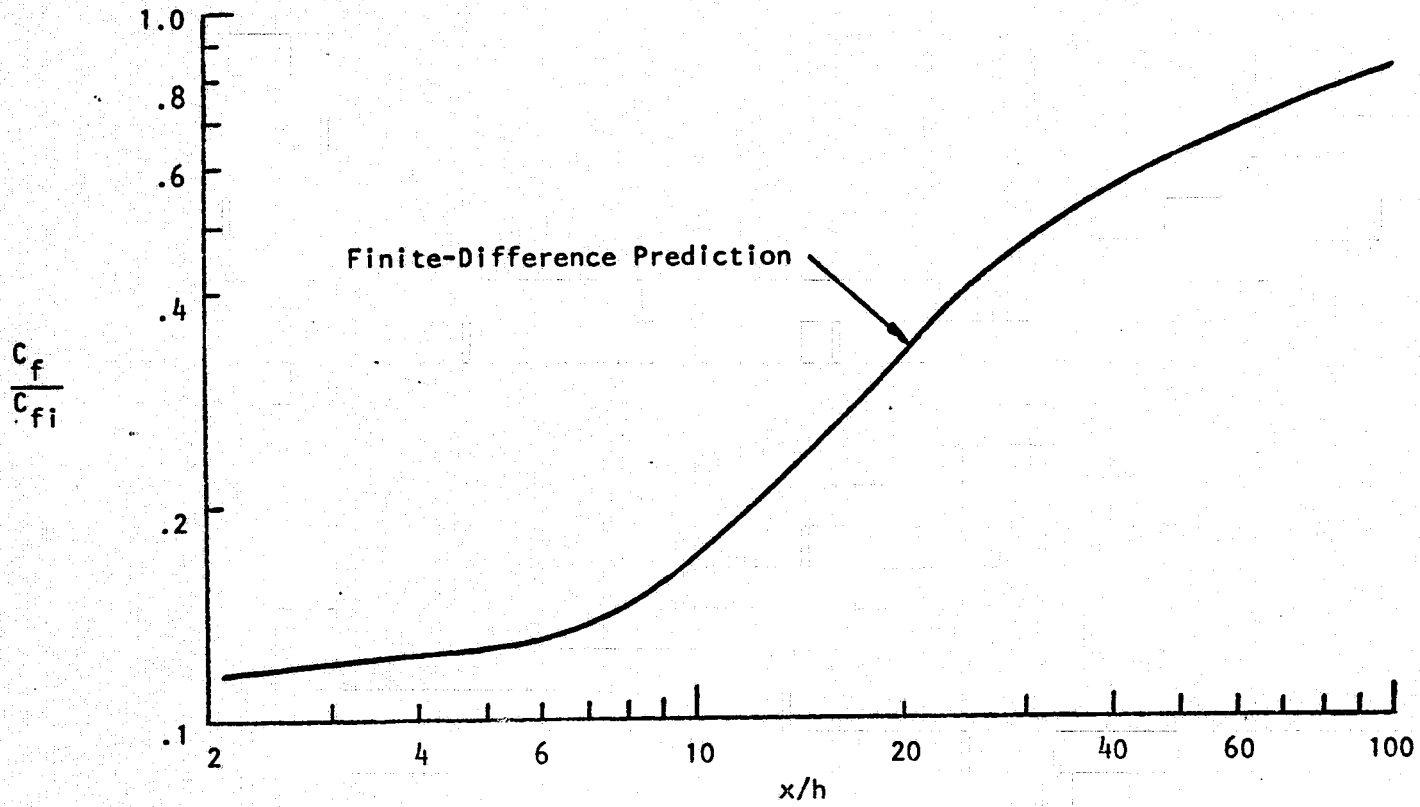
Velocity Profiles

FIGURE 9.   VELOCITY DEVELOPMENT AND SKIN FRICTION BEHAVIOR DOWNSTREAM OF A SINGLE SLOT
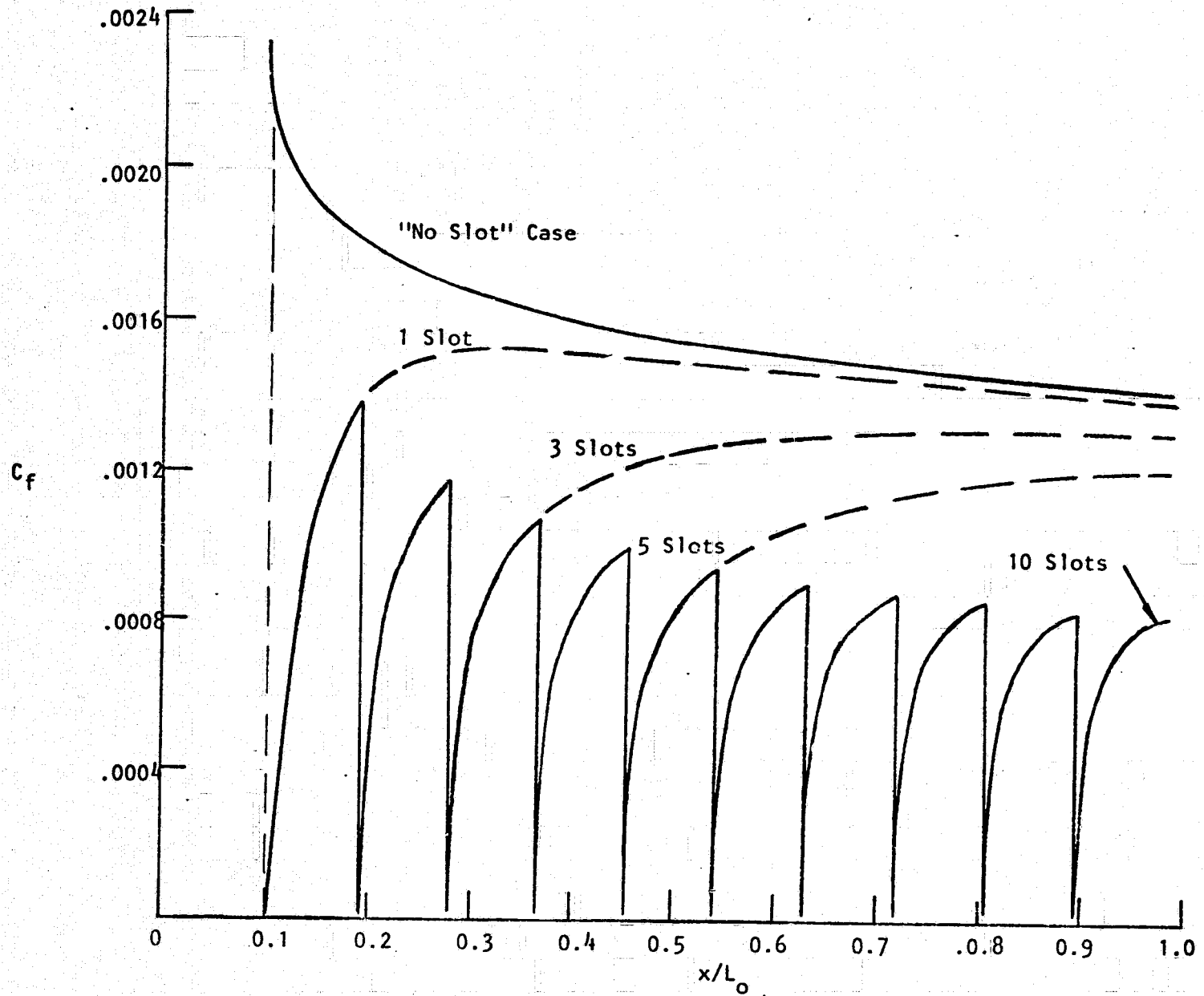
FIGURE 10. SKIN FRICTION REDUCTION WITH SLOT INJECTION, h = 7.62 cm, $(V/V_{\infty})_{max}$ = 0.338
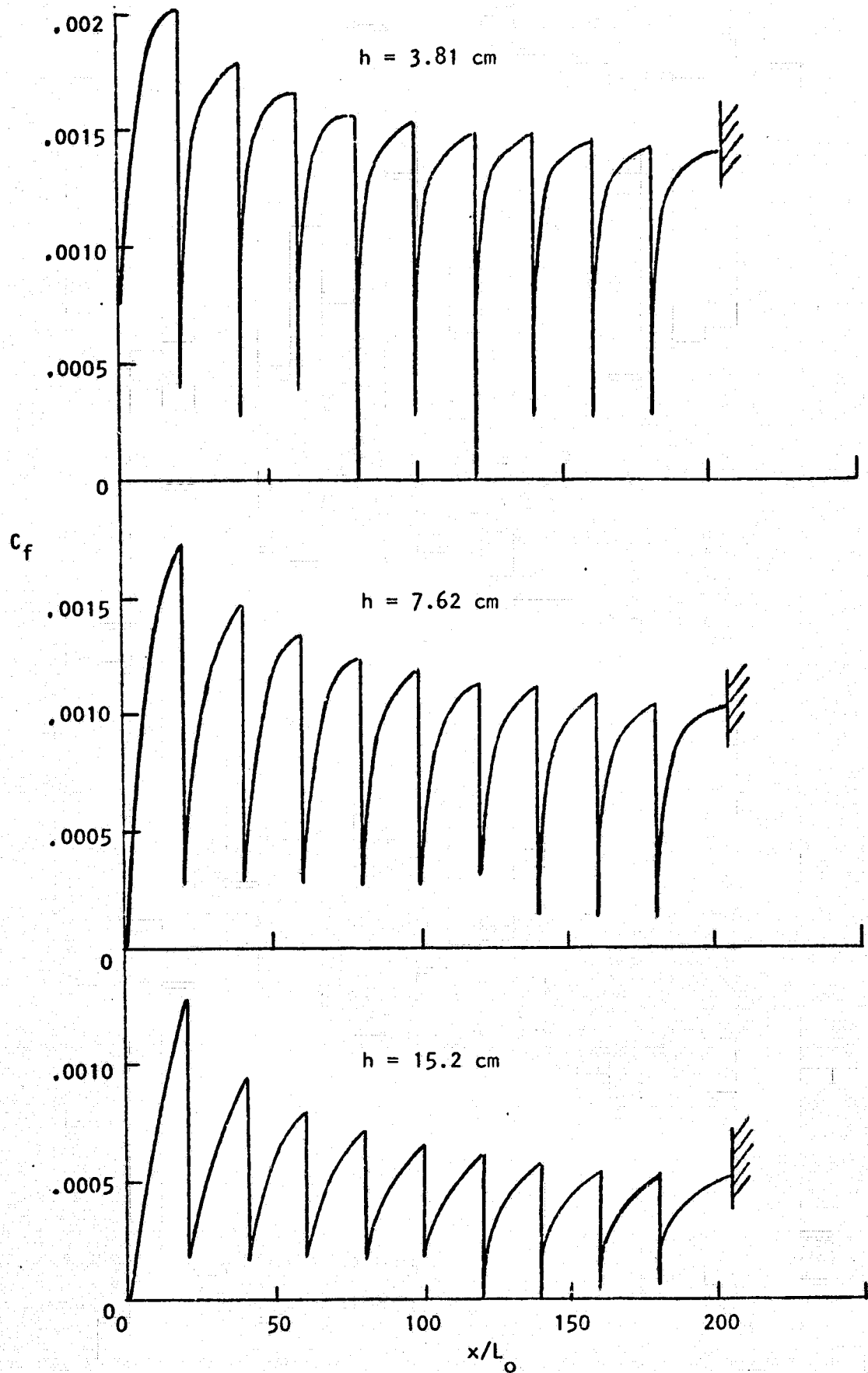
FIGURE 11. VARIATION OF LOCAL SKIN FRICTION ON FUSELAGE WITH SLOT
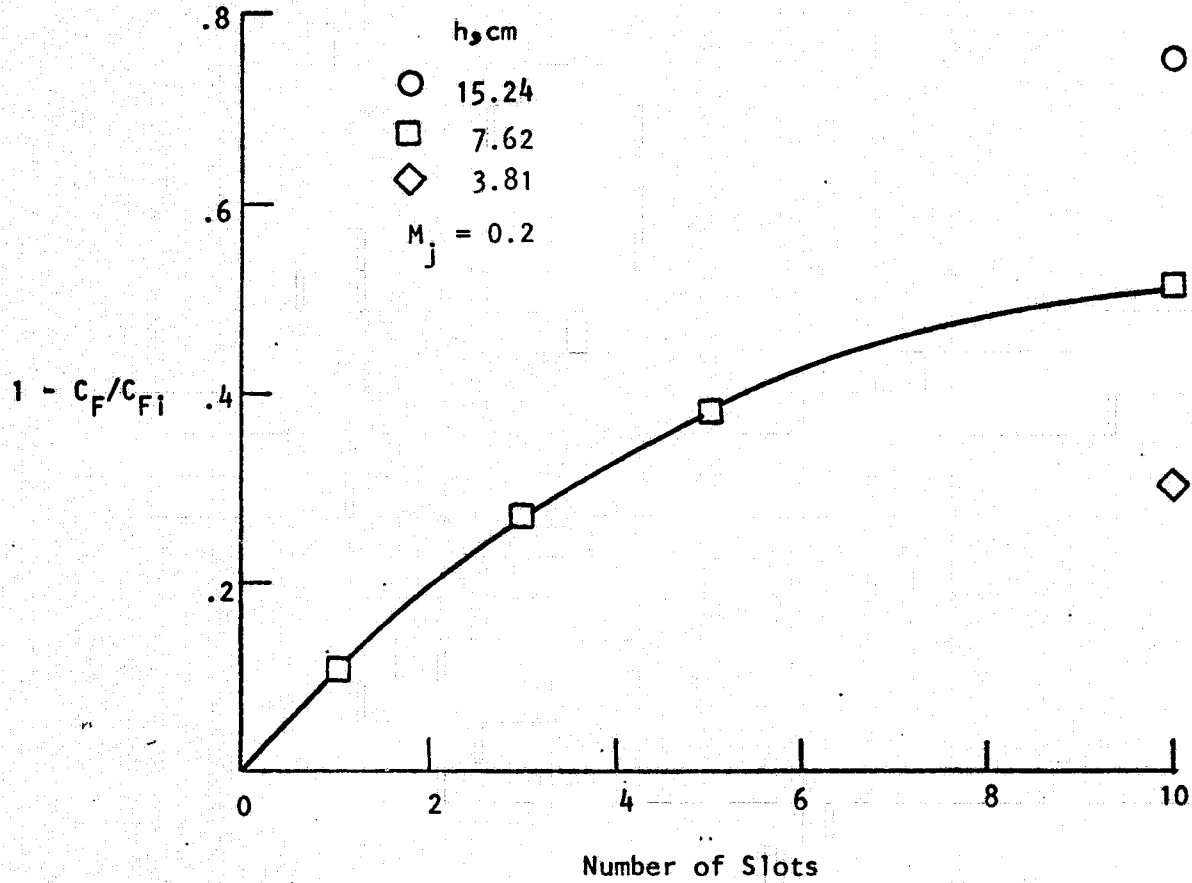INJECTION; $M_j = 0.2$

23

FIGURE 12. SKIN FRICTION REDUCTION EFFECTIVENESS AS A FUNCTION
OF NUMBER OF SLOTS

The improvement with additional slots and increasing slot height, both of which correspond to increasing mass flow, is apparent. It is clear from Figure (12) that large reductions ($\sim$ 50%) in viscous drag are available through the use of slot injection systems.

The results shown in Figures (10), (11) and (12) suggest that the skin friction reduction is improved by increasing the number of injection slots but at a diminishing rate (for constant slot spacing). One probable reason for this is that slot location is very important; for the present study, the most forward slot is the most effective and the most rearward slot is the least effective. Two advantages of a forward slot location in the present study are (1) the no injection skin friction level is high and (2) the boundary layer is thin; slot effectiveness for local skin friction reduction is improved at low ratios of boundary layer thickness to slot height (References 16 and 17). Forward slot injection offers an obvious additional advantage in that the drag reduction occurs over a larger area of the aircraft. This effect of slot location is illustrated when the following comparison is made from Figure (12); consider the case of ten slots with h = 3.81 cm compared with the case of five slots with h = 7.62 cm (the first slot in each case is located at the same position). Although the total mass flow from the five larger slots would be the same as that for the ten 3.81 cm slots, the skin friction reduction is 27% greater for the five slot configuration than for the ten slots (see comparison in Figure 12).

The effect of injection Mach number has also been investigated. The results are summarized in Figure (13), which includes variations in slot height as well as injection Mach number. It appears that reduction of the injection Mach number can provide further reduction in the skin friction for the same total mass flow (i.e., compare points A and B in Figure 13). However, as will be seen subsequently, substantial drag penalties are incurred in the process of capturing the required mass flow and reducing its average Mach number to the level desired at the slot locations. The total mass flow injected through all the slots is captured downstream of the last slot, in the proposed baseline design, and reprocessed. However, due to the mixing which occurs in the fuselage boundary layer downstream of each slot, the captured flow is more energetic than desired. The excess energy

M_j	No. of Slots	h,m	C_F	C_F/C_{Fi}
0.2	10	.0381	.00110	.63
0.2	10	.0762	.000784	.45
0.2	10	.1524	.000411	.24
0.1	10	.0381	.00119	.68
0.1	10	.0762	.00098	.56
0.1	5	.0381	.00135	.77
0.1	5	.0762	.00118	.67
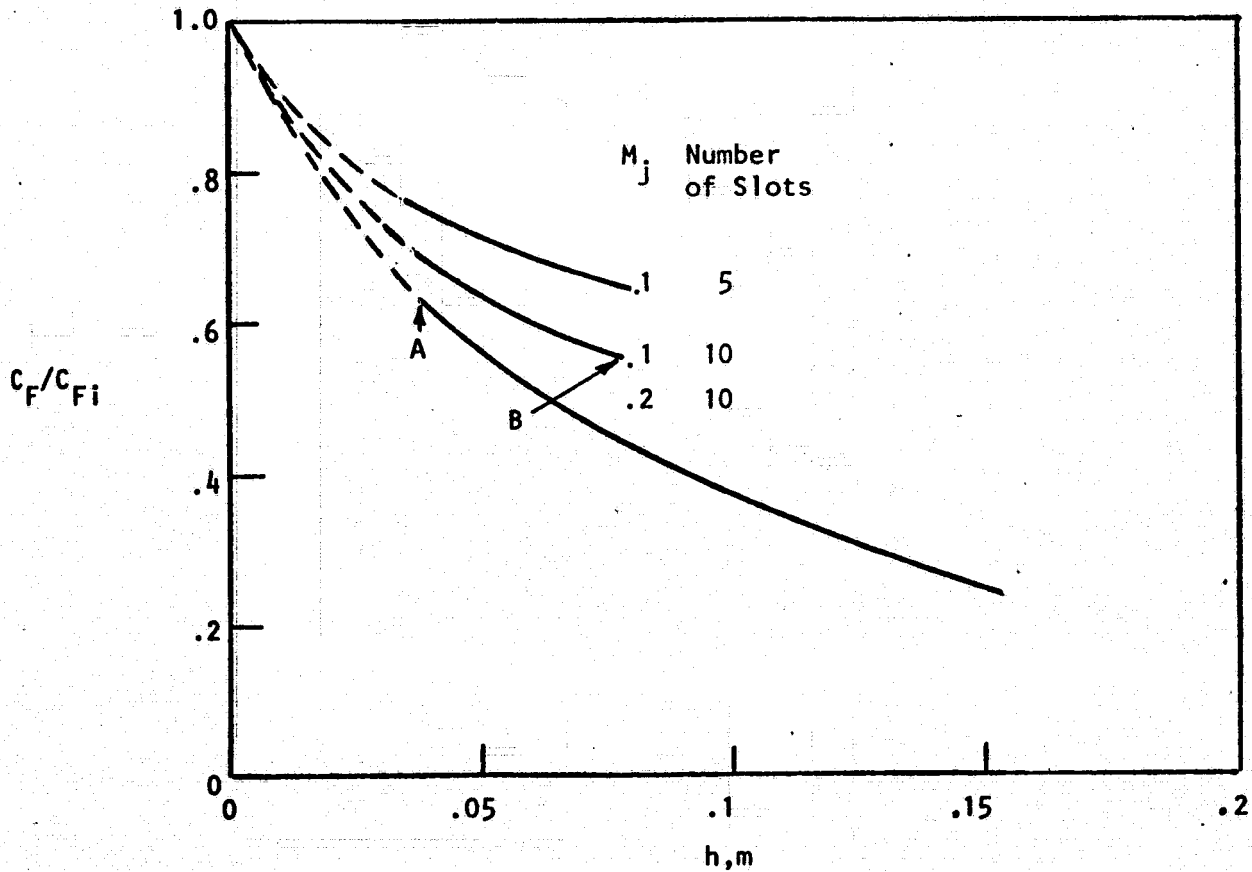
FIGURE 13. SKIN FRICTION REDUCTION EFFECTIVENESS AS A FUNCTION OF SLOT HEIGHT AND INJECTION MACH NUMBER

is removed in the turbo-machinery used for pumping the injected flow, which will be discussed subsequently. This problem is aggravated by reduction of the slot height, which increases the mixing and energization processes, as indicated by the velocity profiles at a station near the end of the fuselage shown in Figure (14), and by reduction of the injection Mach number.
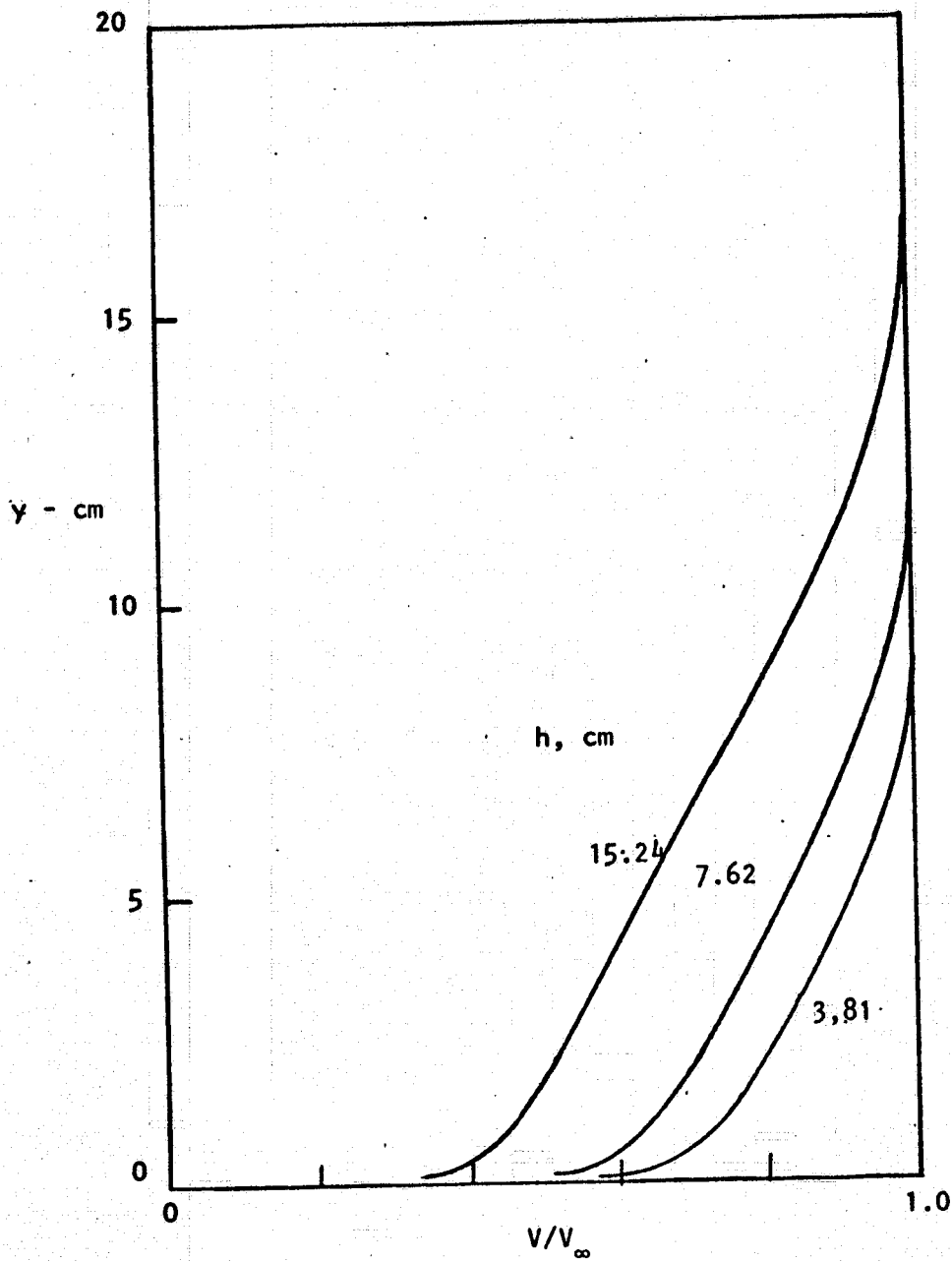
FIGURE 14. VELOCITY PROFILES AT END OF FUSELAGE;
10 SLOTS WITH M_j = 0.2

V. DRAG REDUCTION RESULTS

A. <u>Fuselage Slot Injection</u> - The scheme for utilizing the drag reduction potential of slot injection on the fuselage in conjunction with a turbine/compressor illustrated in Figure (15). The turbine processes the boundary layer air at the end of the series of slots and returns the air through an annular duct around the fuselage from which it is injected to the slots. Since the flow is injected at a low velocity in order to reduce skin friction, there is a drag associated with the turbine flow. The power generated by the turbine is absorbed by the compressor which also processes boundary layer air. The compressor air is discharged at a high velocity producing thrust which partly offsets the drag of the turbine flow.

As noted in Figure (15) there are two ways in which the boundary layer air can be processed. In the first way, the compressor can handle the "inner" or lower velocity flow near the surface while the turbine handles the "outer" or high velocity flow. Alternately, the location of turbine and compressor are reversed, with the turbine handling the "inner" flow and the compressor handling the "outer" flow. The arrangement which would be selected is the one giving the smallest net drag when processing the boundary layer air produced by the injection.

From the velocity profile data such as those presented in Figure (14), the average velocity as a function of boundary layer flow can be determined. Here, the average velocity means the average "momentum" velocity defined by

$$\bar{V} = \frac{1}{W} \int V dW$$

which is judged to be the most pertinent average for use in calculating the drag of the turbo-machine flows. For convenience of application, the average velocity is determined as a function of W/W_j, the boundary layer flow with respect to the injected flow, W_j being the total flow injected from all the slots. The results are presented in Figures (16a) and (16b).

The average velocity enters into the drag calculation of the turbo-machines in a straightforward manner. The drag of the turbine flow is given
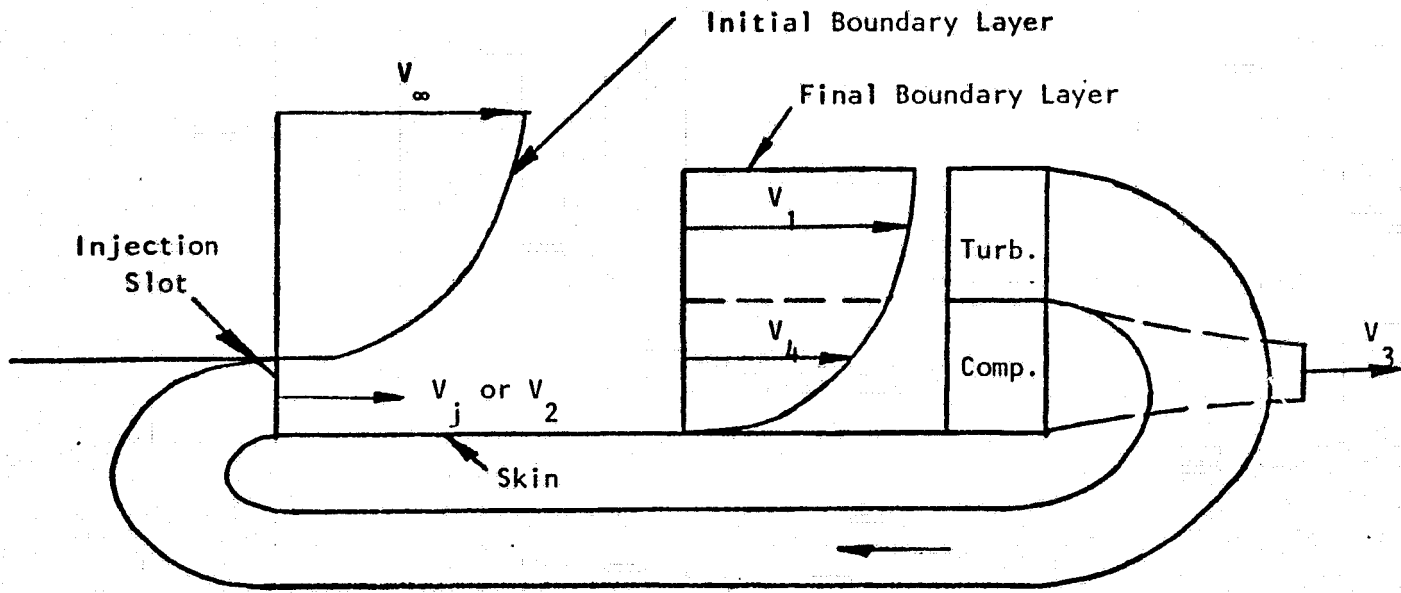
(a) Compressor Handling Inner Flow
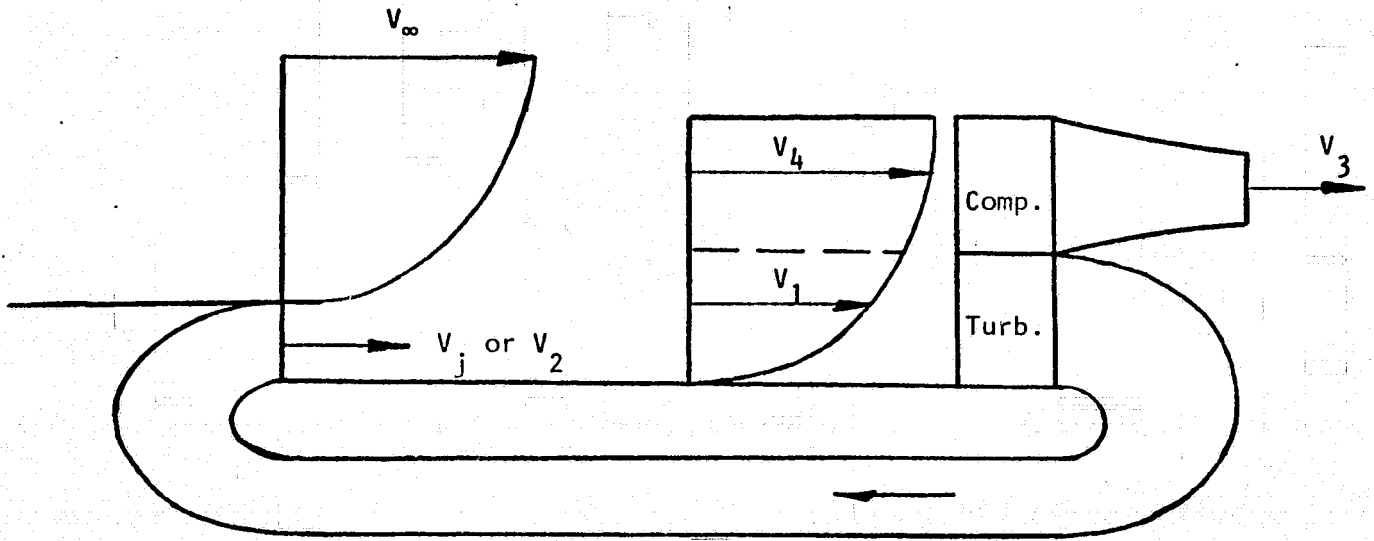
(b) Turbine Handling Inner Flow

FIGURE 15. SCHEMATIC OF SLOT INJECTION SYSTEM
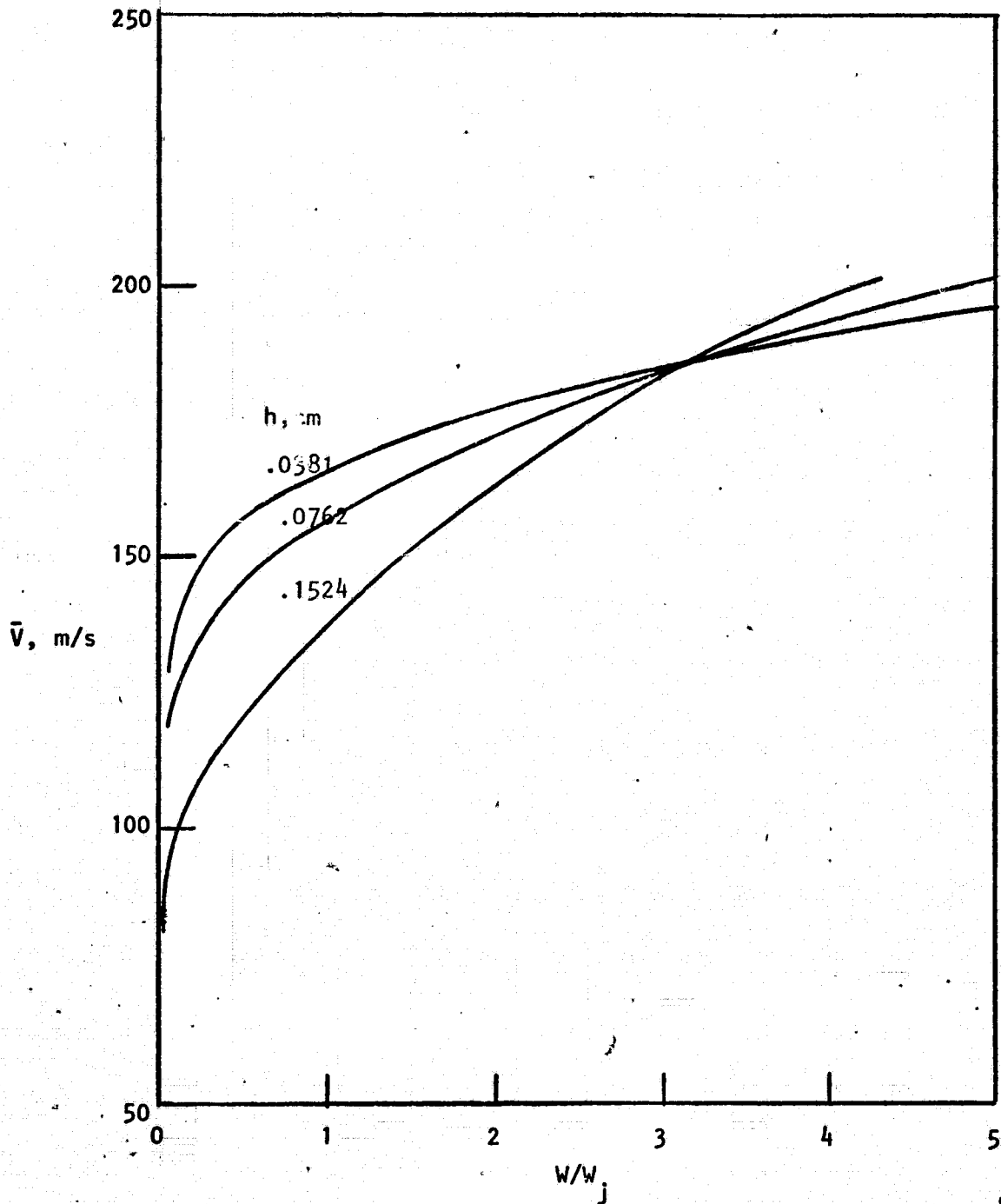
FIGURE 16a. AVERAGE VELOCITY IN BOUNDARY LAYER AT END OF SLOTS; M_j = 0.2

31
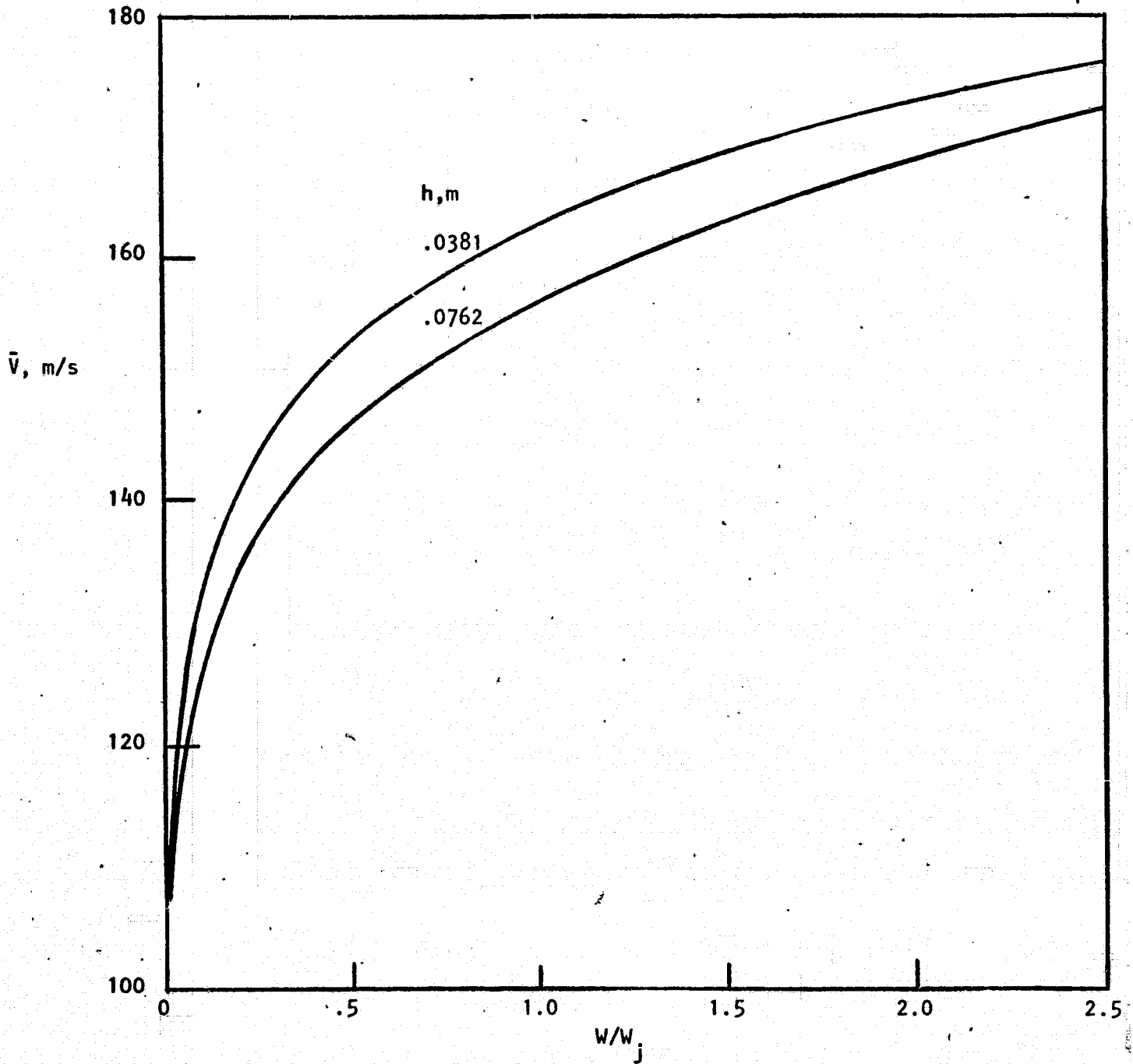
FIGURE 16b.   AVERAGE VELOCITY IN BOUNDARY LAYER AT END OF SLOTS; M_j = 0.1

by

$$\text{turbine drag} = W_t \, (V_1 - V_2)$$

where V_1 is the average velocity in the boundary layer flow handled by the turbine and V_2 is the discharge velocity or the slot injection velocity. This formulation of drag implies that the pressures at intake and discharge are the same (equal to free stream pressure), a basic premise of the boundary layer calculations which is very nearly true in the real case.

In reducing the velocity from V_1 to V_2, the turbine performs work which is transmitted to the compressor. The compressor utilizes the work to increase the velocity of the flow it handles from the intake value V_4 to the discharge value V_3. In this case, the compressor flow results in a thrust given by

$$\text{compressor thrust} = W_c \, (V_3 - V_4)$$

where V_4 is the average velocity of the boundary layer flow handled by the compressor.

The combined turbo-machine drag is then given by

$$\text{turbo-machine drag} = W_t I$$

where

$$I = V_1 - V_2 - \left(\frac{W_c}{W_t}\right) (V_3 - V_4)$$

In application, the quantities V_1, V_2 and V_4 are known. Then, for a given value of W_c/W_t, the value of V_3 can be found by means of a calculation which equates the power output of the turbine to the power input of the compressor and then transforms the power input to an increased energy of the flow which is converted to an increased discharge velocity V_3.

In formulating the production and conversion of power, conventional turbine and compressor efficiencies are included. In addition, ducting losses are taken into account by means of a loss factor (recovery factor or ratio of

total pressures) which accounts for the entire loss in the ducting, both ahead of and behind the machines. The loss factor is especially important in the case of the turbine because of the turning of the flow and the long duct length upstream for injection through the slots.

To convert the average velocity data of Figure (16) to values of average velocity for the turbine and compressor, it is necessary to fix the respective flows. For the turbine, the flow is fixed á priori since it is equal to the injected flow. However, the compressor flow may be chosen arbitrarily with the final choice deferred until the effect on jet drag reduction is determined. In the case where the compressor flow is the "inner" flow (see Figure 15) the average velocity V_4 for a given value of W_c/W_t is the value of $\bar{V}$ read at $W/W_j = W_c/W_t$. Then, since the turbine flow is the same as W_j, the turbine flow extends from $W/W_j = W_c/W_t$ to $W/W_j = 1 + W_c/W_t$. The average velocity for this portion of the boundary layer flow is given by

$$V_1 = (1 + W_c/W_t) \, \bar{V}_1 - (W_c/W_t) \, \bar{V}_2$$

where $\bar{V}_1$ is the value of $\bar{V}$ at $W/W_j = 1 + W_c/W_t$ and $\bar{V}_2$ is the value of $\bar{V}$ at $W/W_j = W_c/W_t$.

The average velocities for this case are shown in Figures (17a) and (17b) as a function of W_c/W_t.

In the case where the turbine flow is the "inner" flow, the average velocity V_1 is determined as the value of $\bar{V}$ at $W/W_j = 1$. For a given value of W_c/W_t, the compressor flow extends from $W/W_j = 1$ to $W/W_j = 1 + W_c/W_t$ and its average velocity is given by

$$V_4 = \frac{(1 + W_c/W_t) \, \bar{V}_2 - \bar{V}_1}{W_c/W_t}$$

where $\bar{V}_1$ is the value of $\bar{V}$ at $W/W_j = 1$ and $\bar{V}_2$ is the value of $\bar{V}$ at $W/W_j = 1 + W_c/W_t$. The average velocities for this case are shown in Figures (18a) and (18b).
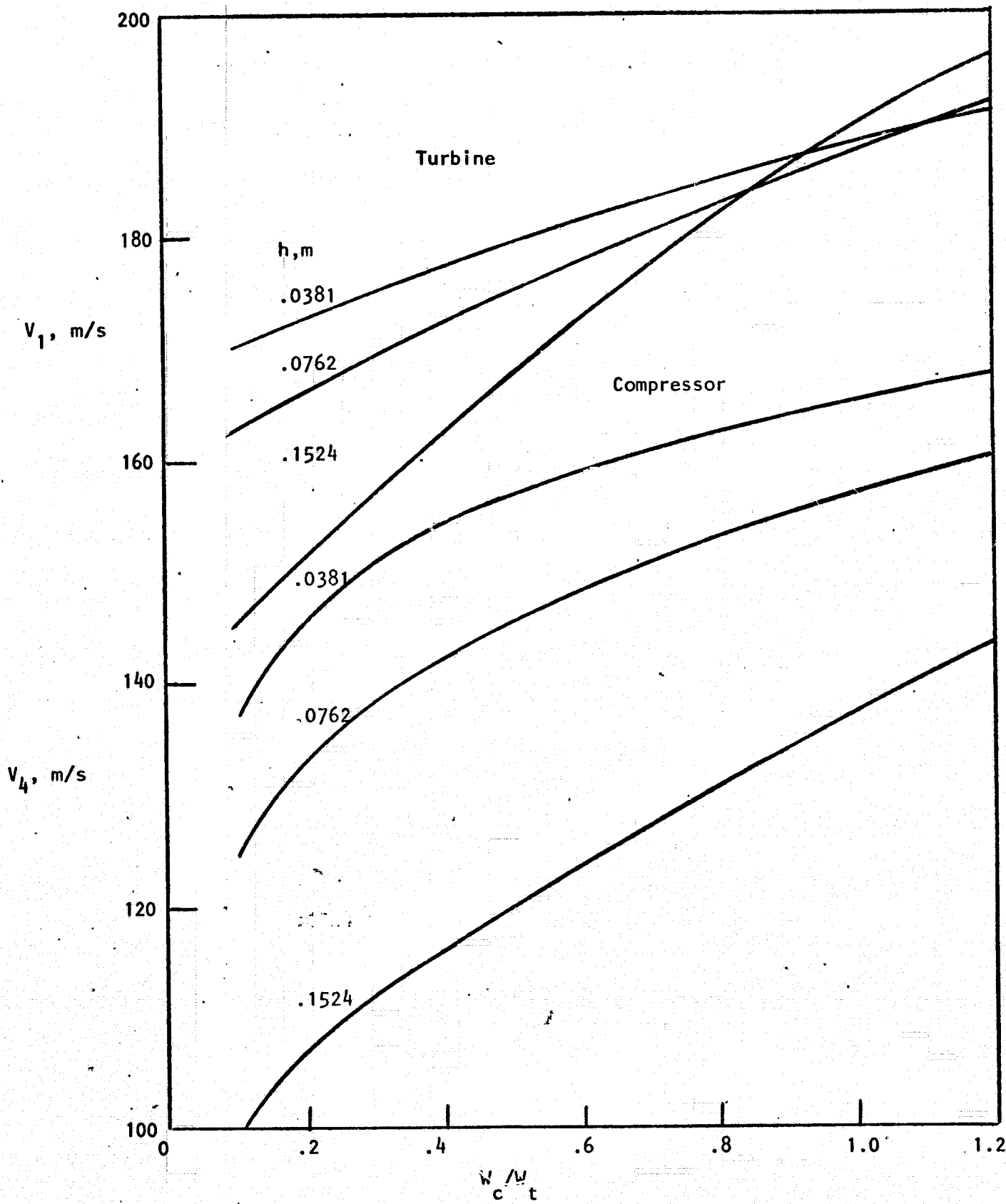
FIGURE 17a. AVERAGE VELOCITIES WITH COMPRESSOR HANDLING INNER FLOW OF
BOUNDARY LAYER; $M_j = 0.2$
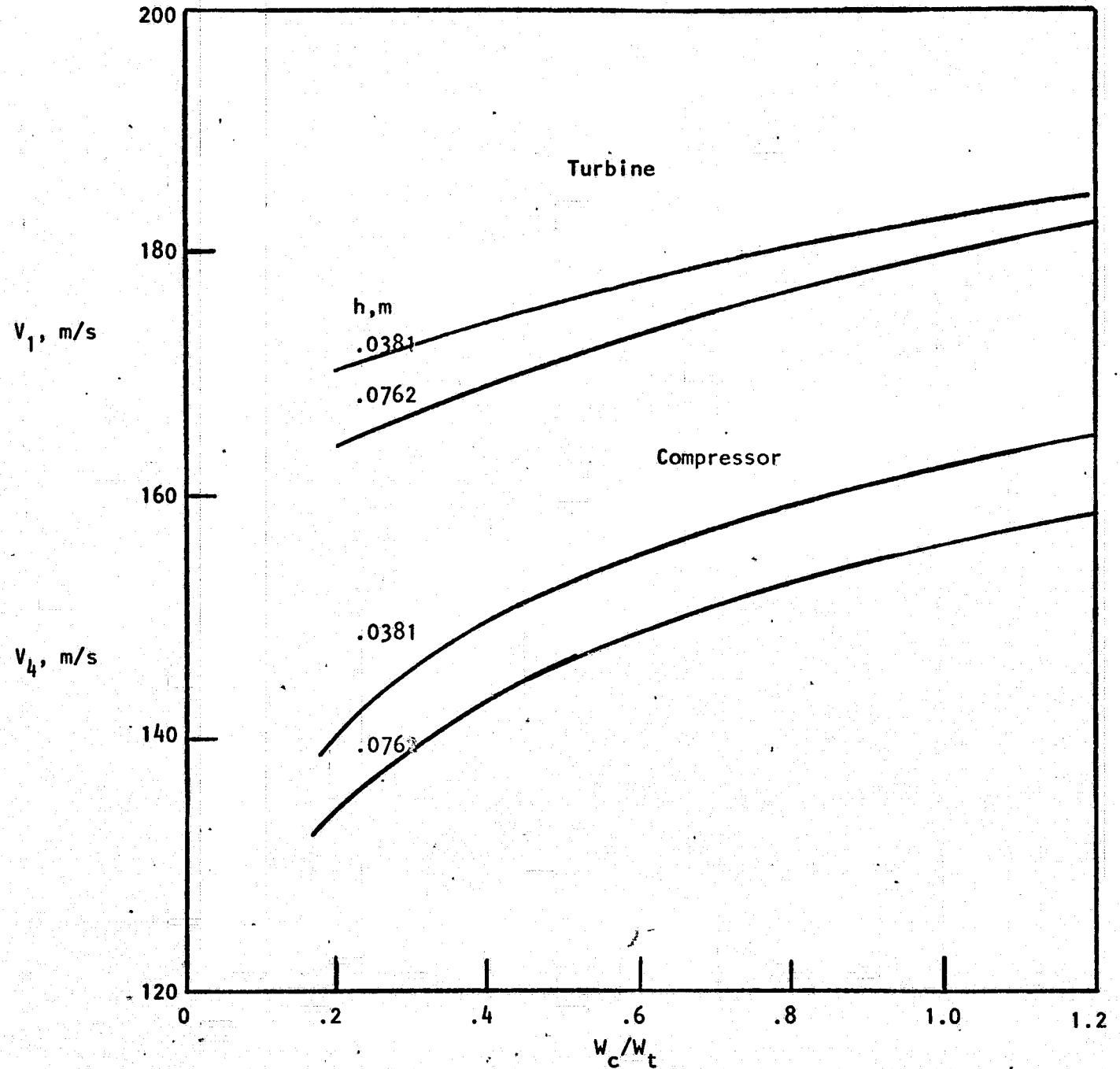
FIGURE 17b. AVERAGE VELOCITIES WITH COMPRESSOR HANDLING INNER FLOW; $M_j = 0.1$
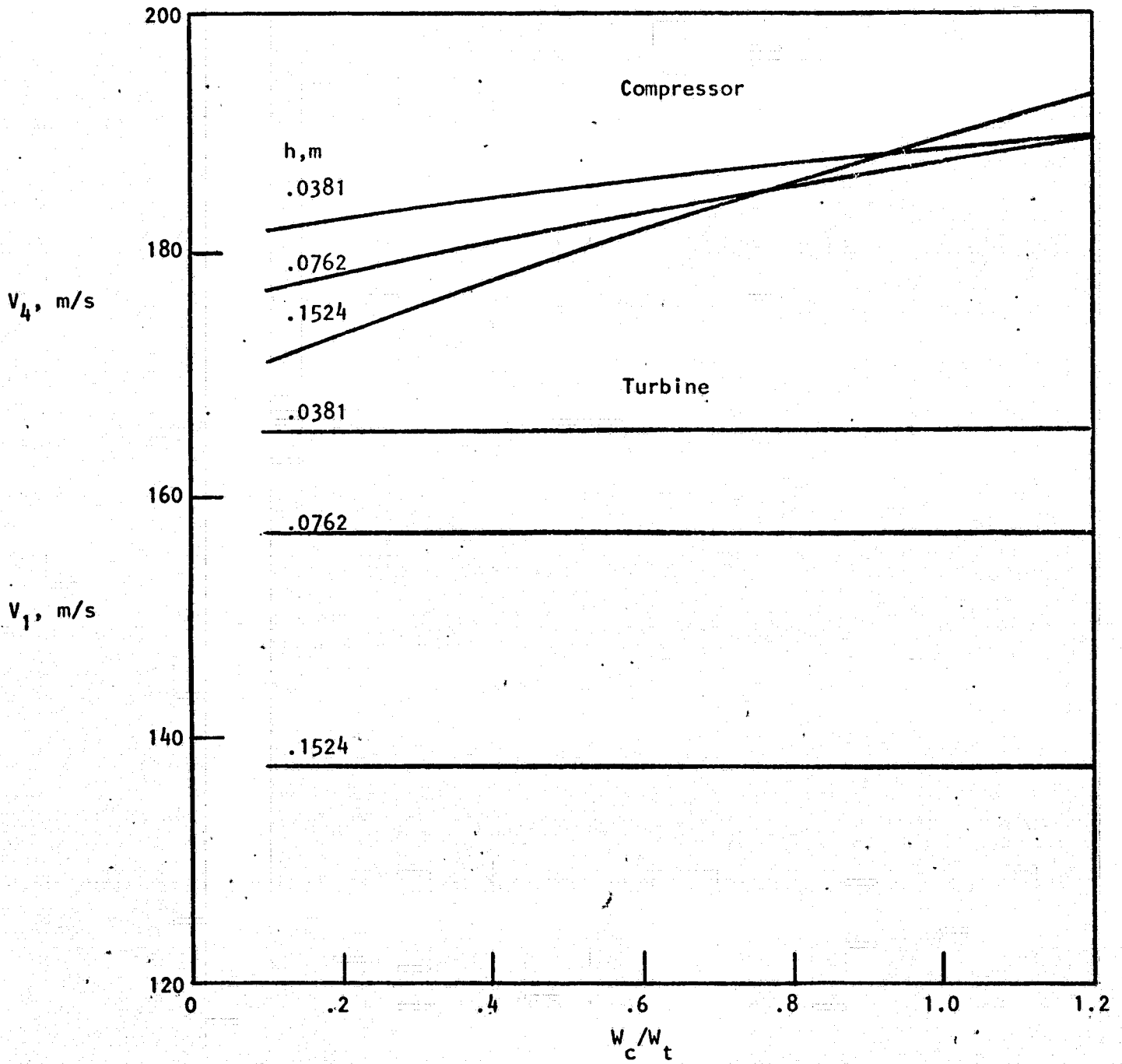
FIGURE 18a.   AVERAGE VELOCITIES WITH TURBINE HANDLING 'INNER' FLOW OF
BOUNDARY LAYER; M_j = 0.2

37
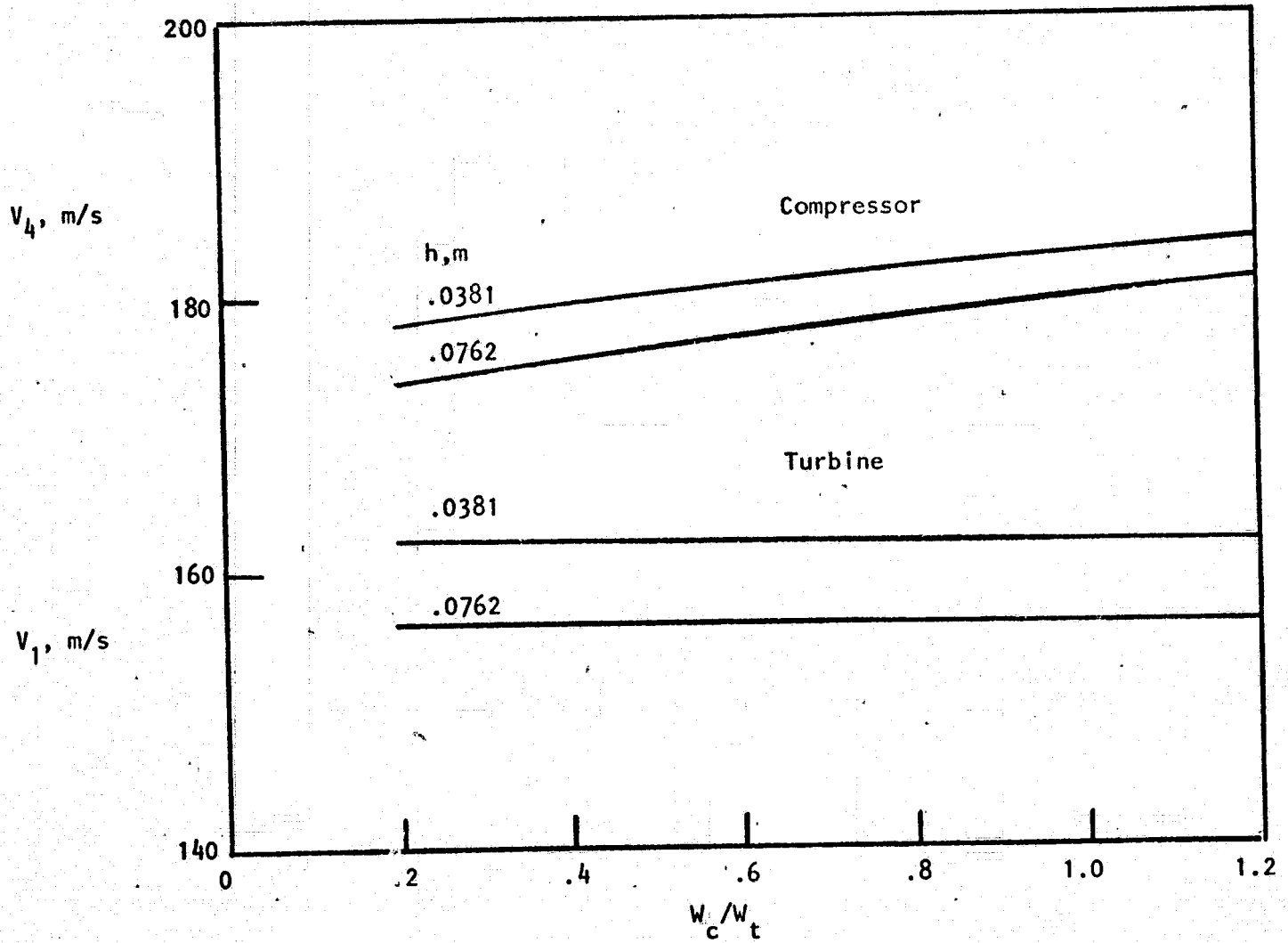
FIGURE 18b.   AVERAGE VELOCITIES WITH TURBINE HANDLING INNER FLOW;
             $M_j = 0.1$

Consider now an airplane with a baseline total drag D_o and fuselage friction drag D_{F_o}. With injection, the fuselage drag becomes

$$D_F = X \, D_{F_o}$$

where X is a factor representing the effect of injection on skin friction.

The net drag of the airplane with the injection system, including the reduction in skin friction, the drag due to the turbine and the thrust due to the compressor, is given by.

$$D = D_o - (1 - X) \, D_{F_o} + W_j I$$

The injection flow produces a reduced skin friction drag, defined by the factor C_F/C_{F_i}, over the portion of the fuselage influenced by the slots. The value of X is not exactly the same as C_F/C_{F_i} because injection starts at some distance from the nose of the fuselage so that there is a small portion of the fuselage where the drag remains unchanged. In this region assume that the friction coefficient varies inversely with distance to the 1/5 power and that the wetted area is proportional to the length. Then the value of X is given by

$$X = C_F/C_{F_i} + (1 - C_F/C_{F_i}) \, (L_i/L_o)^{.8}$$

where

        L_i distance to first slot

        L_o length of fuselage.

Application of these results to the baseline configuration is made assuming the slots to extend completely around the periphery of the fuselage. For the cases which were examined the flow rates W_j are

No. of Slots	M_j	h, m	W_j, kg/s
10	0.2	.0381	156
10	0.2	.0762	312
10	0.2	.1524	624
10	0.1	.0381	78
10	0.1	.0762	156
5	0.1	.0381	39
5	0.1	.0762	78

The results, which are presented as curves of D/D_o (net drag with injection/drag without injection) vs. W_c/W_t (compressor flow/turbine or injection flow) for various values of k_1 (line loss factor of injection flow), are based on turbine and compressor efficiencies equal to 0.9. This would tend to give results which are slightly optimistic. In the same spirit, the line loss factor of the compressor flow was taken to be unity.

Results for the largest slot height considered (h = 15.24 cm) are given in Figures (19a) and (19b) for the compressor handling the "inner" and "outer" flows, respectively. Note that the figure includes a line representing the effect of injection on skin friction only, given by

$$D = D_o - (1 - X) D_{F_o}$$

In addition, a line representing results without the turbine/compressor effect is included. This is given by

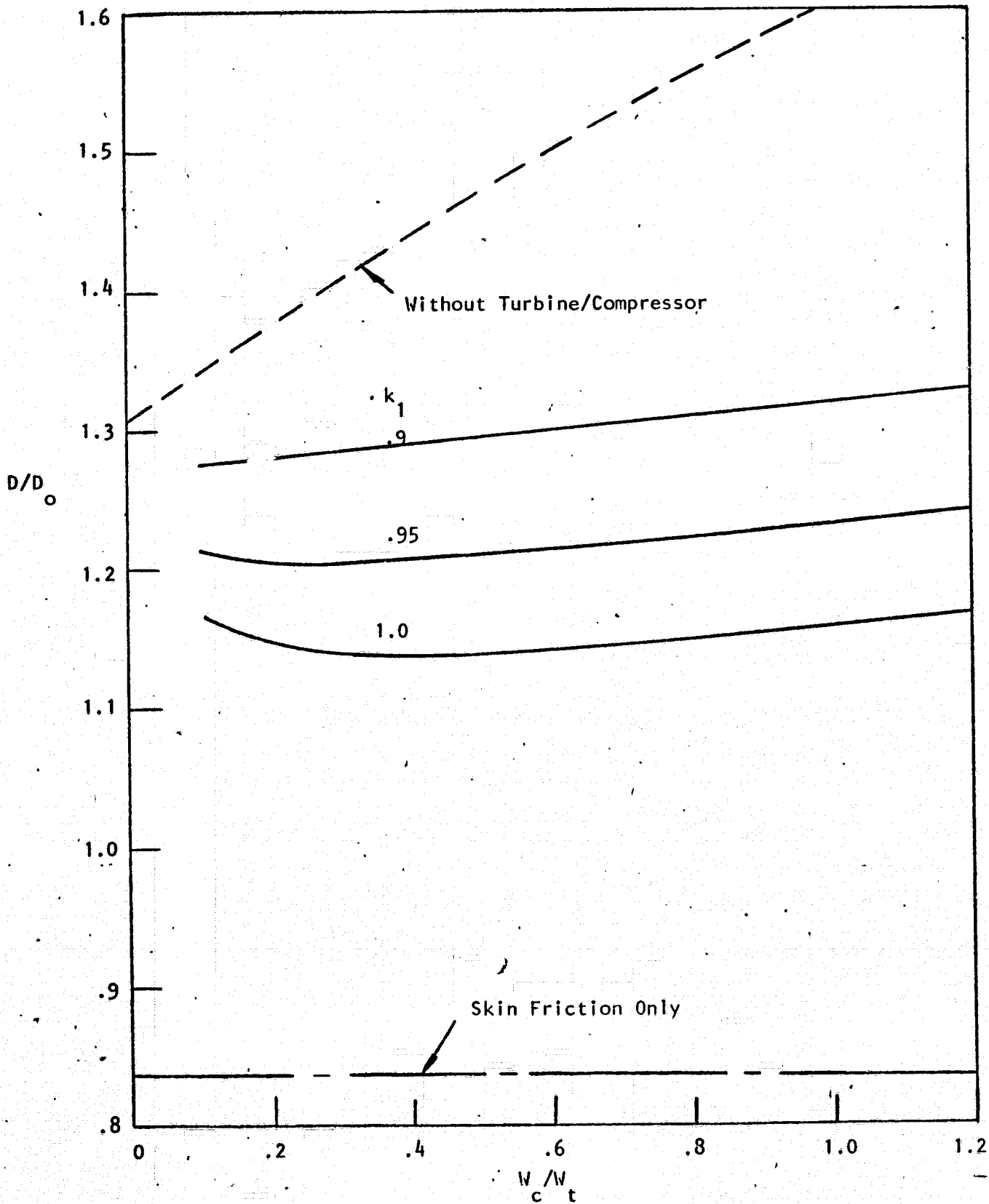$$D = D_o - (1 - X) D_{F_o} + W_j (V_1 - V_2)$$

FIGURE 19a. NET DRAG WITH SLOT INJECTION, COMPRESSOR HANDLING INNER FLOW; h = 15.24 cm, M_j = 0.2

41

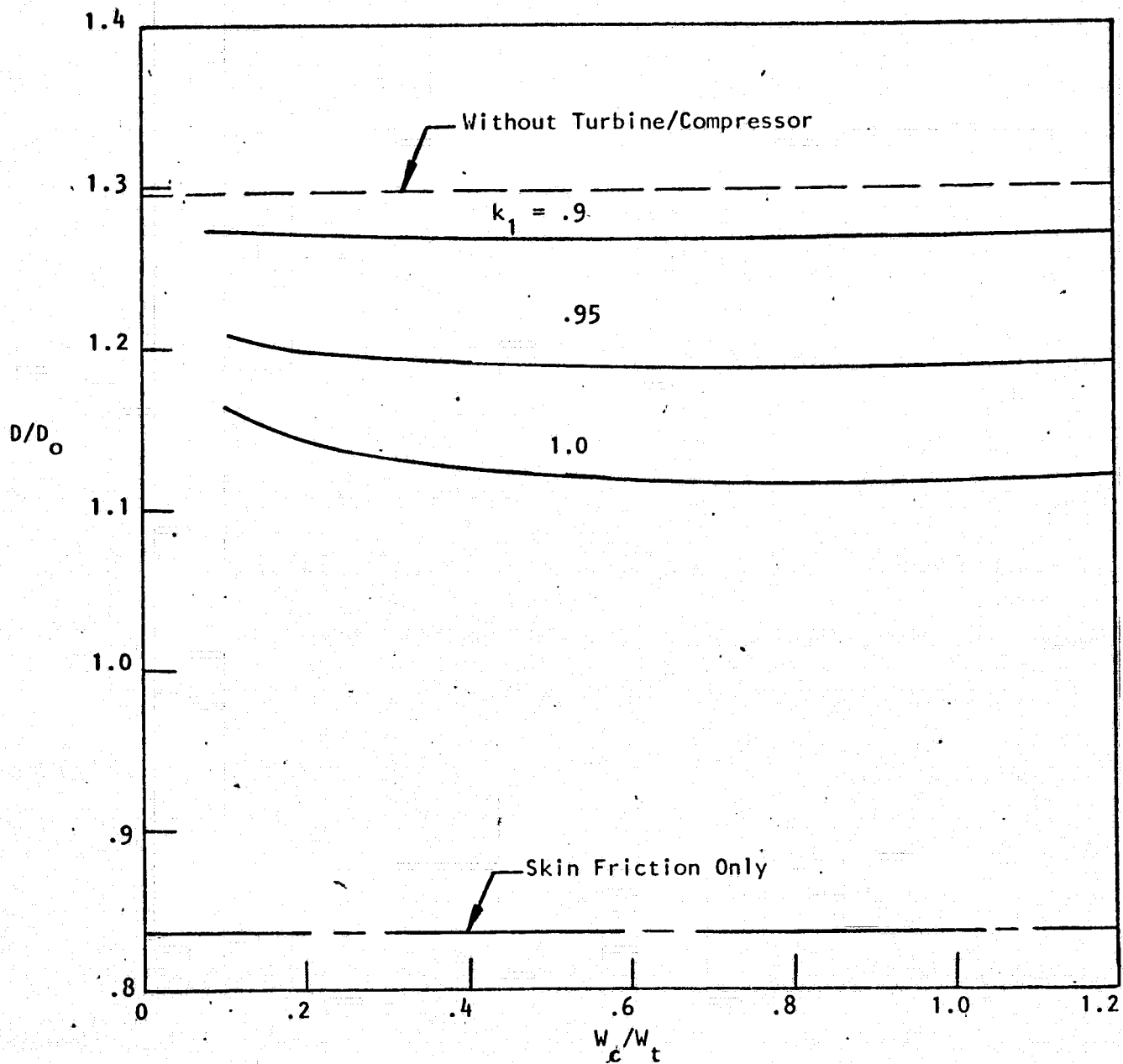FIGURE 19b. NET DRAG WITH SLOT INJECTION, TURBINE HANDLING INNER
FLOW; h = 15.24 cm, M_j = 0.2

It is apparent that the turbine/compressor is quite effective in reducing net drag although not to an extent sufficient to produce a positive result (D/D_o less than unity). Comparison of the results given in Figures (19a) and (19b) also indicates that slightly better results can be achieved with the turbine processing the lower momentum "inner" flow and that in neither case is the compressor flow of critical importance. These trends prevailed for all of the configurations examined.

Additional results for the smaller slot heights are presented in Figures (20) and (21). Furthermore, to demonstrate the basic soundness of the concept of having the turbo-machines process boundary layer flow, some calculations were made with the machines handling free stream flow ($V_1 = V_4 = V_\infty$). The comparison shown in Figure (22) demonstrates the potential benefits.

Comparison of the results shown in Figures (20) and (21) with those presented in Figure (19) indicates that the smallest slot height, despite its inferiority in terms of reducing viscous drag, gives the best net performance. This is, of course, a reflection of the large penalty in momentum drag which increases directly with total injector flow rate and, therefore, with slot height and/or injection Mach number. It should be noted also that the effect of the loss factor k_1 is greatest for the largest slot height and decreases systematically with decreasing height. This is, again, an indication of the large penalty in drag associated with increased flow rates.

As can be seen in Figure (21), even for a loss-free system ($k_1 = 1$), net drag reduction is not attainable with $M_j = 0.2$. Accordingly, additional calculations at a lower jet Mach number ($M_j = 0.1$) were carried out for the small and intermediate slot heights. These results are presented in Figures (23) and (24). Again, even with the decreased effectiveness of slot injection in reducing wall shear (c.f. Figure 13) some improvement in overall performance is attained due to the lower mass flow rates involved.

Although the results shown in Figures (23) and (24) indicate some net drag reduction the actual values are quite small amounting to only 1 or 2% for realistic values of line loss factors. Further reduction in jet Mach
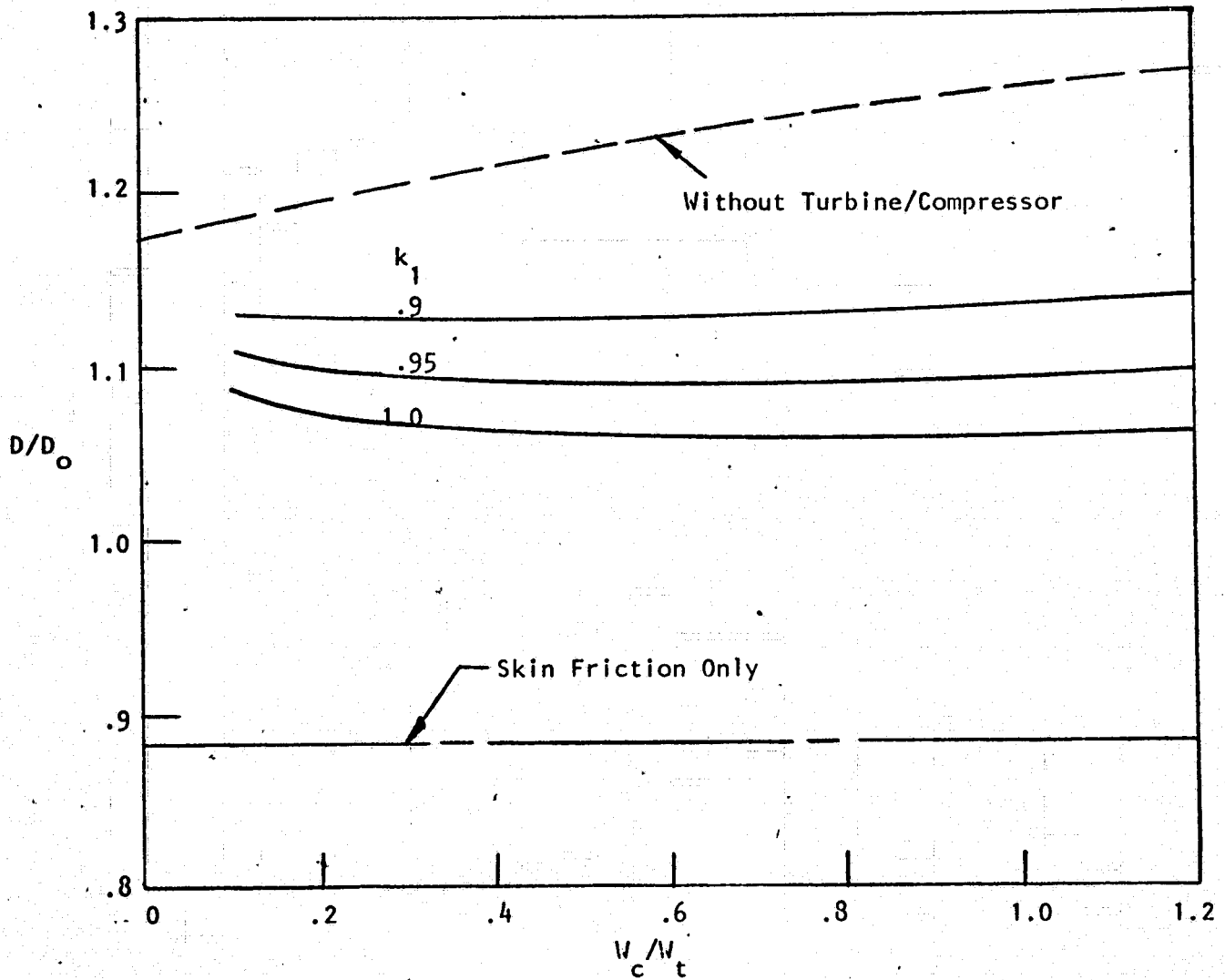
FIGURE 20a. NET DRAG WITH SLOT INJECTION, COMPRESSOR HANDLING
'INNER FLOW; h = 7.62 cm, M_j = 0.2
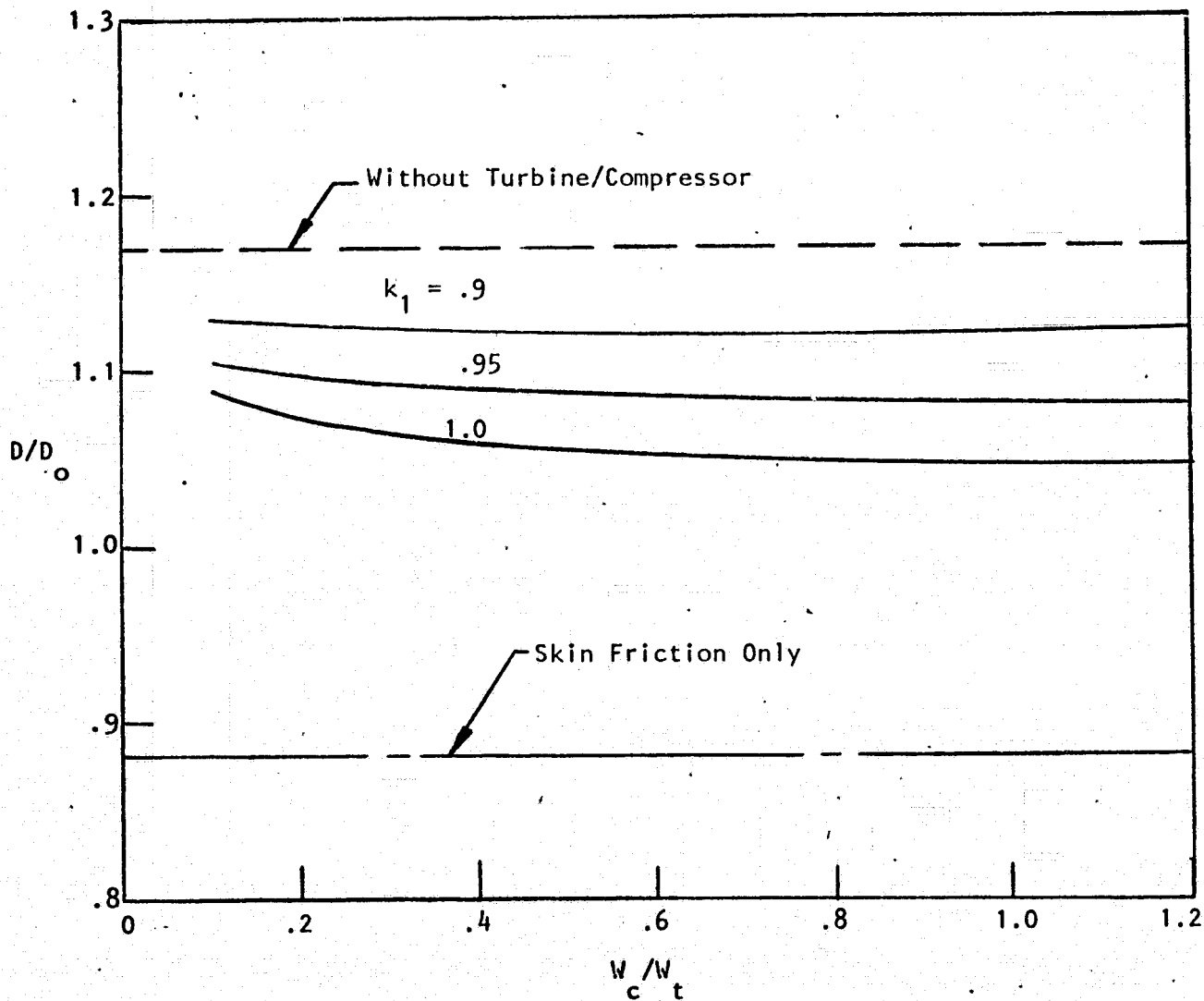
FIGURE 20b. NET DRAG WITH SLOT INJECTION, TURBINE HANDLING   INNER
FLOW; h = 7.62 cm, M_j = 0.2

45

FIGURE 21a. NET DRAG WITH SLOT INJECTION, COMPRESSOR HANDLING INNER FLOW; h = 3.81 cm, M_j = 0.2

FIGURE 21b. NET DRAG WITH SLOT INJECTION, TURBINE HANDLING INNER
FLOW; h = 3.81 cm, M_j = 0.2

FIGURE 22. COMPARISON OF NET DRAG WITH TURBINE/COMPRESSOR USING FREE STREAM FLOW AND BOUNDARY LAYER FLOW; $M_j = 0.2$

48
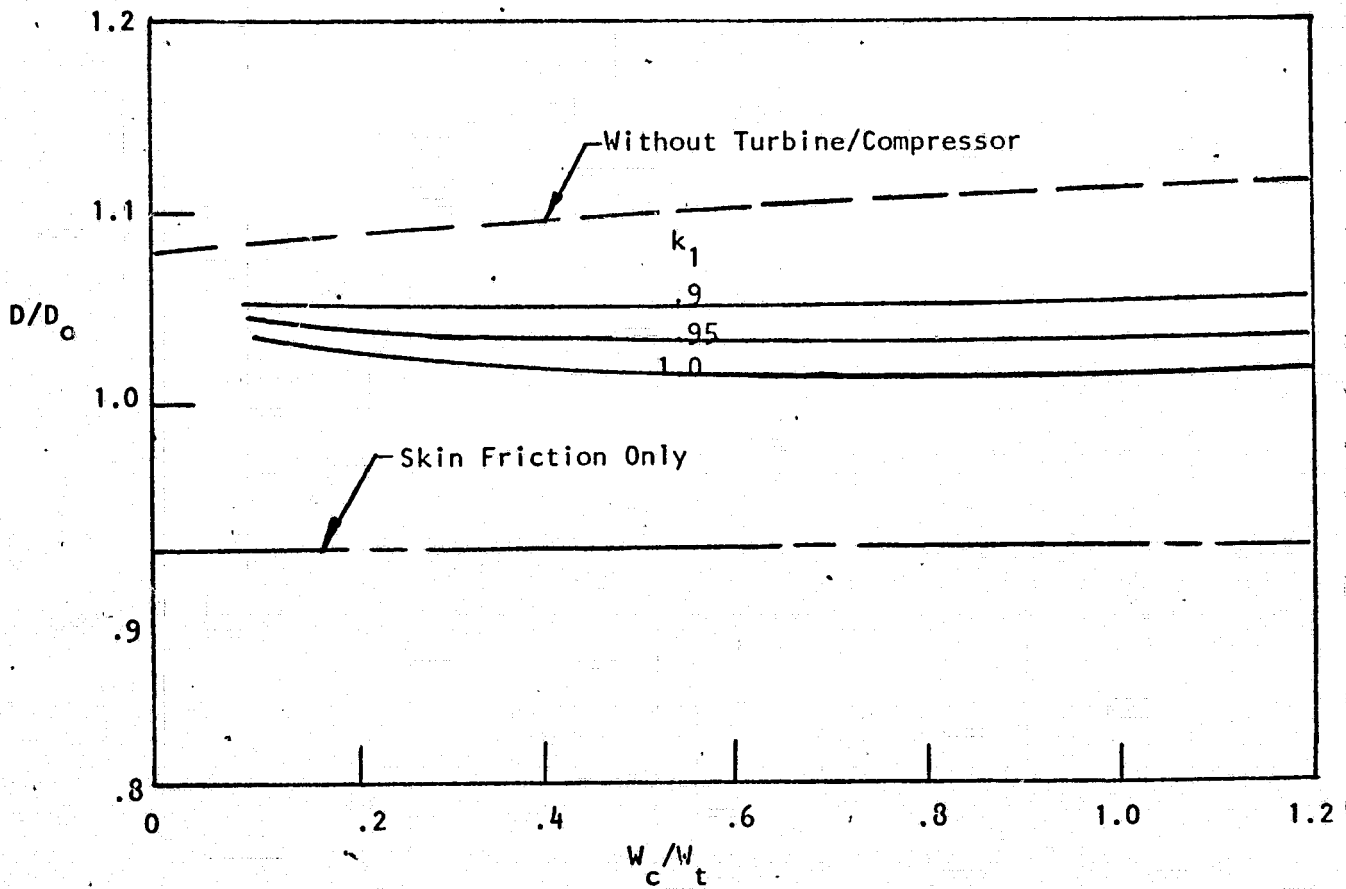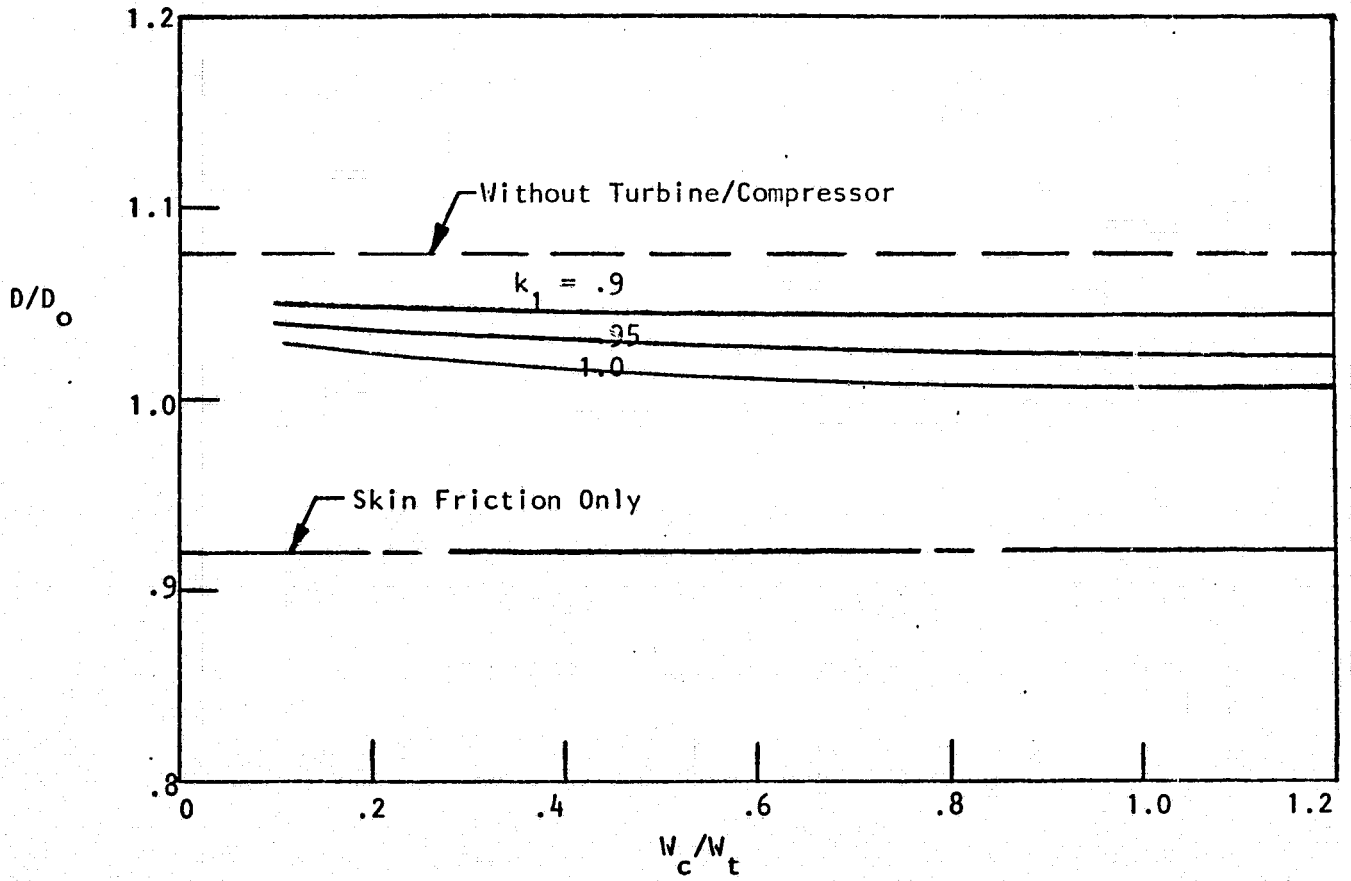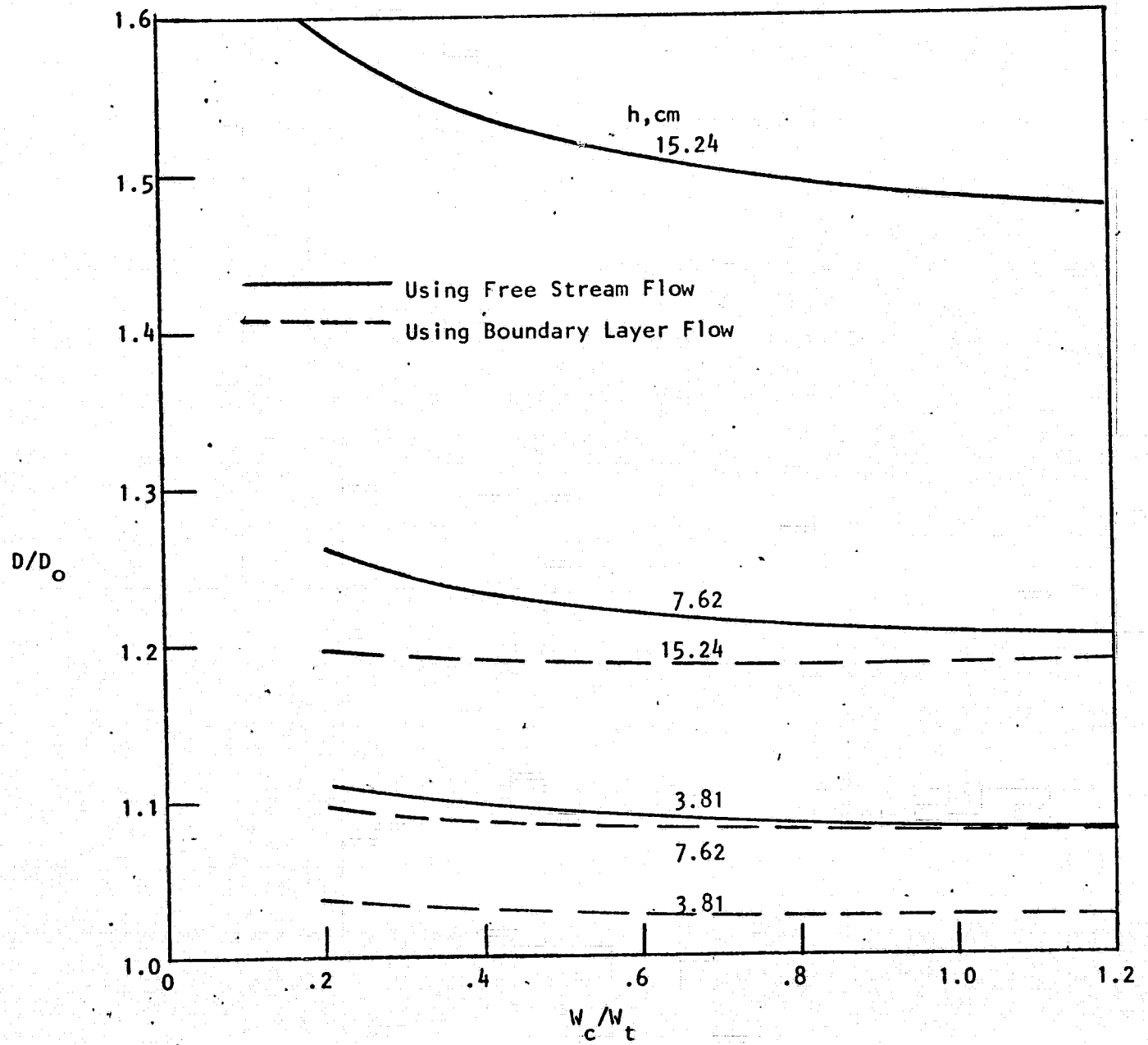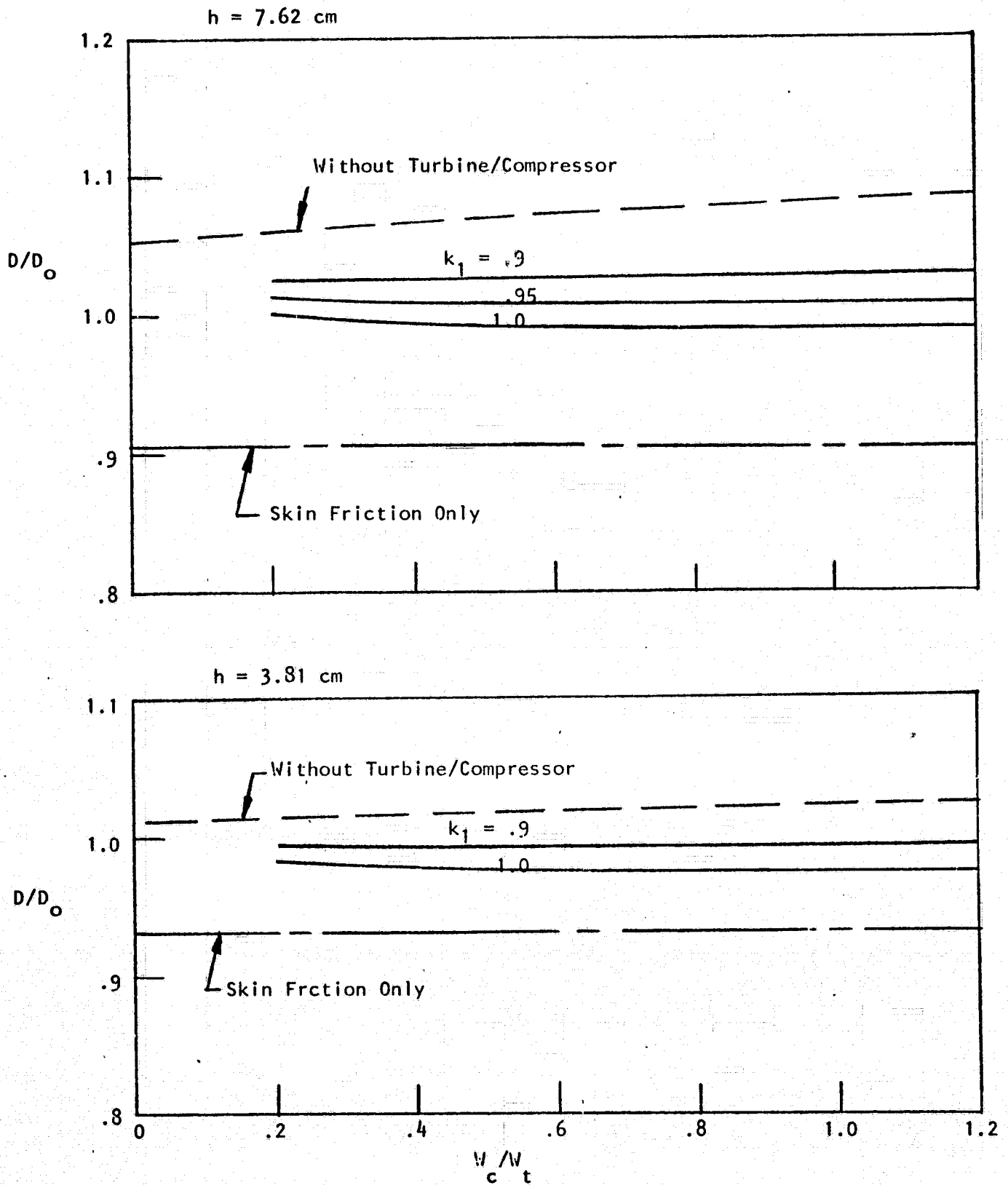
FIGURE 23. NET DRAG WITH COMPRESSOR HANDLING INNER FLOW; $M_j = 0.1$
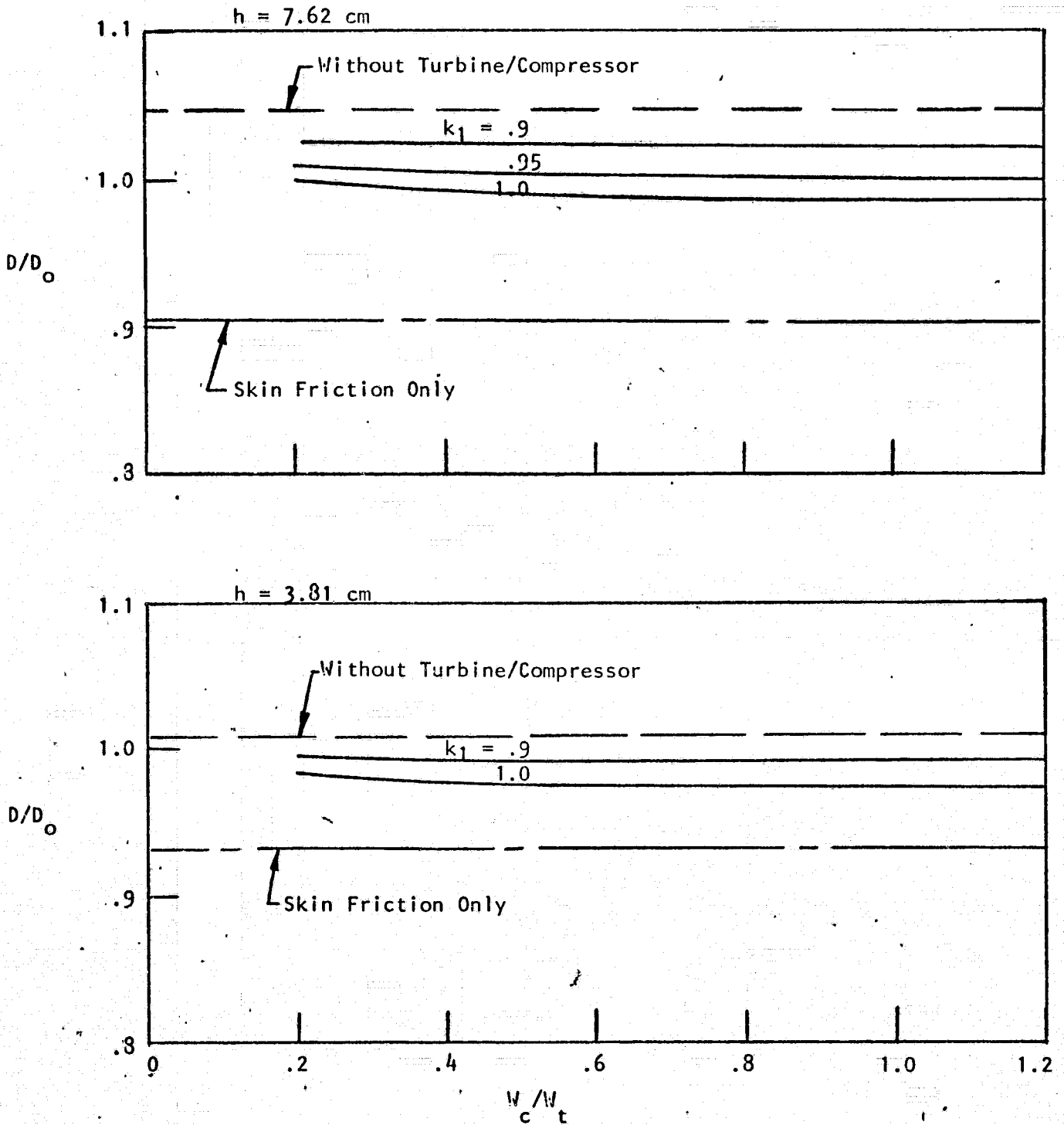
FIGURE 24.   NET DRAG WITH TURBINE HANDLING INNER FLOW; M_j = 0.1

number, or injector flow rate in general, is not likely to provide signifi-
cant improvement since the wall shear ratio would approach unity. This ef-
fect is demonstrated in Figure (25) in which the curve of D/D_o versus M_j
goes through unity at $M_j \rightarrow 0$.

In summary, these results indicate that the baseline design, which makes
exclusive use of multiple slot injection and captures the required mass for
injection downstream of the last slot, will provide, at best, marginal drag
reduction. It appears that alternate schemes are needed, possibly combining
slot injection with other drag reduction methods, to provide significant
improvement in performance. Several alternate schemes are examined in the
subsequent sections; however the considered schemes do not encompass all pos-
siblities by any means.

B. Combined Fuselage Suction and Slot Injection - This scheme consists
of a passive system requiring no pumping or turbo-machinery. The system
depends for its operation on the pressure difference which exists between
the upper and lower surfaces of the fuselage at a small angle of attack. The
high pressure lower surface is composed of a porous or slotted surface through
which suction takes place. The flow is ducted to the top surface of the fuse-
lage where it is discharged by slot injection. The physical arrangement
would consist of a series of 10 suction surfaces encompassing the lower half
of the fuselage, each of 6.1 m length. At the end of each section, the suc-
tion flow is collected and discharged through a slot on the top of the fuse-
lage, thus comprising a system of 10 slots at 6.1 m intervals.

As indicated in Figure (5) suction at an excessive rate can produce an
increase in skin friction rather than a decrease. The largest drag reduc-
tion is obtained with the "optimum rate" corresponding to the stability
limit for sustaining a laminar boundary layer.

The injection at low velocity on the top of the fuselage produces a re-
duction in skin friction. With the flow fixed by the suction requirement,
the question arises about the best way to distribute the flow on the top of
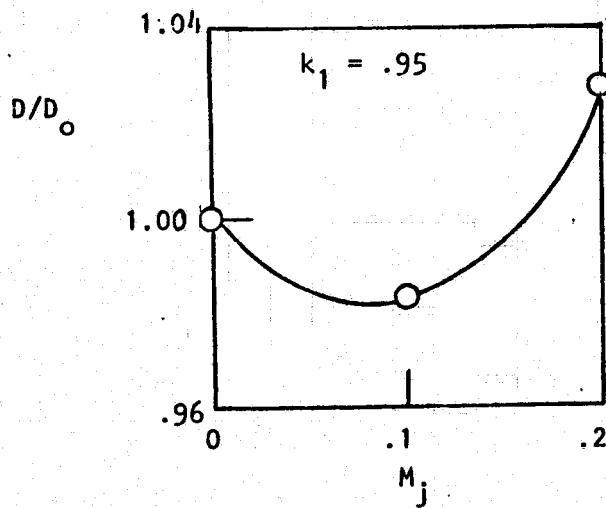
FIGURE 25.   EFFECT OF INJECTION MACH NUMBER ON NET DRAG;
h = 3.81 cm

the fuselage. The same flow may be injected with a larger slot height by limiting the peripheral extent of the slot. The skin friction reduction increases as slot height increases, but the extent of surface affected by injection decreases. The best slot height is the one which gives the greatest net gain from the two opposing effects.

The following simple analysis shows that the best slot height is the smallest slot height; that is, the flow should be distributed over the largest possible lateral extent of surface area. For a given injection flow, W, the slot height h and the slot lateral extent b are related by

$$W = \rho_j \, V_j \, hb$$

For the length of the slot coverage L, the area of surface affected by injection is bL. The friction drag on this surface is given by

$$D_F = (C_F/C_{F_i}) \, C_{F_i} \, q_\infty \, bL$$

where C_F/C_{F_i} is the reduced skin friction factor due to injection.

The drag reduction is then given by

$$\Delta D_F = (1 - C_F/C_{F_i}) \, C_{F_i} \, q_\infty \, bL$$

which may also be written

$$\Delta D_F = \frac{(1 - C_F/C_{F_i}) \, C_{F_i} \, q_\infty \, LW}{\rho_j \, V_j \, h}$$

Since C_{F_i}, q_∞, L, W, ρ_j and V_j are all constant, the drag reduction is written

$$\Delta D_F = \text{constant} \, \frac{(1 - C_F/C_{F_i})}{h}$$

It is apparent that the maximum drag reduction is obtained when the value of $(1 - C_F/C_{F_i})/h$ is a maximum. The data in Figure (13) are converted to this

expression with results presented in Figure (26) showing that the largest drag reduction corresponds to the smallest slot height.

The suction surfaces are arranged in 10 sections of 6.1 m length on the bottom half of the fuselage. At the end of each section, the suction flow is collected and ducted around the fuselage along which it is injected in a slot encompassing the top half of the fuselage. Thus, the slot injection consists of 10 slots at 6.1 m intervals. This arrangement does not present serious difficulties with regard to internal ducting, especially in view of the low flow rates characteristic of suction requirements. It is estimated that with a 1/2 inch gap around the bottom of the fuselage, the suction flow of each 6.1 m section can be handled with a pressure drop of one-half of one percent. Including the ducting loss and the required velocity head for injecting the flow through the slot on the upper half of the fuselage, the total pressure drop will be around 4 or 5 percent. Such a pressure differential between the lower and upper part of the fuselage can be obtained with a small angle of attack.

The flow through the suction surface is

$$W = C_s \, \rho_\infty \, V_\infty \, \frac{\pi d}{2} \, L$$

and the flow through the injection slot is

$$W = \lambda \, \rho_\infty \, V_\infty \, \frac{\pi d}{2} \, h$$

Hence, the slot height is given by

$$h = C_s L$$

The value of C_s determines the skin friction reduction factor due to suction $(C_F/C_{F_i})_s$ and the value of h determines the skin friction reduction factor due to injection $(C_F/C_{F_i})_j$. It should be noted that in order to determine $(C_F/C_{F_i})_s$, it is necessary to fix a Reynolds number. The value used in the
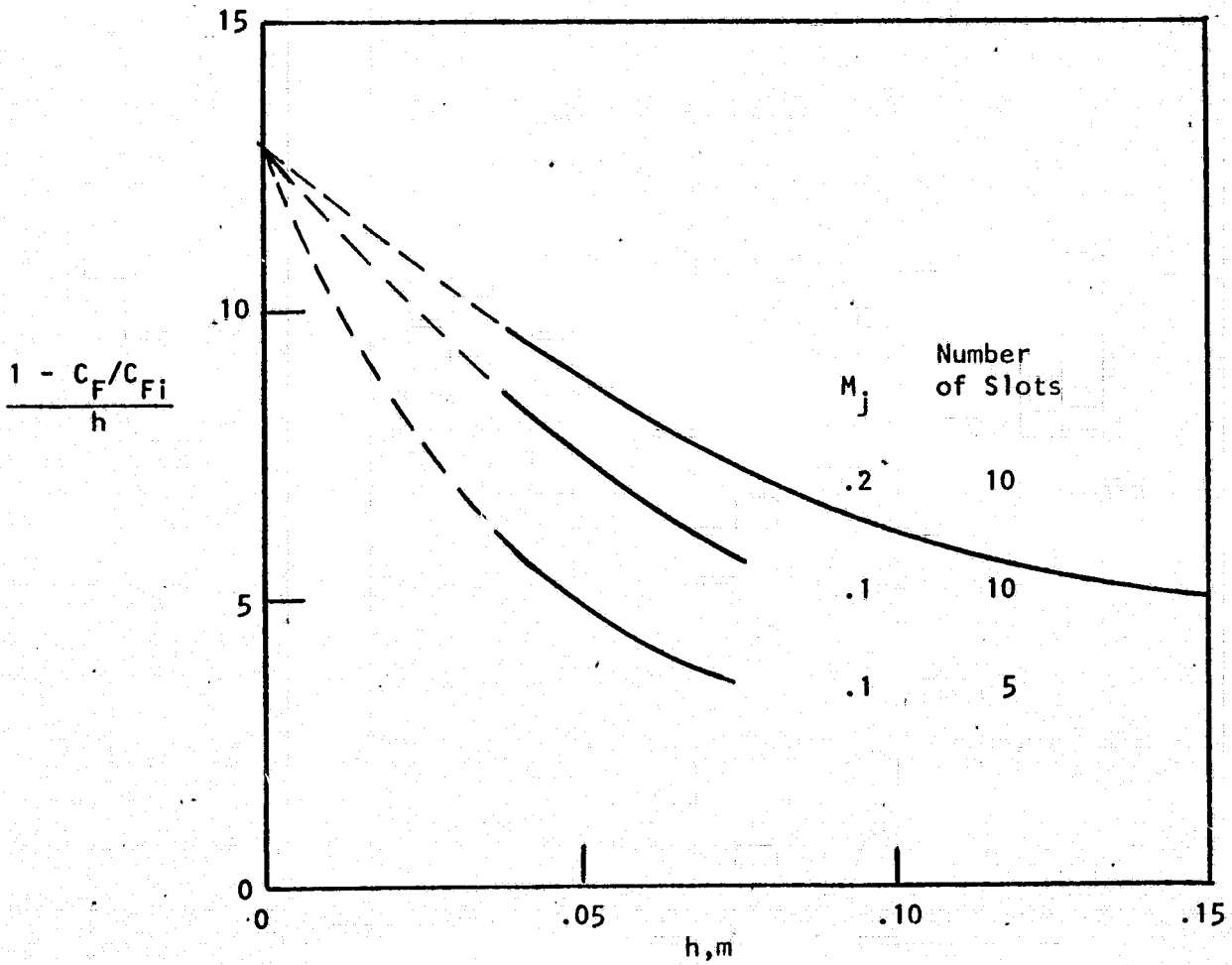
FIGURE 26. PARAMETER DESCRIBING DRAG REDUCTION AS A FUNCTION OF SLOT HEIGHT

55

present application is 10^8, roughly corresponding to the average fuselage length.

The drag reduction due to suction is given by

$$\Delta D_s = (1 - (C_F/C_{F_i})_s) \ C_{F_i} \ q_\infty \ \frac{\pi d}{2} \ L$$

and that due to injection is

$$\Delta D_j = (1 - (C_F/C_{F_i})_j) \ C_{F_i} \ q_\infty \ \frac{\pi d}{2} \ L$$

the drag increase due to the momentum change of the flow is given by

$$\Delta D_m = W \ (V_\infty - V_j)$$

which in terms of the suction flow coefficient is written

$$\Delta D_m = 2C_s \ q_\infty \ \frac{\pi d}{2} \ L \ (1 - V_j/V_\infty)$$

If it is assumed that the injection density is the same as the free stream density (which is very nearly true) then the velocity ratio is the same as the injection flow parameter

$$V_j/V_\infty = \lambda$$

The net drag reduction is given by

$$\Delta D = \Delta D_s + \Delta D_j - \Delta D_m$$

The original skin friction drag without suction or injection, determined by both the upper and lower halves of the fuselage is given by

$$D_{F_i} = C_{F_i} \ q_\infty \ \pi d L$$

Hence,

$$\frac{\Delta D}{D_{F_i}} = \frac{1 - (C_F/C_{F_i})_s}{2} + \frac{1 - (C_F/C_{F_i})_j}{2} - \frac{C_s}{C_{F_i}} \ (1 - \lambda)$$

56

The values of Δ/D_{F_i} determined as a function of the suction flow coefficient C_s are shown in Figure (27), calculated with $C_{F_i} = .00175$ and $\lambda = .244.$ * The figure shows the contribution of each of the three components of drag, indicating that suction contributes the largest part of the drag reduction.

In order to evaluate the effect of drag reduction on airplane performance, it is necessary to establish the drag reduction with respect to the overall drag. In the application treated earlier, the overall drag was established as equal to four times the fuselage drag or $D_o = 4 \times D_{F_o}$. This relationship will also be used here. However, in order to do so, it is necessary to establish the realtionship between D_{F_o} and D_{F_i}.

As in the earlier application, it is assumed that there is an initial fuselage length of 6.1 m which is not treated by suction or injection. The drag D_{F_i} excludes this length since it represents the original drag on that portion of the fuselage treated with suction or injection. Adopting the same assumptions used before (turbulent skin friction coefficient varying inversely with distance to a .2 power and surface area varying directly with distance), the relationship between D_{F_i} and D_{F_o} is determined as

$$\frac{D_{F_i}}{D_{F_o}} = 1 - \left(\frac{L_i}{L_o}\right)^{.8}$$

With $L_i = 6.1$ m and $L_o = 67$ m,

$$\frac{D_{F_i}}{D_{F_o}} = .853$$

The net drag is found from

---

*This corresponds to slot injection at $M_j = 0.2$. All performance estimates for this scheme are made using (C_F/C_{F_i}) values corresponding to $M_j = 0.2$ since this provides greater reduction in wall shear than the $M_j = 0.1$ case.
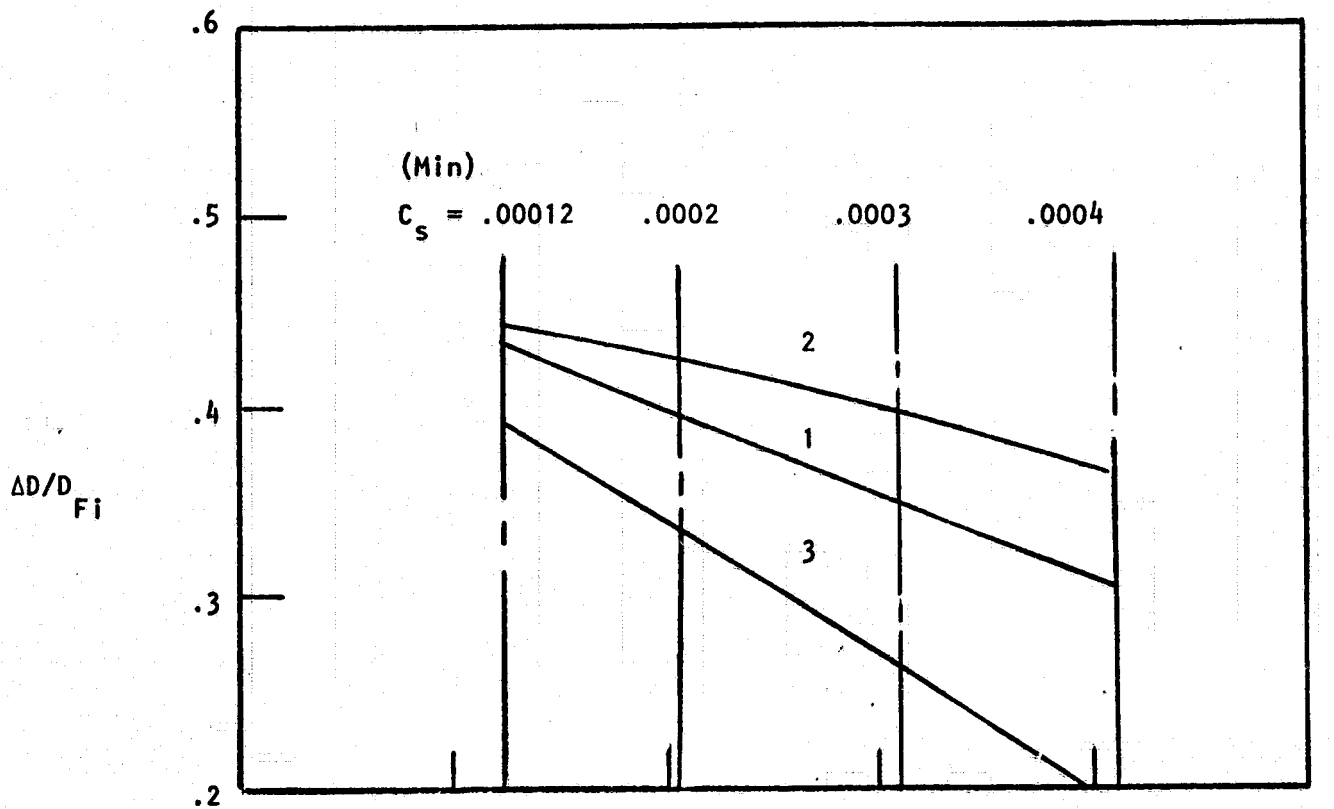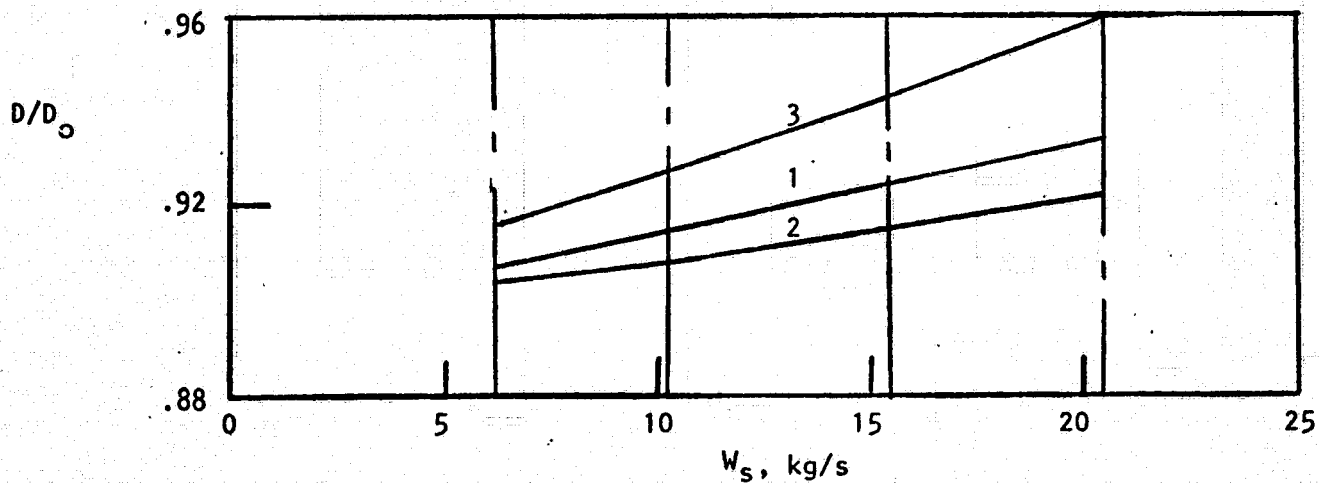
FIGURE 27. REDUCED DRAG WITH COMBINED SUCTION AND INJECTION

58

$$\frac{D}{D_o} = 1 - \frac{\Delta D}{D_{F_i}} \frac{D_{F_i}}{D_{F_o}} \frac{D_{F_o}}{D_o} = 1 - .213 \frac{\Delta D}{D_{F_i}}$$

with results as shown in Figure (27).

It is apparent that the greatest net drag reduction is obtained with the minimum suction flow. The injection slot height corresponding to this condition is extremely small, approximately one-tenth of an inch. It is possible that a practical installation would require a larger slot height, obtainable by restricting the lateral extent of the slot. In this case, the contribution to drag reduction would be less than for the fully extended slot. However, the slot injection contributes a minor part of the net drag reduction so that a larger slot height would not seriously affect the net reduction.

Figure (27) shows that the minimum reduced drag ratio corresponding to the minimum suction flow is around .91 (9% drag reduction). The interpretation of this ratio in terms of mission performance (range increase with the same fuel load or fuel load decrease with the same range) is presented in a later section.

C. Fuselage Suction - The scheme of combined suction and injection indicated that the contribution of injection to the net drag reduction is very small. The real advantage of the injection is that it takes place in a low pressure region on the top half of the fuselage, thus providing a means of discharging the suction flow without the need of pumping or turbo-machines. The disadvantage of the scheme is that it precludes achieving the larger drag reduction which would result if the upper part of the fuselage were also treated with suction. The use of suction over both halves of the fuselage would nearly double the reduction in skin friction and would more than offset the drag due to the pumping required.

The use of turbo-machines to perform the pumping is neatly adaptable to the scheme of suction over the entire fuselage perimeter, permitting a system which eliminates the need for complicated ducting. As illustrated in Figure

(28) the suction surface forms a shell around the pressurized fuselage surface with the annular space between the two surfaces forming a passageway which leads the suction flow to the compressor located at the aft end of the terminal fuselage taper. The turbine is located on the outside of the suction surface where it handles the free stream boundary air produced by the suction process. The turbine and compressor comprise a single wheel with turbine blades on the outside and compressor blades on the inside. The system thus consists of an extremely simple and convenient arrangement of surface, ducting and turbo-machinery.

To determine the net drag reduction of this scheme, the drag due to the turbo-machinery is accounted for by assuming intake and discharge pressures equal to free stream pressure. Then the drag of the compressor (suction flow) is given by

$$\text{compressor drag} = W_c \ (V_\infty - V_3)$$

and for the turbine

$$\text{turbine drag} = W_t \ (V_1 - V_2)$$

The value of V_1 is the average velocity (based on momentum) of the boundary layer flow ingested by the turbine. To evaluate this parameter the asymptotic velocity profile for suction is assumed to prevail at this station. According to Reference (6) (page 231) this is given by

$$V/V_\infty = 1 - \exp \ (-\xi)$$

where
$$\xi \equiv C_s \ \rho_\infty \ V_\infty \ y/\mu$$

Here y denotes distance measured normal to the wall. The suction flow coefficient is taken at the optimum value $C_s = .00012$ for this calculation.

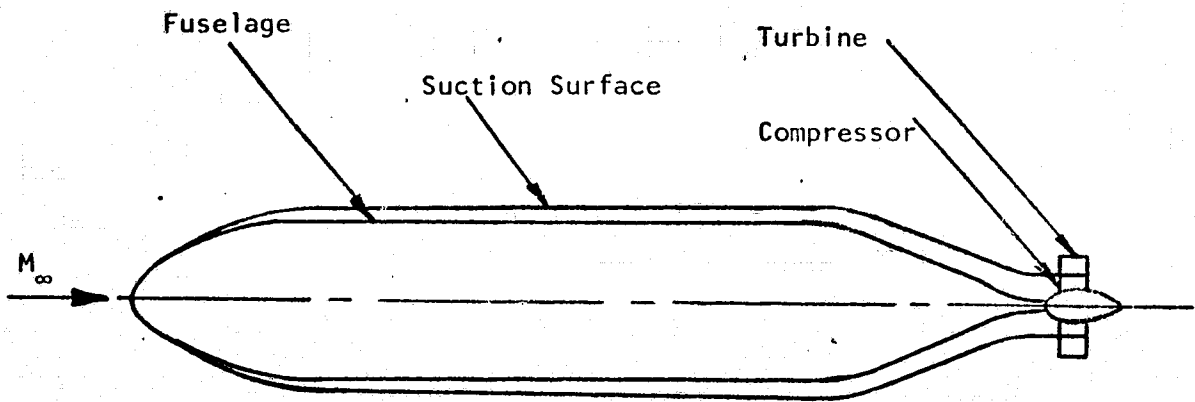From the assumed velocity profile the average velocity is given by

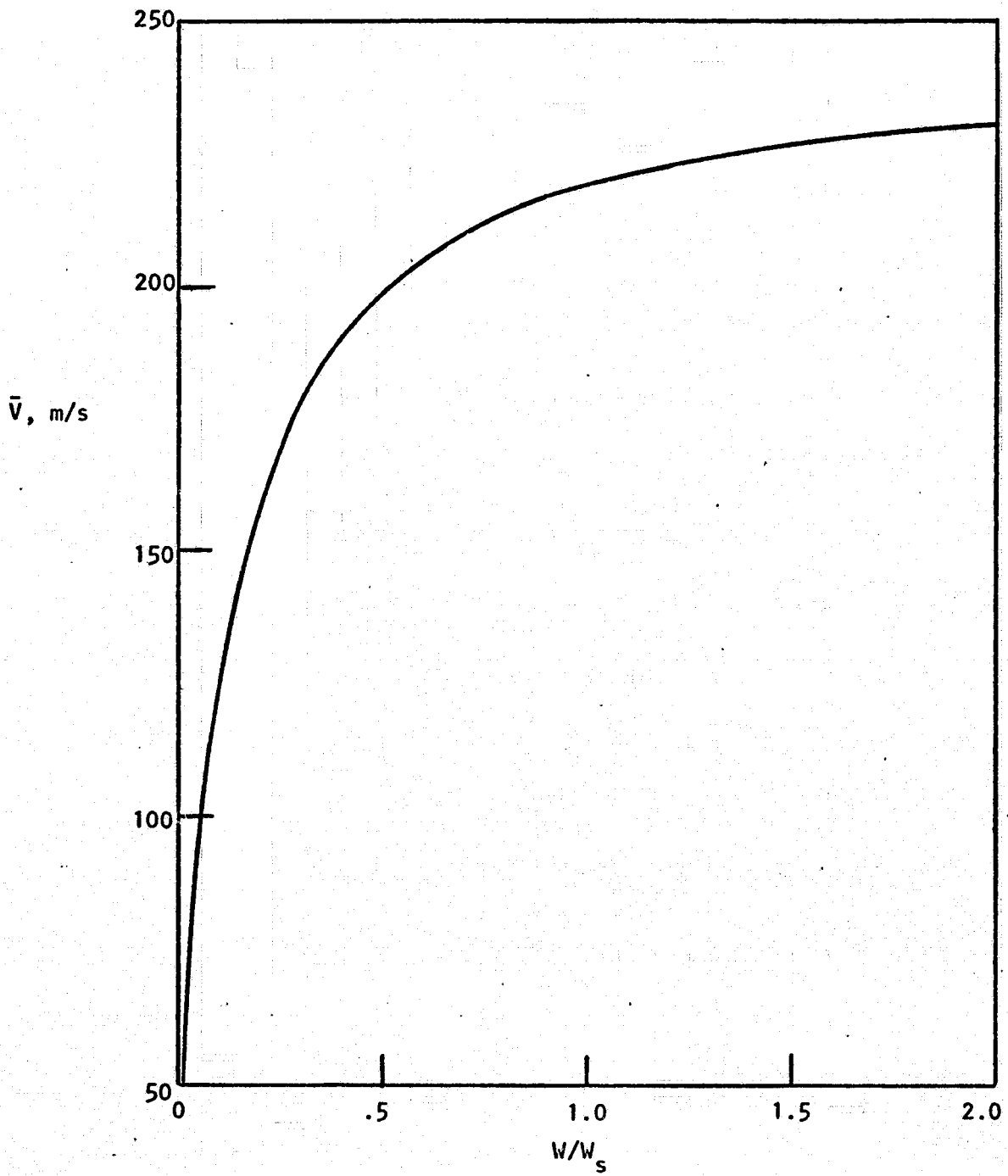FIGURE 28. SCHEMATIC OF FUSELAGE SUCTION SYSTEM WITH TURBO-MACHINES

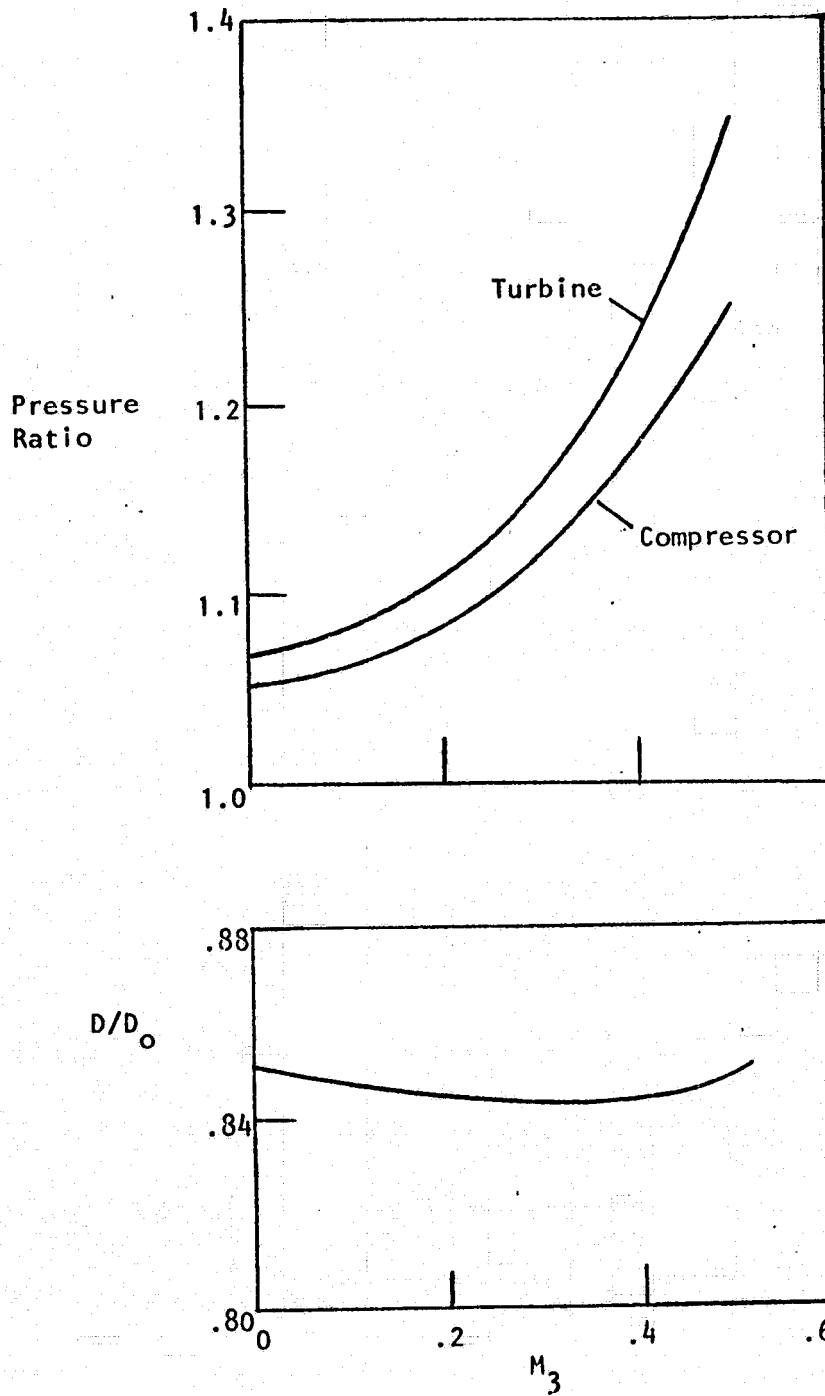FIGURE 29. AVERAGE VELOCITY IN SUCTION BOUNDARY LAYER

FIGURE 30. EFFECT OF COMPRESSOR DISCHARGE MACH NUMBER ON PRESSURE
RATIOS AND NET DRAG WITH FUSELAGE SUCTION

$$\bar{V}/V_\infty = \frac{x - 2(1 - 3^{-\xi}) + 1/2(1 - e^{-2\xi})}{\xi - 1 + e^{-\xi}}$$

The flow in the boundary layer in terms of the suction flow is given by

$$\frac{W}{W_s} = \frac{\mu}{\rho_\infty V_\infty L c_s^2} (\xi - 1 + e^{-\xi})$$

By means of these equations, the average velocity $\bar{V}$ may be found as a function of W/W_s. The results are shown in Figure (29).

In applying these data to the turbo-machine, it is considered that the suction flow W_s is the compressor flow W_c and the boundary layer flow W is the turbine flow W_t. While the compressor flow is fixed by the suction requirements, the turbine flow may be chosen at will, with the choice depending on the effect on overall performance.

The power generated by the turbine in reducing the velocity from V_1 to V_2 is absorbed by the compressor and utilized to reduce its drag by increasing the discharge velocity V_3. In calculating the exchange and utilization of power, turbine and compressor efficiencies are taken as .9 (justified by the low pressure ratio of the machines) and line loss recovery factors as .95 (justified by the small flows involved so that ducting losses can be made very small without compromising weight or space). It is also assumed that all the free stream velocity head is lost in the suction process so that the total pressure at the compressor face is given by $k_1 \times P_\infty$ where k_1 is the line loss recovery factor.

The compressor flow is fixed by the suction flow requirements, but the turbine flow is an independent design parameter which may be chosen for best overall performance. The compressor discharge velocity V_3 (or the corresponding Mach number M_3) is also an independent design parameter.

The effect of M_3 is illustrated in Figure (30) which shows a typical variation (calculated with $W_c = W_t$) of the net drag (reduced skin friction

drag plus the momentum drags of the turbo-machine flows). It appears that the optimum M_3 is around .4. However, the effect on net drag is quite small and a value of M_3 = .2 is preferable because it entails smaller pressure ratios of the compressor and turbine.

The effect of turbine flow is calculated with M_3 = .2 and with V_1 determined as a function of W_t from the boundary layer data in Figure (29) with $W/W_s = W_t/W_c$. The results (Figure 31) indicate that for practical purposes the net drag is independent of turbine flow. Therefore, the flow rate may be chosen on the basis of convenience of design. The lower the flow rate, the higher is the required pressure ratio, two effects which are generally to be considered as opposing in achieving an optimum design. However, in the present application, because flow rates and pressure ratios are very mild, neither quantity is of overriding importance. Therefore, it is considered that using a turbine flow equal to the compressor flow, leading to a turbine pressure ratio which is slightly higher than the compressor pressure ratio, is a good solution.

Included in Figure (31) is a line showing the drag reduction due to the suction only, indicating that the drag due to the turbo-machine is relatively small. Also shown on the figure is the result for the previous scheme of suction on only the lower half of the fuselage. The comparison indicates the greatly superior drag reduction with full fuselage suction and turbo-machine. Reduced drag as a function of turbo-machine efficiencies and line loss recovery factor is illustrated in Figure (32). These results indicate that the effect of low efficiency is not significant and the effect of line loss is moderate.

Of course, a fair comparison must take into account the difference in weight of the two schemes, the difference being favorable to the half-suction scheme without turbo-machine. Such a comparison involves the mission performance treated in a later section.
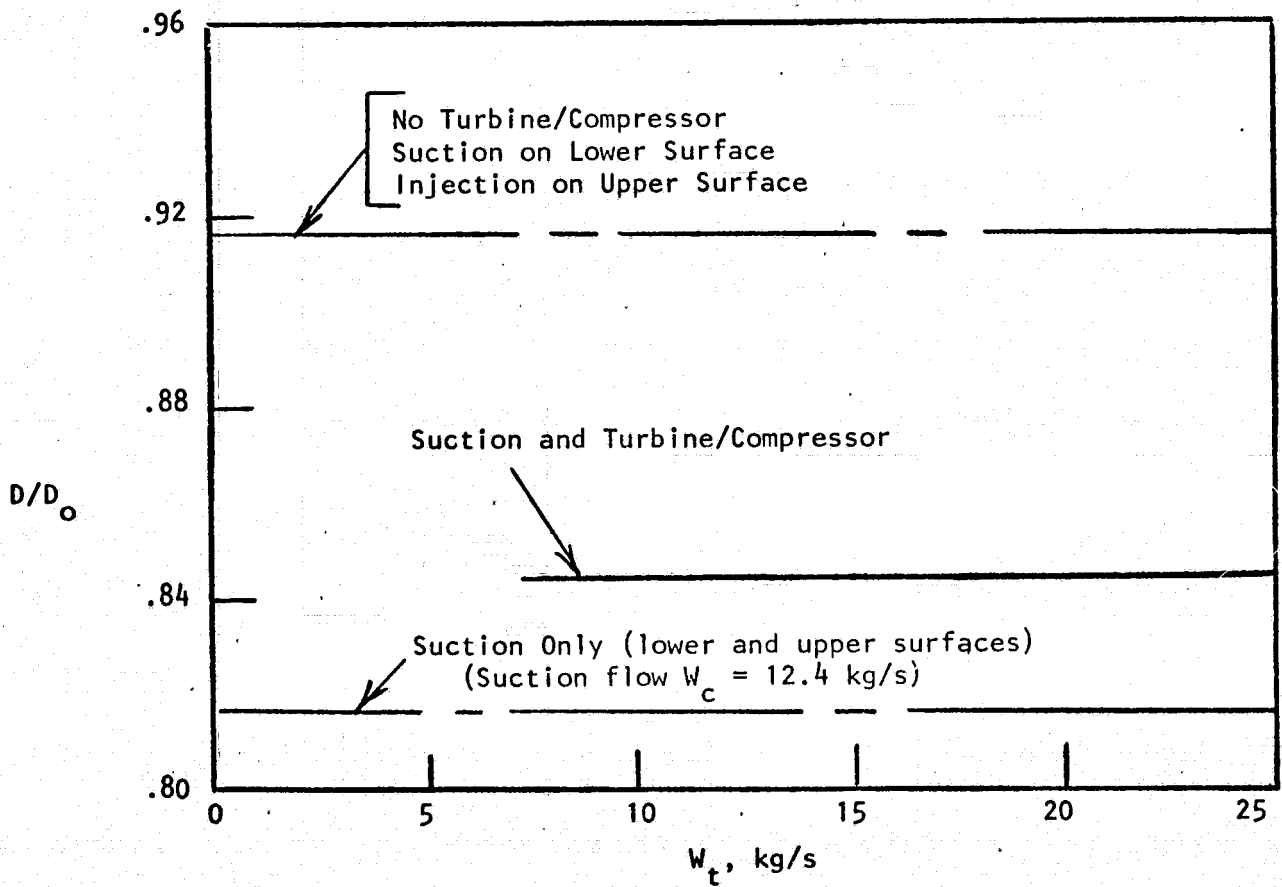
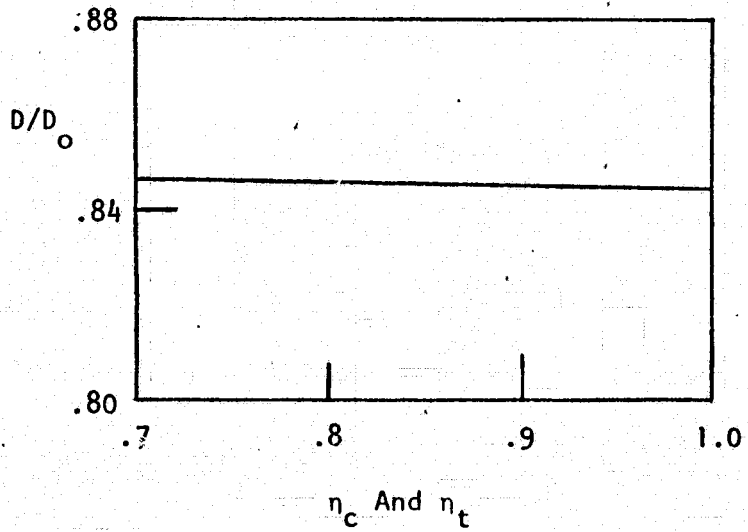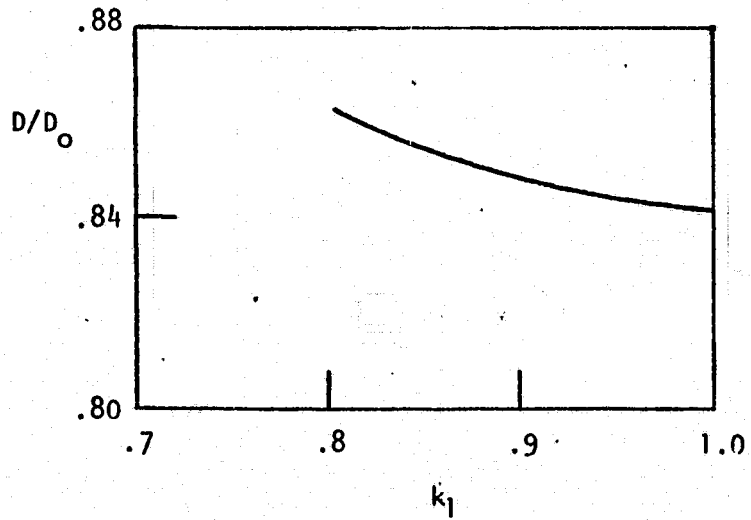FIGURE 31. NET DRAG WITH FUSELAGE SUCTION

FIGURE 32.   EFFECT OF TURBO-MACHINE EFFICIENCIES AND LINE LOSS RECOVERY
FACTOR ON NET DRAG WITH FUSELAGE SUCTION

67

D. Wing Suction - To estimate potential drag reduction due to wing suction the two-dimensional results developed in Section IV-B were applied, on the average, to the total wing surface of the baseline configuration. The essential features of this scheme are indicated in Figure (33).

Since the suction air processed by the compressor was collected at variable presure, a certain ambiguity arises in defining the total pressure P_4. Accordingly, an appropriate average value is needed to treat compressor performance. One approach is to weigh the pressure with respect to mass flow. If χ represents the fraction of the flow at total pressure P, the average is given by

$$\bar{P} = \int P d\chi$$

or if the flow is considered to consist of discrete fractions or individual flow filaments

$$\bar{P} = \Sigma \chi_i P_i$$

In order to achieve this average in practice, it is necessary to preserve the individual flow filaments up to the compressor blading, a procedure which involves transcendent ducting problems. A much more feasible approach is to consider the flows mixed before proceeding to the compressor, the ducting problem being reduced to providing a chamber where the individual flow filaments may be mixed efficiently. In the case where this mixing is allowed to occur at constant area, mass and momentum conservation imply that

$$\bar{W} \bar{N} = \Sigma W_i N_i$$

where the W_i represent the flow rates of the individual filaments and

$$N_i = N_i(M_i) \equiv (\frac{1}{M_i}) \ (1 + \gamma M_i^2) \ (1 + \frac{\gamma-1}{2} M_i^2)^{-\frac{1}{2}}$$

$$\bar{N} = \bar{N}(\bar{M}) \equiv (\frac{1}{\bar{M}}) \ (1 + \gamma \bar{M}^2) \ (1 + \frac{\gamma-1}{2} \bar{M}^2)^{-\frac{1}{2}}$$

Wing Suction

M_∞

M_3

Compressor Flow W_c

Total Pressure P_4

Compressor

M_2

Fuselage
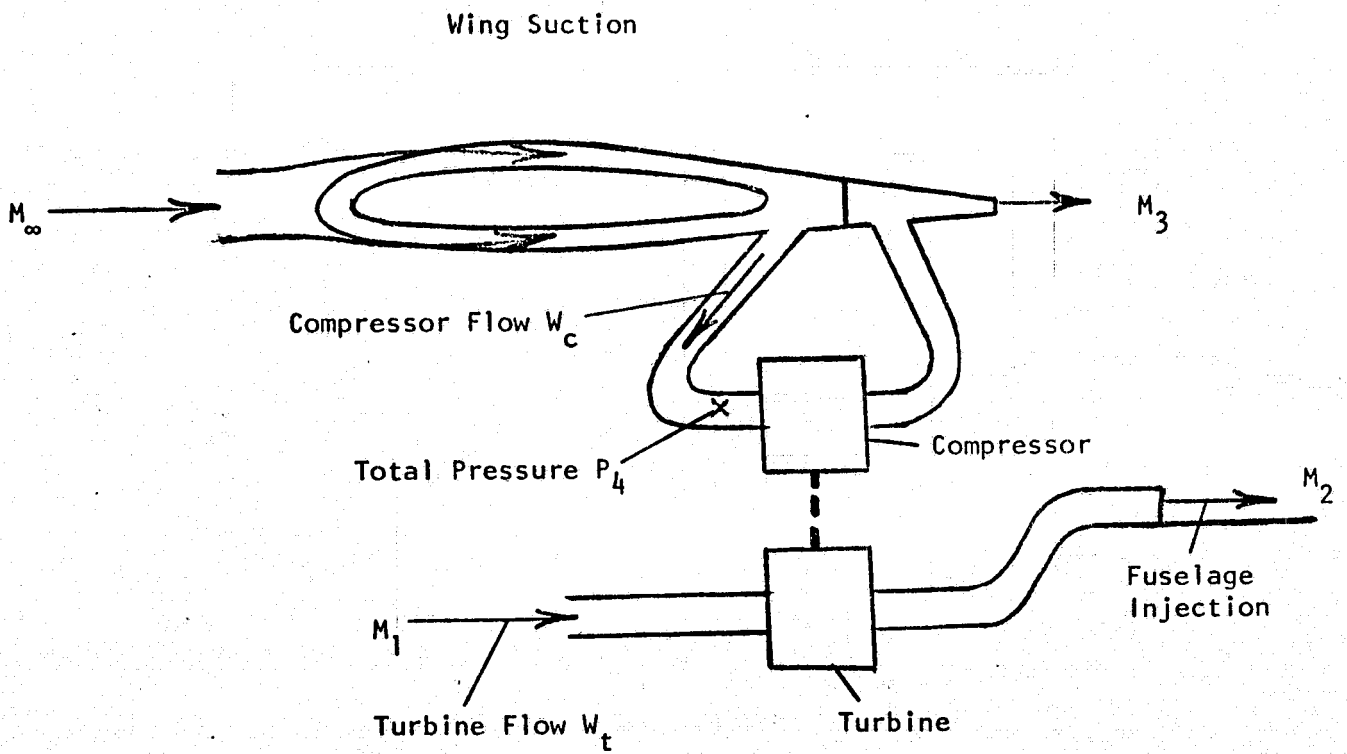Injection

M_1

Turbine Flow W_t

Turbine

FIGURE 33.   SCHEMATIC OF WING SUCTION ARRANGEMENT

In the latter expressions the M_i represent the Mach numbers of the individual filaments at the start of the mixing process and $\bar{M}$ is the final Mach number of the total mixed flow. W, of course, is the total mass flow and is related to the W_i by $\bar{W} = \Sigma W_i$. In deriving these relations it has been assumed that all the filaments are parallel at the start of the mixing process and that each have the same total temperature.

If it is now further assumed that all of the individual filaments are expanded to sonic velocity at the entrance to the mixing chamber then

$$N_i = N^* \equiv N(i) \quad \text{for all } i$$

Accordingly, the relation for $\bar{N}$ yields

$$\bar{N} = (N^*/\bar{W}) \, \Sigma \, W_i = N^*$$

That is, the Mach number of the mixed flow is also sonic. It follows, therefore, that

$$X_i \equiv \frac{W_i}{\bar{W}} = \frac{P_i \, A_i}{\bar{P}\bar{A}}$$

where X_i is the fraction of flow at stagnation pressure P_i, $\bar{P}$ is the stagnation pressure of the mixed flow, and A_i and $\bar{A}$ the respective flow areas. Since we have assumed constant area mixing $\bar{A} = \Sigma A_i$. Thus

$$\Sigma \, \frac{X_i}{P_i} = \frac{1}{\bar{P}\bar{A}} \, \Sigma A_i$$

or

$$\frac{1}{\bar{P}} = \Sigma \, \frac{X_i}{P_i}$$

Applying this concept to the pressure distribution on the wing (Figure 2) the effective total pressure is determined as approximately

$$\bar{P}/P_\infty = .75$$

It is worth noting that this average pressure is around 90% of the basic average determined by weighing with respect to flow.

The momentum drag of the turbo-machine flows is determined in a manner similar to that described previously. The compressor provides a pressure ratio sufficient to increase the pressure of the suction flow from its initial value $\bar{P}$ to its discharge value P_∞, with due allowance for the discharge Mach number and the line loss recovery factor. The compressor flow is fixed by the suction flow requirements but the turbine flow is an independent design parameter which may be chosen at will. In making calculations, it is best to treat the turbine exit Mach number M_2 and the compressor exit Mach number M_3 as independent design parameters which may be chosen for best performance. The turbine entrance Mach number M_1 is also a design parameter to some extent since the inlet of the turbine flow can be arranged to ingest the boundary layer flow along the fuselage or wing.

The effect of the compressor exit Mach number M_3 is illustrated in Figure (34) which shows curves of net drag with $M_1 = M_\infty = .82$ and with various M_2. The value of $M_3 = .2$ is chosen for design since it gives very nearly the lowest net drag and the smallest turbine flow.

The effect of the turbine exit Mach number M_2 is illustrated in Figure (35) which shows that a value of .3 or .4 gives the best results. The figure also illustrates the effect of the turbine inlet Mach number M_1, indicating that a serious deterioration of performance would occur with the use of boundary layer flow. For best overall performance (low net drag and low turbine flow) the turbine inlet should be free of the boundary layer and should handle only free stream flow.

It should be noted that the results in Figures (34) and (35) were determined with the average total pressure at the compressor defined by $\bar{P}/P_\infty = .75$ which was chosen as a realistic average value. It is interesting to consider the effect of this pressure on performance, illustrated by the results in Figure (36) calculated with $M_1 = M_\infty = .82$ and $M_2 = .4$. It is apparent that the average pressure has a large effect on both the net drag and the turbine flow.

The effect of machine efficiencies and line loss factors are presented in Figure (37). The design values, shown by the circled points, result in a
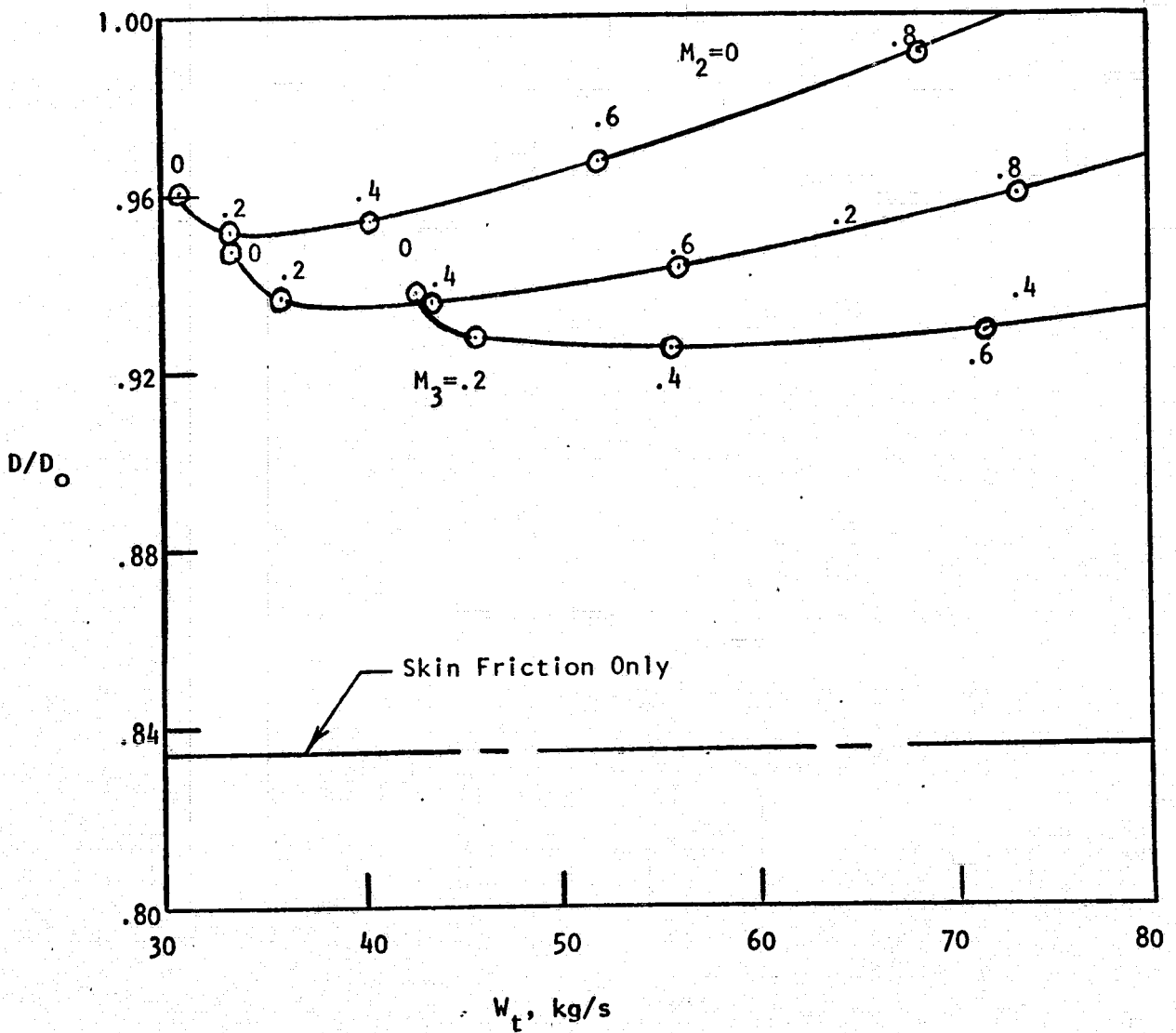
FIGURE 34. EFFECT OF EXIT MACH NUMBERS ON NET DRAG WITH WING SUCTION.
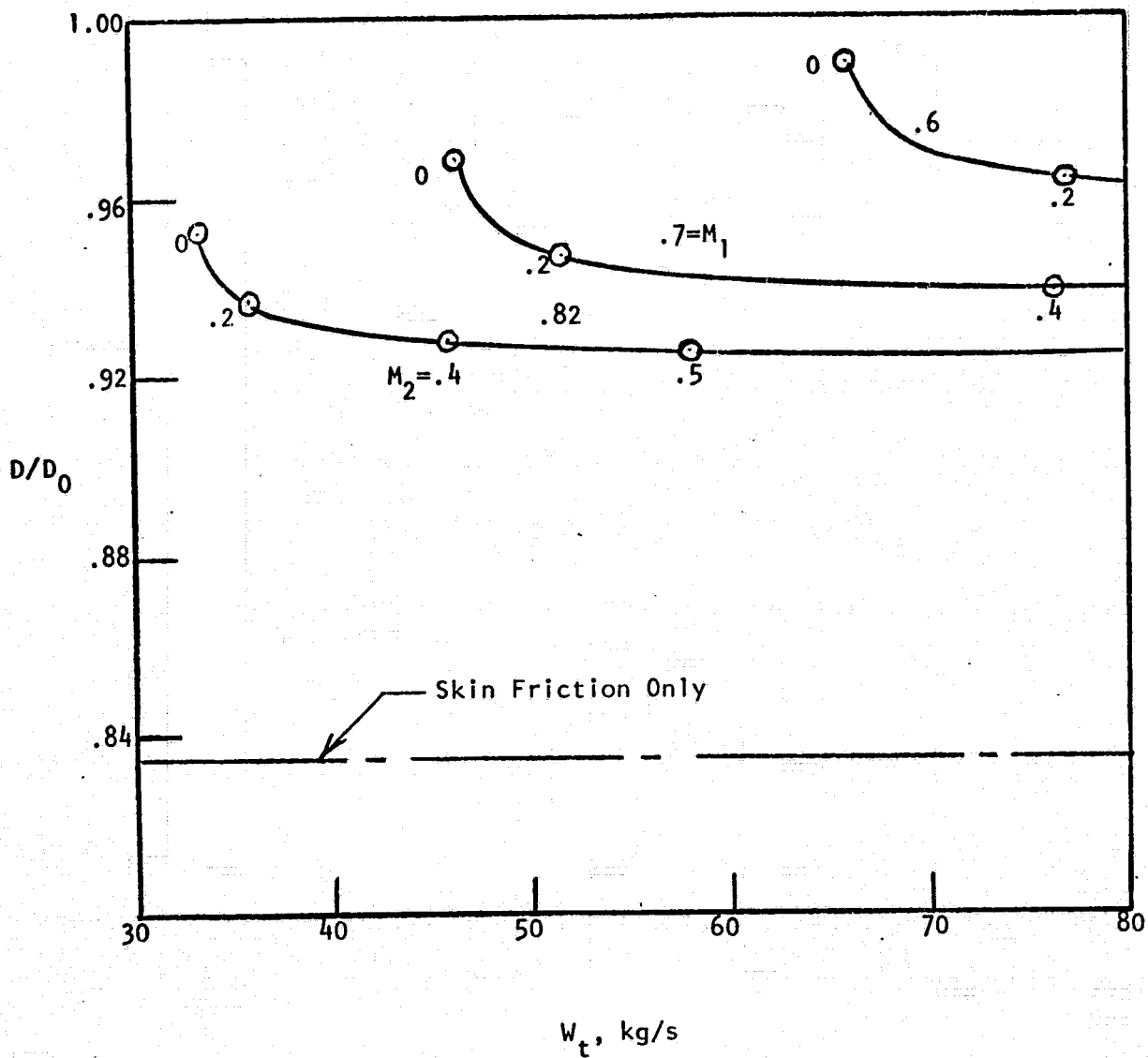
FIGURE 35.   EFFECT OF TURBINE ENTRANCE AND EXIT MACH NUMBERS ON NET DRAG
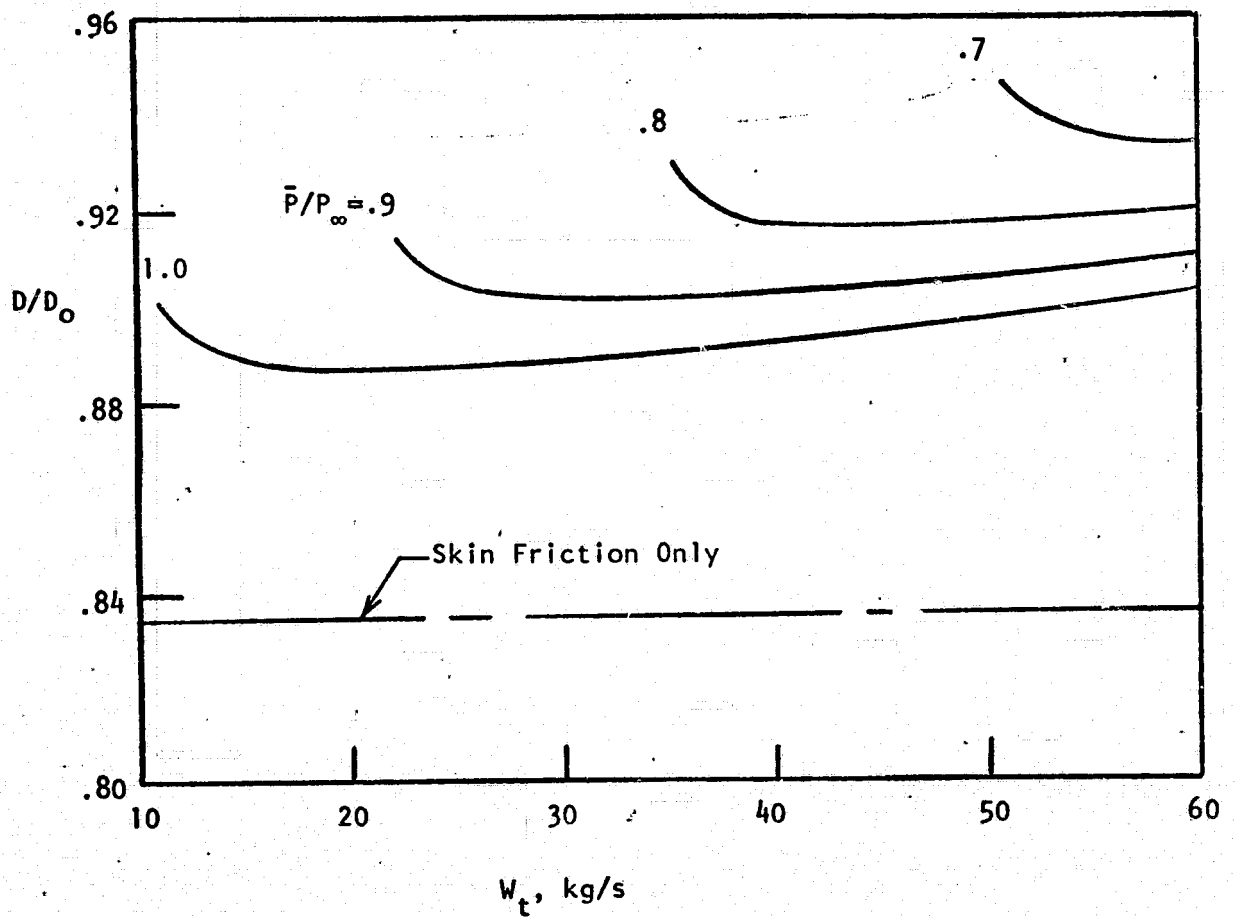WITH WING SUCTION.

73

FIGURE 36.   EFFECT OF AVERAGE SUCTION PRESSURE ON NET DRAG WITH
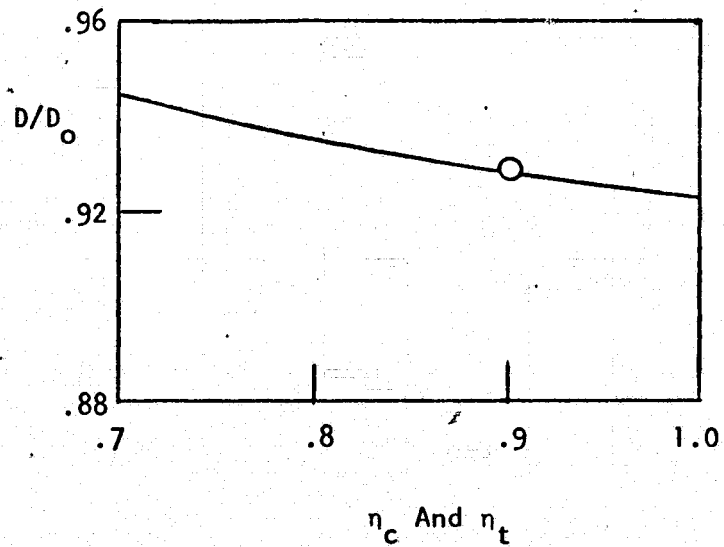   WING SUCTION
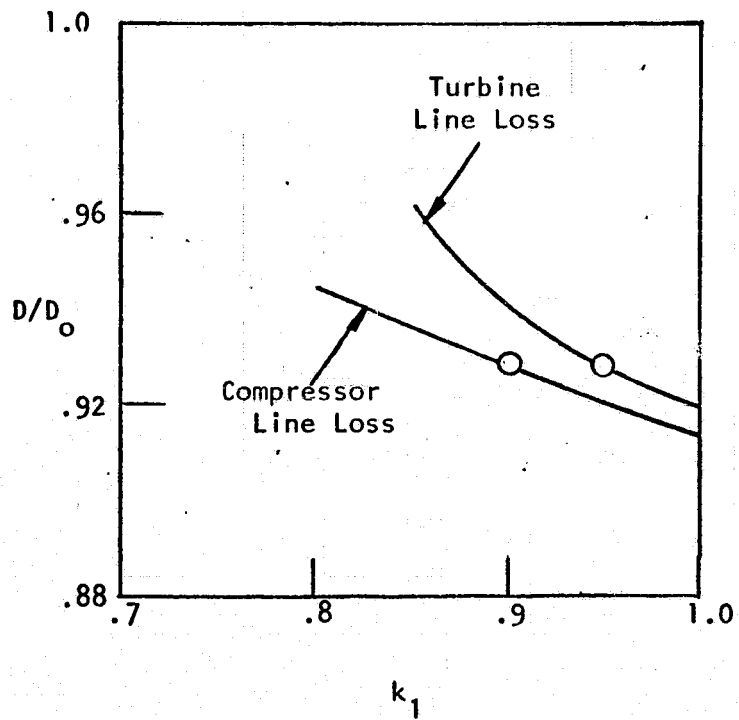
FIGURE 37. EFFECT OF TURBO-MACHINE EFFICIENCIES AND LINE LOSS RECOVERY
FACTORS ON NET DRAG WITH WING SUCTION

75

reduced net drag D/D_o = .928. This is less than obtained with suction on the fuselage for which D/D_o = .844. Nevertheless, the reduction is significant and especially when used together with fuselage suction can produce much improved mission performance as will be demonstrated in the next section.

The physical layout of the wing-suction scheme is conceived as two separate symmetrical arrangements of ducting and turbo-machine, one for each of the port and starboard wings. The ducting of the suction flow proceeds from the wing tip to the wing root where the turbo-machine is located. For the baseline configuration the wing thickness at the root is approximately 2.1 m. This is large enough to accommodate the turbo-machine, the diameter of which is estimated to be around 1.2 m. The inlet for the turbine flow may be located on the bottom of the wing or on the side of the fuselage. The size of the inlet is very small, the area being around .2 m^2 for each side. The flow exits may be located on the fuselage near the trailing edge of the wing root or at the trailing edge of the wing itself. This latter arrangement could produce some improvement in airplane performance by delaying separation on the wing.

VI. MISSION PERFORMANCE

In order to evaluate the drag reduction schemes properly it is necessary to consider the effect on the mission performance of the airplane. For a realistic evaluation the added weight introduced by the scheme must be included in the analysis.

To keep the analysis simple, the mission is considered to consist of three parts.

      (1)   Initial operation prior to cruise

      (2)   Cruise

      (3)   Final operation after cruise

It is assumed that range is accomplished only in the cruise part of the mission and that all the fuel has been consumed at the end of the final operation.

Let us consider first the mission for the baseline configuration i.e., in the absence of any drag reduction. Each part of the mission is characterized by a certain fuel consumption defined by the three parameters.

$$Y_1 = F_1/W_o$$

$$Y_2 = F_2/W_o$$

$$Y_3 = F_3/W_o$$

where F_1, F_2 and F_3 are the fuel weights consumed during operations 1, 2 and 3 and W_o is the gross weight of the airplane (weight at the start of operation 1). The total fuel consumed is given by

$$F = Y_o W_o$$

where

$$Y_o = Y_1 + Y_2 + Y_3$$

and the airplane weight after the mission is over is

$$W_e = W_o - F$$

The range accomplished during the mission is given by

$$R = \text{constant} \quad (L/D) \log \frac{(W_o - F_1)}{(W_o - F_1 - F_2)}$$

where (L/D) is the maximum lift to drag ratio of the airplane.

The constant is a function of the cruise speed and the engine performance, but its value is not pertinent for the present purpose since we will be dealing with _relative_ mission performance.

Consider now the airplane with a drag reduction scheme which decreases drag but increases weight. The decrease in drag increases the maximum L/D. With the assumption that the drag polar of the original airplane is parabolic and does not change in shape, the new maximum L/D, denoted with a prime, may be expressed in terms of the reduced drag D/D_o determined in the previous sections of this report.

$$\frac{(L/D)'}{(L/D)} = \frac{1}{2(D/D_o) - 1}$$

The variation of this ratio with D/D_o is shown in Figure (38). If the drag reduction scheme did not introduce an increase in weight, this ratio would represent the relative increased range which would be accomplished by the airplane with the same fuel load.[*]

---

[*]It is important to note that the effect illustrated in Figure (38) assumes that changes in the drag polar are due solely to changes in zero-lift drag. This is essentially true for the fuselage drag reduction schemes. However, for schemes involving wing-suction an additional influence must be accounted for, viz., the effect of suction on lift characteristics. For the present example it is estimated that an additional 2 percent increase in maximum L/D is provided by the wing-suction scheme. The basis for this estimate is outlined in Appendix B.
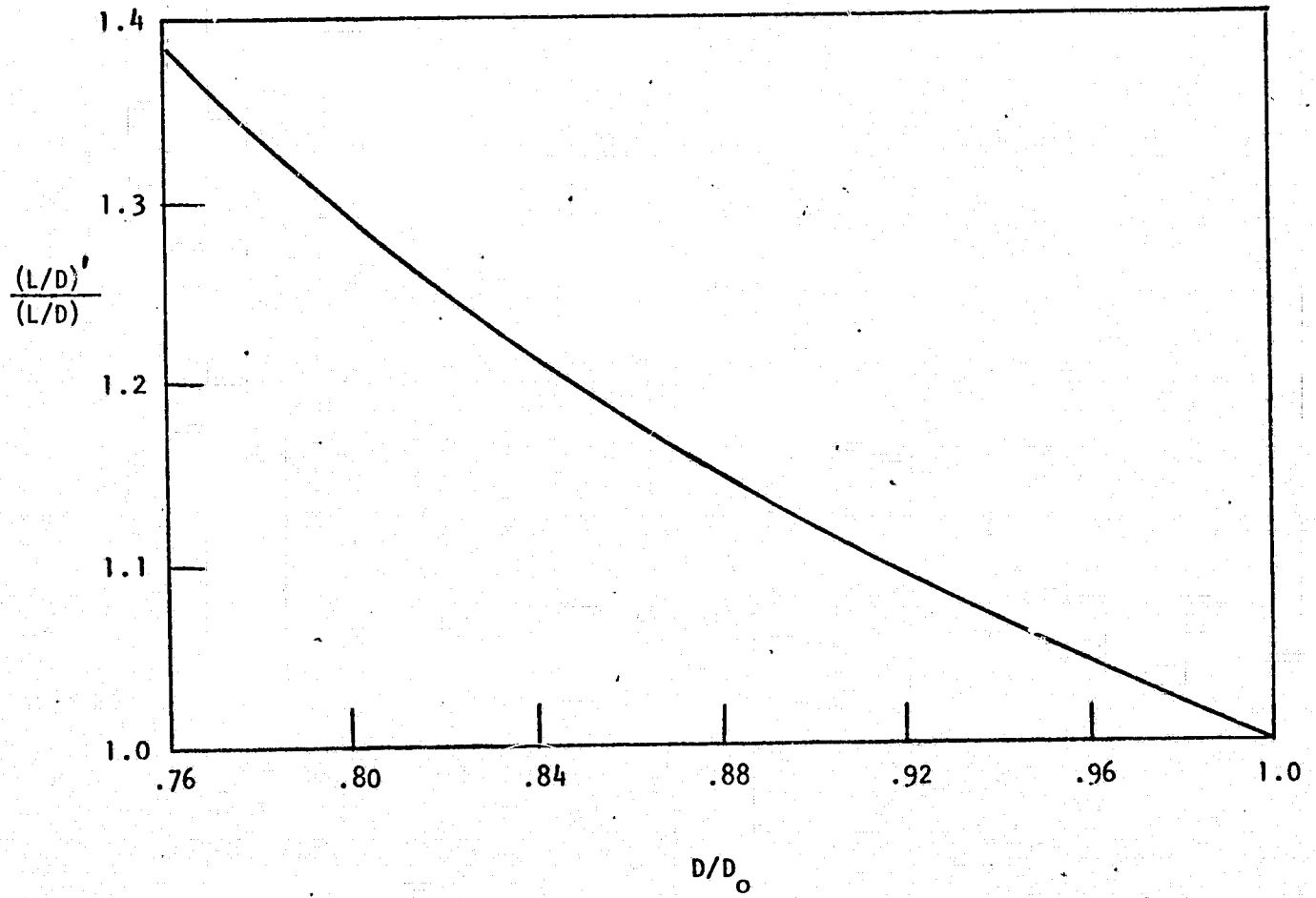
FIGURE 38.   INCREASED MAXIMUM L/D WITH NET REDUCED DRAG

The weight increase of the airplane is responsible for increased fuel consumption required to accomplish the various parts of the mission. The fuel consumed in parts 1 and 3 is assumed to increase directly with the weight of the airplane at the start or end of these parts, denoting the case of the airplane with the drag reduction by prime quantities.

$$\frac{F_1'}{F_1} = \frac{W_1'}{W_0} = \frac{W_e' + F'}{W_e + F}$$

$$\frac{F_3'}{F_3} = \frac{W_e'}{W_e}$$

The drag reduction scheme introduces an increase in weight ΔW so that

$$W_e' = W_e + \Delta W$$

Now for completeness of the comparison two relative missions are considered. For the first mission the fuel load is considered to be the same or $F = F'$. In this case, there is an increase in range given by

$$\frac{R'}{R} = \frac{(L/D)'}{(L/D)} \frac{\log (1 + X_2')}{\log (1 + X_2)}$$

where

$$X_2 = \frac{Y_2}{1 - Y_1 - Y_2}$$

$$X_2' = \frac{Y_2 (1 - Y_0) - B (Y_1 (1 - Y_0) + Y_3)}{(1 - Y_1 - Y_2)(1 - Y_0 + B)}$$

In the latter expression for X_2', the quantity B represents the increased weight introduced by the drag reduction scheme, defined by

$$B = \Delta W / W_0$$

In the second mission the range is considered to be the same or $R = R'$. In this case, there is a reduction in the fuel load given by

$$F'/F = \frac{1 - Y_o + B}{1 - Y_o} \frac{(Z_2' (1 - Y_1 - Y_2) + Y_o (1 - Y_1) - Y_2)}{Y_o (1 - Y_1)}$$

where

$$Z_2' = (1 = X_2)^a - 1$$

$$a = (L/D)/(L/D)'$$

In applying these equations, the weight increase is expressed by the parameter w which defines the weight increase per square foot of surface,

$$\Delta W = w \times surface\ area$$

In the case of complete suction on the fuselage, the surface area is taken as the complete suction surface $\pi \times 6.1 \times 61 = 1170\ m^2$. In this case the value of w represents the weight of the suction surface which is conceived as an additional surface applied over the original fuselage, the gap between the two surfaces forming the duct which leads the suction flow to the turbo-machine. The value of w does not have to be increased for extraneous ducting, but it must include some fraction for the structure which supports the suction surface. The value of w may also be adjusted to account for the weight of the turbo-machines. However, the turbo-machine is so small that its weight is unimportant compared to the weight of the suction surface.

In the case of combined fuselage suction and injection, the surface is taken as the suction surface on the bottom part of the fuselage or $1/2 \times 1170 = 585\ m^2$. In this case the value of w is larger than the weight of suction surface, since it must include the weight required to duct and inject the suction flow on the top half of the fuselage.

Calculations were made using an original gross weight $W_o = 340,000$ kg and representative values for the fuel fractions of the original mission as follows:

$$Y_1 = .05$$
$$Y_2 = .30$$
$$Y_3 = .15$$

The values of D/D_o were taken as .844 for the case of complete suction with turbo-machine and .916 for the case of half-suction and half-injection without turbo-machine.

The results are presented as curves of increased range (Figure 39) and decreased fuel load (Figure 40) as a function of the weight parameter. It is considered that the suction surface weight is around 2.5 kg/m^2 (aluminum skin .076 cm thick with some allowance for structural support). Therefore, for the case of complete suction, the range increase is around 18% or the fuel reduction is around 11%. For the case of combined suction and injection the value of w is increased 20% to account for the weight of ducting required for injection. In this case the range increase is approximately 8% or the fuel reduction is around 6%.

It is apparent that complete suction offers superior mission performance. This is true even when the added weight of the turbo-machine is taken into account. It has been estimated that the size of the wheel is less than 1.2 m in diameter. Since it is a single stage machine, the weight is probably around 150 kg. The added surface weight based on w = 2.5 kg/m^2 is 2830 kg. Therefore, the weight of the turbo-machines increases w from 2.5 to 2.65. This increase does not reduce mission performance significantly.

The effect of turbo-machine efficiencies and line loss recovery factor on mission performance (determined with w = 2.5) are shown in Figures (41) and (42) for the case of full fuselage suction. It is evident that the effects are extremely mild, a direct result of the small flow involved in the suction process.

Mission performance for an aircraft utilizing the wing drag reduction scheme whether alone or in combination with the two fuselage drag reduction schemes is shown in Figures (43) and (44).

For the case of wing suction, mission performance is determined for the surface area of 900 m^2 and a value of D/D_o = .928. (Note that the L/D factor in Figure 38 is increased by 2 percent to account for the improvement of lift
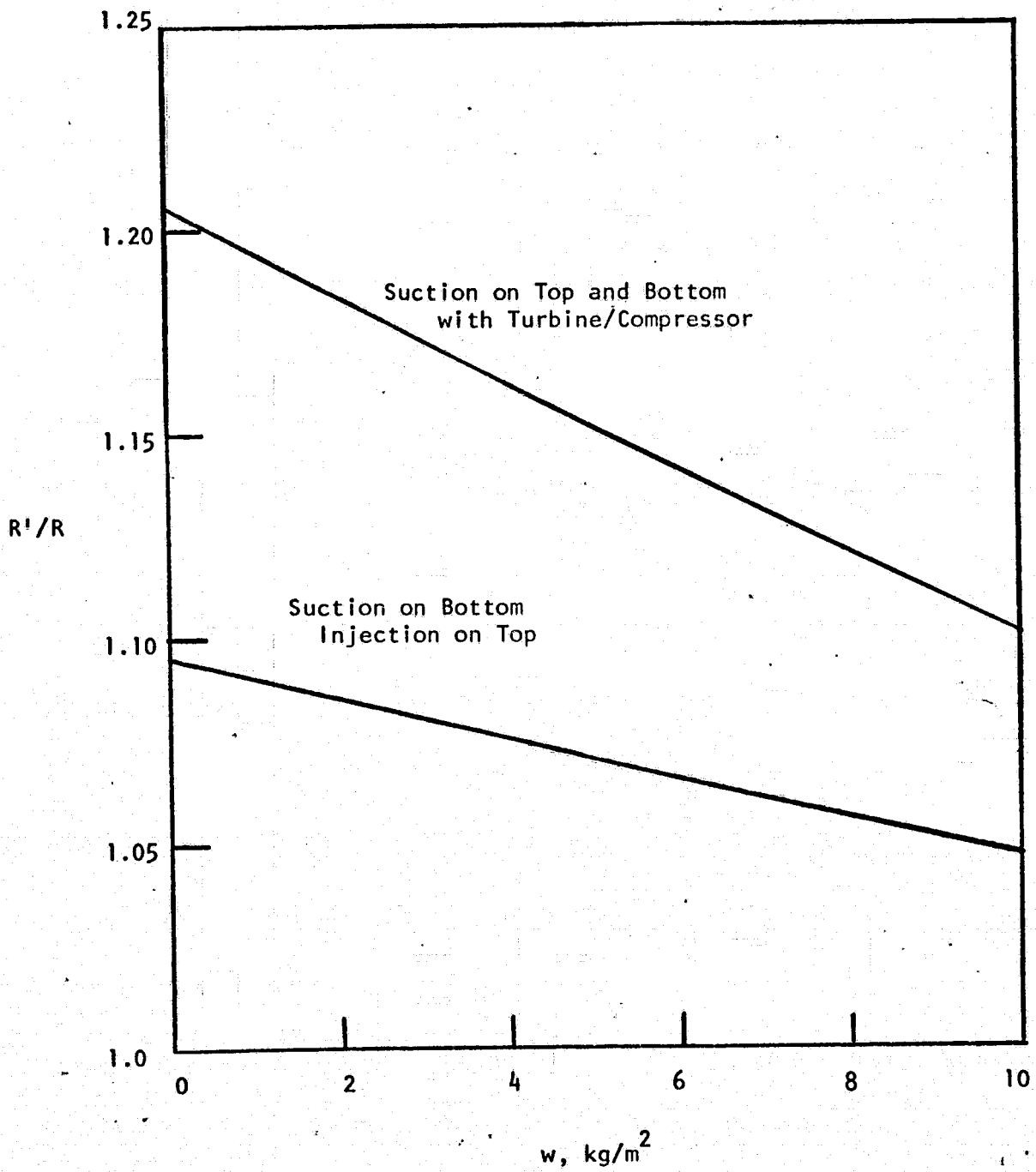
FIGURE 39. INCREASED RANGE WITH FUSELAGE DRAG REDUCTION AS FUNCTION OF SURFACE WEIGHT PARAMETER

83
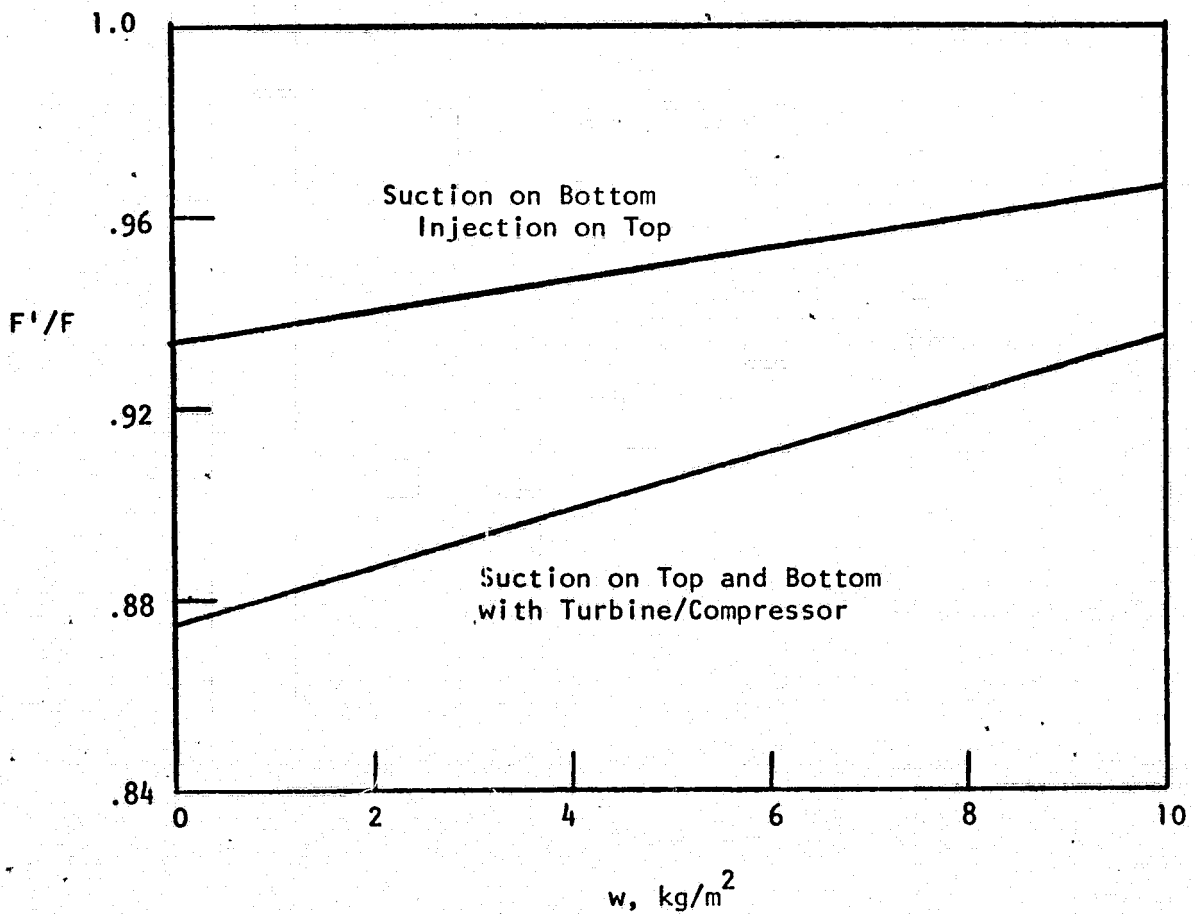
FIGURE 40.   DECREASED FUEL LOAD WITH FUSELAGE DRAG REDUCTION AS
FUNCTION OF SURFACE WEIGHT PARAMETER

84
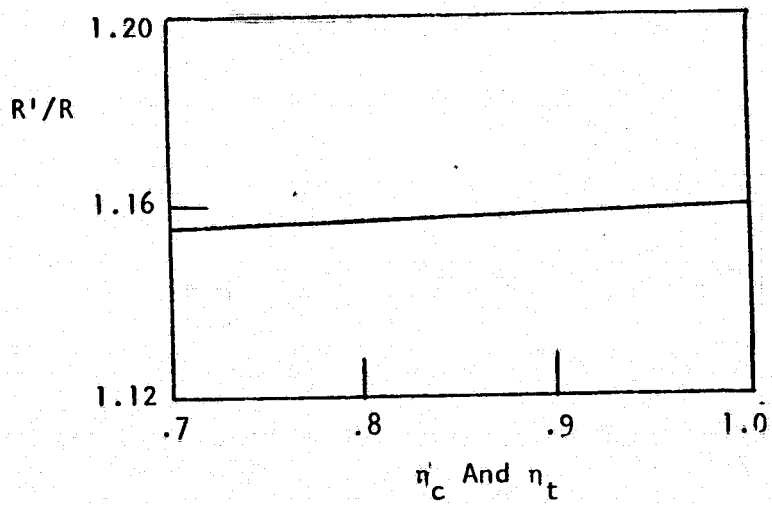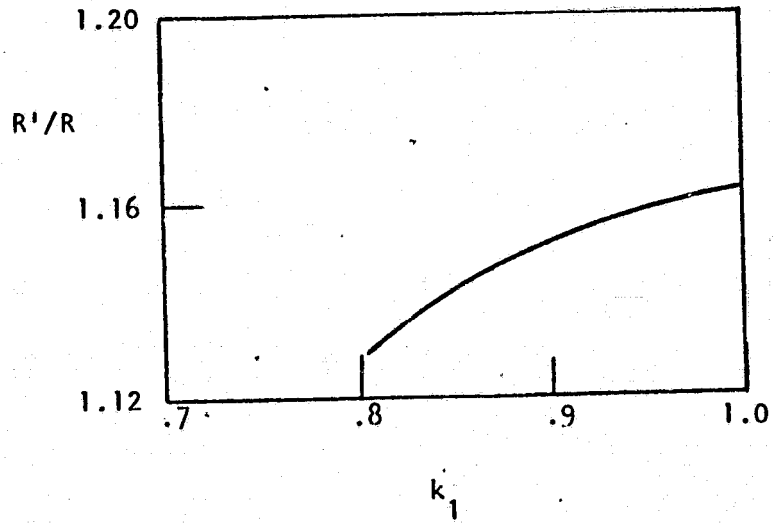
FIGURE 41.   EFFECT OF TURBO-MACHINE EFFICIENCIES AND LINE
LOSS RECOVERY FACTOR ON INCREASED RANGE WITH
FUSELAGE SUCTION
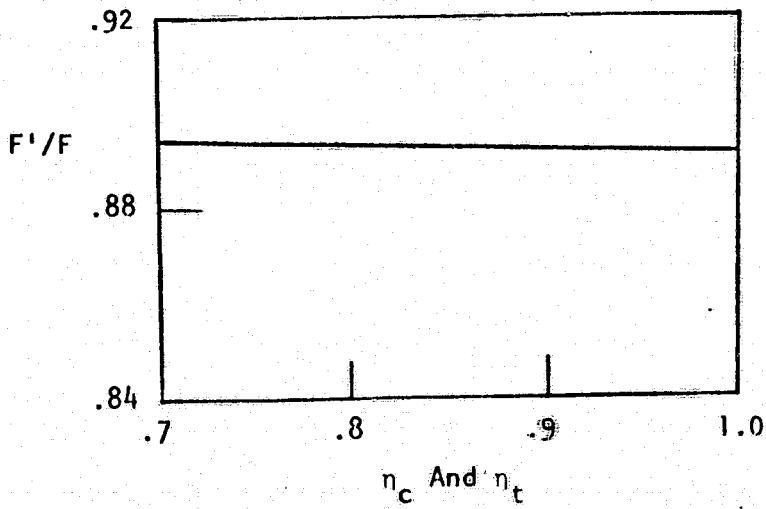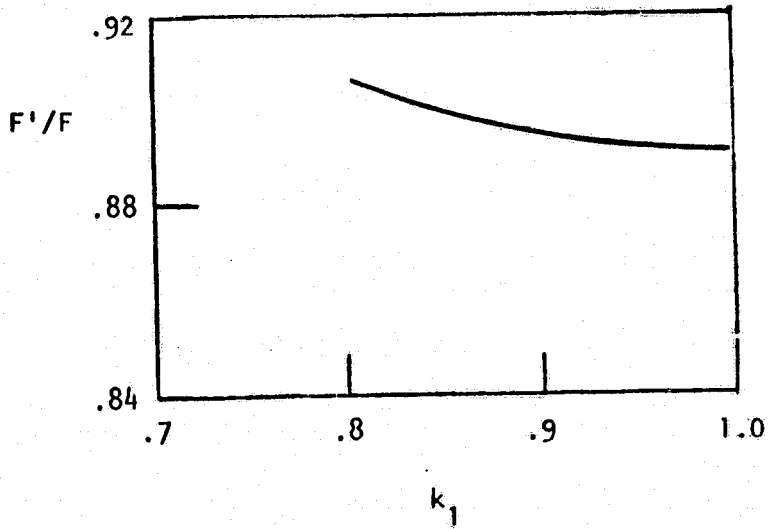
FIGURE 42.   EFFECT OF TURBO-MACHINE EFFICIENCIES AND LINE LOSS
RECOVERY FACTOR ON REDUCED FUEL LOAD WITH FUSELAGE
SUCTION

86

FIGURE 43. INCREASED RANGE WITH DRAG REDUCTION SCHEMES AS FUNCTION OF SURFACE WEIGHT PARAMETER

1 - Wing Suction
2 - Fuselage Half Suction and Injection
3 - Fuselage Suction
4 - Combined 1 & 2
5 - Combined 1 & 3

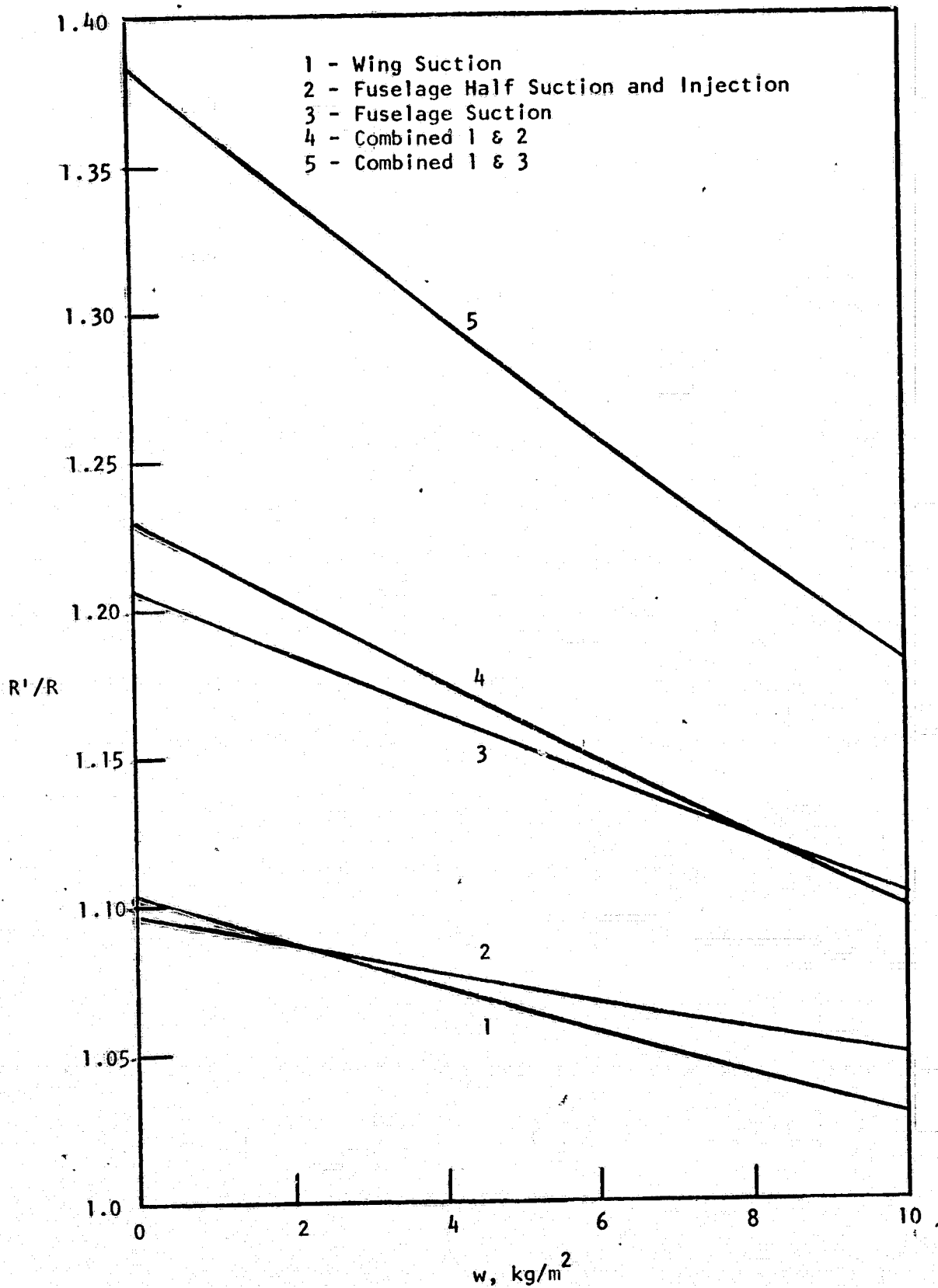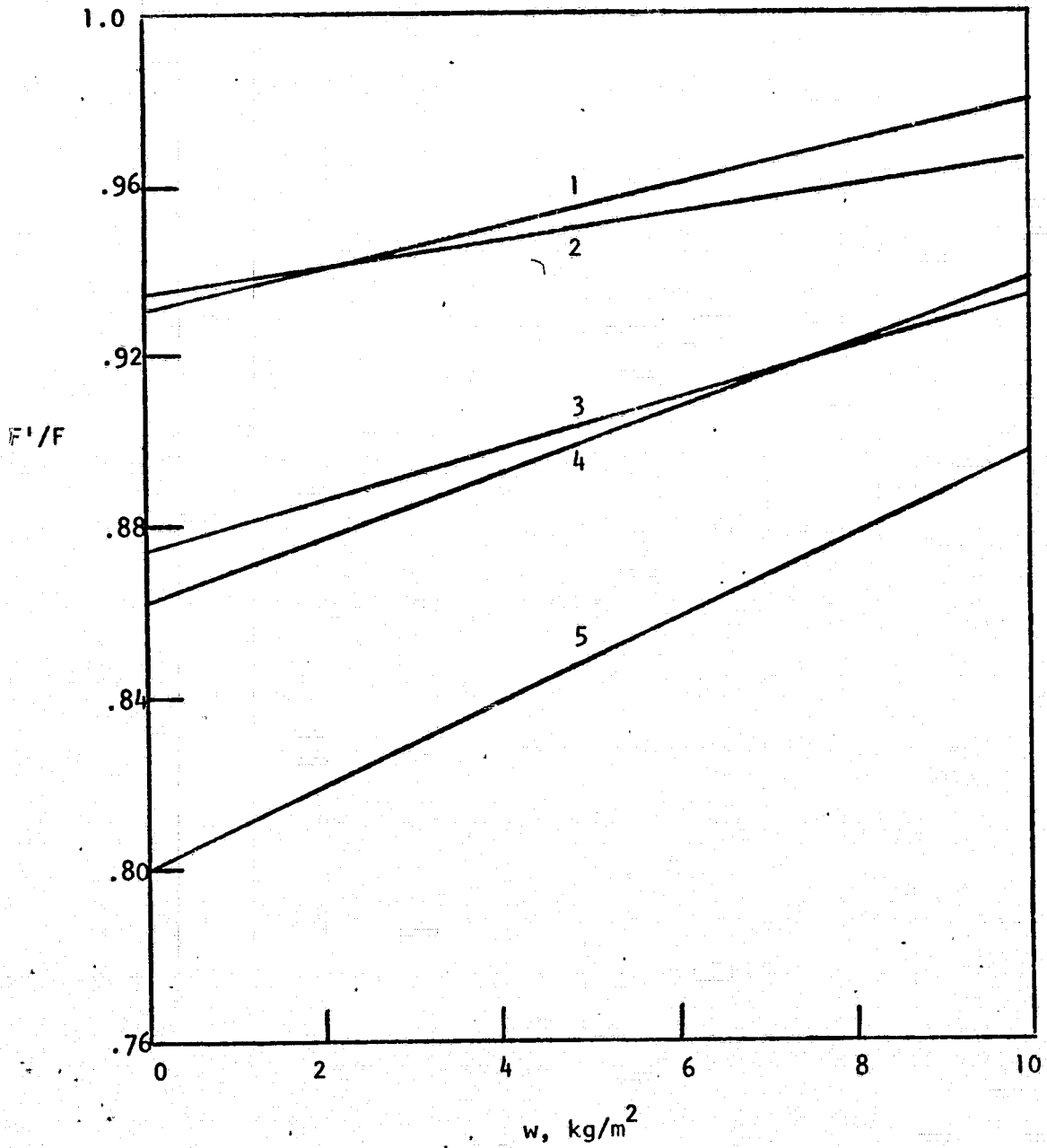FIGURE 44. DECREASED FUEL LOAD WITH DRAG REDUCTION SCHEMES AS FUNCTION OF SURFACE WEIGHT PARAMETER

characteristics with suction.) The appropriate value of the surface weight parameter is taken to be 40% higher then the basic weight 2.5 kg/m^2 to account for the ducting and turbo-machinery or $w = 3.5$ kg/m^2. As can be seen, the wing drag reduction scheme produces only moderate improvement, 8% increase in range or 5% decrease in fuel load. However, when combined with either of the fuselage drag reduction schemes the effect is magnified.

For the combined systems the value of D/D_o for determining the L/D factor is given by

$$D/D_o = (D/D_o)_1 + (D/D_o)_i - 1$$

where $i = 2$ or 3. The significance of the subscripts is defined at the top of Figure (43). The 2 percent factor due to lift augmentation is applied to the combined L/D which is an approximation considered sufficiently accurate for the present purpose.

The approximate surface areas for the combined systems to which the respective weight parameters are applied are given by

$$S = S_1 + S_i$$

The corresponding weight parameters are given by

$$w = \frac{w_1 S_1 + w_i S_i}{S}$$

There is obtained

$$w_4 = 3.3; \quad w_5 = 3.0$$

Using the results shown in Figures (43) and (44) together with these values of w the performance of the various drag reduction schemes can be established. These are summarized in Table II below.

TABLE II

SUMMARY OF MISSION PERFORMANCE FOR
VARIOUS DRAG REDUCTION SCHEMES

Scheme	w, kg/m^2	% Range Increase	% Fuel Load Decrease
1	3.5	8	5
2	3.0	8	6
3	2.5	18	11
4	3.3	18	11
5	3.0	32	17

It is interesting to note that the combined performance is more than the sum of the individual performances.

The effect of turbo-machine efficiencies and line loss recovery factor on mission performance with the combined systems is shown in Figures (45) and (46). The efficiencies and recovery factor refer to the wing suction system since this system is much more sensitive to these quantities. Furthermore, the recovery factor refers to the suction or compressor flow circuit since this is the circuit where ducting can become a problem. The results indicate that even with poor turbo-machine efficiencies and low recovery factor or high duct loss, the combined fuselage and wing drag reduction schemes produce large improvements in mission performance.
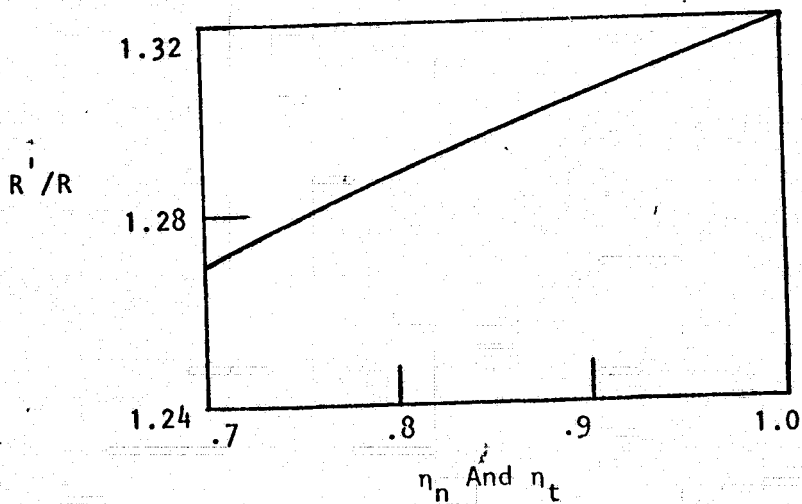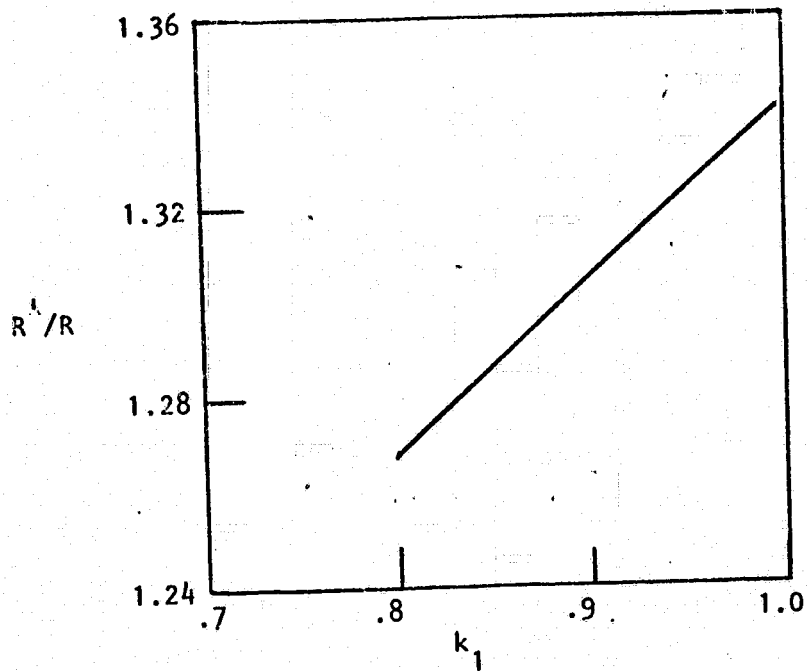
C.2

FIGURE 45. EFFECT OF TURBO-MACHINE EFFICIENCIES AND LINE LOSS RECOVERY FACTOR ON INCREASED RANGE WITH COMBINED FUSELAGE AND WING DRAG REDUCTION SCHEME
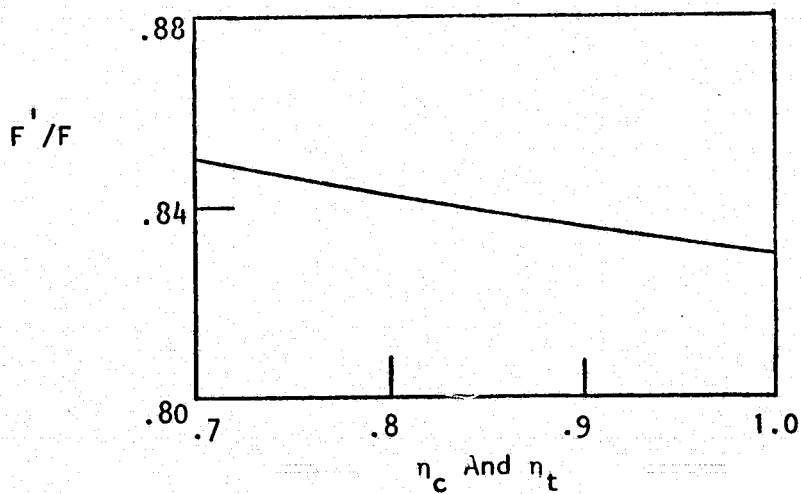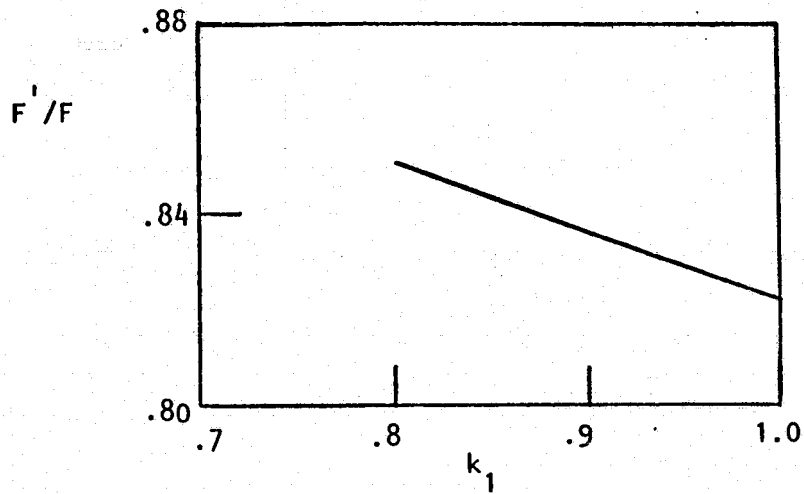
91

FIGURE 46. EFFECT OF TURBO-MACHINE EFFICIENCIES AND LINE LOSS
RECOVERY FACTOR ON DECREASED FUEL LOAD WITH COM-
BINED FUSELAGE AND WING DRAG REDUCTION SCHEME

VII. CONCLUDING REMARKS

On the basis of the results presented in the previous section it is concluded that significant drag reduction and corresponding improvement in the performance of subsonic transport aircraft can be achieved by judicious application of certain boundary layer control schemes. These include combinations of suction and slot injection applied to various surfaces of the aircraft.

It is emphasized that the results obtained in this study are subject to a number of important restrictions and/or assumptions, which render the above cited conclusion provisional both qualitatively and quantitatively. These restrictions will be delineated here.

The most fundamental assumption implicit in these studies relates to the possibility of preserving the laminar boundary layer state with distributed surface suction. This assumption is particularly crucial since, if transition did occur under these conditions, the viscous drag would actually be increased above the undisturbed turbulent values. Although the feasibility of the technique appears to have been established in both wind tunnel and flight tests no applications have been made to date on either commercial or military aircraft (Reference 1). Accordingly, our performance results have to be considered overly optimistic at the present time.

On the other hand, if the aforementioned assumptions do prove to be valid, the performance estimates which have been obtained are probably conservative for a variety of reasons. As an example the wing drag reduction results outlined in Section V-D indicated that net reduction was quite sensitive to the average pressure at the compressor (cf: Figure 36). The performance results presented in Section VI were made with a single value of this parameter taken as $\bar{P}/P_\infty = 0.75$. Higher values of this average would lead to substantial increases in performance. These could be achieved by installation of more compelx ducting possibly at the cost of increased vehicle weight. Furthermore, this parameter is a function of wing geometry. Thus, optimization of this parameter would be useful and could lead to im-

proved performance.

Additional examples of possible improvement in performance would include application of suction on empennage surfaces. The results given in Appendix A are indicative of the large reduction in drag that can be achieved by application of this technique on airfoil sections at zero angle of attack.

We also note that the contribution of those schemes to lift-augmentation has hardly been examined. Specifically, the angle of attack for which our wing results were made was substantially below representative values for flight at $(L/D)_{max}$. It is expected that much greater improvement in $(L/D)_{max}$ would result at higher angles of attack. Also, the use of slot injection on the wings to energize the boundary layer and prevent separation has also not been examined.

In summary, the results of this study indicate a real potential in terms of the development of low-drag subsonic transport. However, the extent of this potential has not been completely established and further in-depth studies directed toward optimizing this potential are recommended.

REFERENCES

1. Head, M. R., Johnson, D. and Coxon, M., "Flight Experiments on Boundary Layer Control for Low Drag," ARC R & M 3025, March, 1955.

2. Whites, R. C., Sudderth, R. W. and Wheldon, W. G., "Laminar Flow Control on the X-21," Astronautics and Aeronautics, July, 1966.

3. Pfenninger, W., "Recent Development in Boundary Layer Research," AGARDOgraph 97, Vol. 4, 1965.

4. Groth, E. E. et al, "Experimental Aerodynamic Investigations at Supersonic Speeds," Section II, Part 2 of Summary of Laminar Boundary Layer Control Research, Technical Documentary Report ASD-TDR-63-554, March, 1964.

5. Janes All The Worlds Aircraft 1968-1969, McGraw-Hill Book Co., New York.

6. Schlichting, H., "Boundary Layer Theory," Pergamon Press, 1955.

7. Beckwith, I. E. and Bushnell, D. M., "Calculation by a Finite-Difference Method of Supersonic Turbulent Boundary Layers with Tangential Slot Injection," NASA TN D-6221, April, 1971.

8. Laitone, E. V., "Subsonic Flow About a Body of Revolution," Quart. App. Math., 5, 2, 227 (1947).

9. Bavitz, P., "An Analysis Method for Two-Dimensional Transonic Viscous Flow," NASA TN D-7718, 1974.

10. Torda, T. P., "Boundary Layer Control by Continuous Surface Suction or Injection," J. Math. Phys., Vol. 31, p. 206, 1952.

11. Thwaites, B., "The Development of Laminar Boundary Layers under Conditions of Continuous Suction. Part II: Approximate Methods of Solution," Rep. Aero. Res. Coun., London, No. 12699.

12. Economos, C. and Fort, R., "Two-Dimensional and Axisymmetric Laminar and Turbulent Boundary Layer with Transition Criterion and Entropy Swallowing," General Applied Science Laboratories, Technical Report No. 772, March, 1972.

13. Howard, F. G., J. N. Hefner and Srokowski, A. J., "Multiple Slot Skin Friction Reduction," to be published in the AIAA Journal of Aircraft.

14. Price, J. M. and Harris, J. E., "Computer Program for Solving Compressible Nonsimilar-Boundary-Layer Equations for Laminar, Transitional or Turbulent flows of a Perfect Gas," NASA TM X-2458, April, 1972.

REFERENCES (Continued)

15. Cary, A. M. Jr. and Hefner, J. N., "Film Cooling Effectiveness and Skin Friction in Hypersonic Turbulent Flow," AIAA J. Vol. 10, No. 9, September, 1972.

16. Kacker, S. C. and Whitelaw, J. H., "Prediction of Wall-Jet and Wall-Wake Flows," Journal of Mechanical Engineering Science, Vol. 12, No. 6, pp. 404-420, 1970.

17. Saland, H. J., "Velocity Profiles for Tangential Slot Injection in Turbulent Incompressible and Compressible Flows," Ph. D. Thesis, New York University, 1970.

18. Grey, J., Aircraft Fuel Conservation: An AIAA View, Proceedings of a Workshop Conference, Reston, Virginia, June, 1974.

19. AGARD, Transonic Aerodynamics, AGARD Conference Proceedings No. 35, September, 1968.

APPENDIX A
LAMINAR BOUNDARY LAYER WITH SIMULTANEOUS
MASS TRANSFER AND PRESSURE GRADIENT

The starting point for this analysis is the Von Karman momentum integral equation for two-dimensional incompressible laminar boundary layer flow which takes the form (cf: Reference 6, p. 236)

$$u_e^2 \frac{d\theta}{dx} + (2\theta + \delta^*)\, u_e \frac{du_e}{dx} = \frac{\tau_w}{\rho} + v_w u_e \qquad (A-1)$$

where v_w represents the normal velocity at the wall (negative for suction) and the remaining variables are defined in the conventional manner.

Equation (A-1) can be written in the alternate form

$$U^2 T' + T(H + 2)\, UU' = C_f/2 + VU \qquad (A-2)$$

where the transformed variables are defined by

$$
\begin{aligned}
U &\equiv u_e/u_{e\infty} \\
V &\equiv v_w/u_{e\infty} \\
T &\equiv u_{e\infty}\theta/\nu \\
H &\equiv \delta^*/\theta \\
(\ )' &\equiv d/dX \\
X &\equiv u_{e\infty}x/\nu
\end{aligned}
\qquad (A-3)
$$

Following Torda (Reference 11) we assume a velocity profile of the form

$$\tilde{u} = A\eta + B\eta^2 + C\eta^3 + D\eta^4 \qquad (A-4)$$

where

$$
\begin{aligned}
\tilde{u} &= u/u_e \\
\eta &= y/\delta
\end{aligned}
$$

Equation (A-4) satisfies the no-slip condition $u(x,0) = 0$. The remaining coefficients are evaluated by imposing the following additional boundary conditions

$$u = u_e; \quad \frac{\partial u}{\partial y} = 0 \quad @ \; y = \delta$$

$$v_w \left(\frac{\partial u}{\partial y}\right)_w = u_e \frac{du_e}{dx} + \nu \left(\frac{\partial^2 u}{\partial y^2}\right)_w \tag{A-5}$$

$$v_w \left(\frac{\partial^2 u}{\partial y^2}\right)_w = \left(\frac{\partial^3 u}{\partial y^3}\right)_w$$

Application of (A-5) to the profile (A-4) yields

$$A = (24 + 6N + MN)/K$$

$$B = 3(4M - 3N)/K$$

$$C = (4M^2 - 3MN)/K$$

$$D = (3N - 6 + 2MN - 6M - 3M^2)/K$$

where

$$K \equiv 18 + 6M + M^2$$

$$M \equiv VR$$

$$N \equiv R^2 U'$$

$$R \equiv u_{e\infty}\delta/\nu$$

also

$$C_f/2 = AU/R$$

Substitution of these results in Equation (A-2) yields the following equation relating R, the Reynolds number based on boundary layer thickness, to the variation of mass transfer V and velocity U.

$$V' = G_1/UR^3 + G_2 U'' R + G_3 R'/R^2 \tag{A-6}$$

where

$$G_1 = (1260K^3/B_3) \; \{N \; (B_4/1260K^3-1) + M + B_5/K\}$$

$$G_2 = 2B_2/B_3$$

$$G_3 = 6B_1/B_3$$

and

$$B_1 = (9180N^2 + 7128N - 175392) + M(7290N^2 - 10584N - 181728)$$
$$+ M^2(2112N^2 - 11388N - 86112)$$
$$+ M^3(291N^2 - 3276N - 21936) + M^4(19N^2 - 416N - 3768)$$
$$- M^5(26N + 432) - 24M^6$$

$$B_2 = (11016N + 7128) + M(9126N - 6156) + M^2(3114N - 8064)$$
$$+ M^3(513N - 3048) + M^4(38N - 546) - 39M^5$$

$$B_3 = (1890N^2 + 26568N + 19008) + M(2898N^2 + 19944N + 12672)$$
$$+ M^2(909N^2 + 1368N - 19008) + M^3(76N^2 - 780N - 4032)$$
$$- M^4(78N + 144)$$

$$B_4 = 72(17N^2 + 211N + 1778) + 6M(101N^2 + 1007N + 10838)$$
$$+ 2M^2(38N^2 + 321N + 9108) + 3M^3(11N + 936) + 216M^4$$

$$B_5 = 6N + 24 + MN$$

For given distributions of V and U the variation of boundary layer thickness can be determined from Equation (A-6). Subsequently, all other boundary layer parameters (momentum thickness, skin friction, etc.) can be computed from appropriate algebraic auxiliary relations. Alternately, the condition R≡0 can be imposed leading to

$$V' = G_1/UR^3 + G_2U'' \; R \tag{A-7}$$

Then for U specified the requisite distribution of suction needed to maintain a constant boundary layer thickness can be established.

Two features of Equations (A-6) and (A-7) are important to note here. First, the solution depends on the second derivative of the axial velocity distribution. Accordingly, in the numerical integration procedure which was utilized to obtain solutions a cubic-spline fit of the input velocity distribution was employed to assure smooth variation of this parameter.

The second feature to be noted is that the leading term on the right hand side of either (A-6) or (A-7) is singular at a stagnation point; i.e.: G_1 has no real roots. Accordingly, this method cannot be utilized to initiate a calculation at a stagnation point. Thus, the approximate scheme due to Thwaites (Reference 11) was employed for this purpose and the two methods matched at a small distance away from the singularity. The method of Reference (11) takes the following form. Equation (A-2) can be written

$$Z' = P/U \tag{A-8}$$

where

$$Z \equiv T^2$$

$$P \equiv 2 \{c_f/2U - T^2 U' (H + 2) + VT\}$$

Thwaites approximates the function P by

$$P = 0.45 - 6T^2 U' - 1.28 VT + 0.76 V^2 T^2$$

Real roots of this function can be found. Accordingly, the indeterminate form P/U at a stagnation point can be evaluated permitting integration to be initiated there.[*] Specifically, it can be shown that

$$Z'_o = \frac{2 T_o^2 U''_o P_1 - V'_o T_o P_2}{U'_o (1 - P_1) - V_o P_2/2 T_o}$$

---

[*]This procedure represents a generalization of the method employed in the Karman-Pohlhausen technique to evaluate stagnation conditions in the absence of mass transfer (see p. 210 of Reference 6).
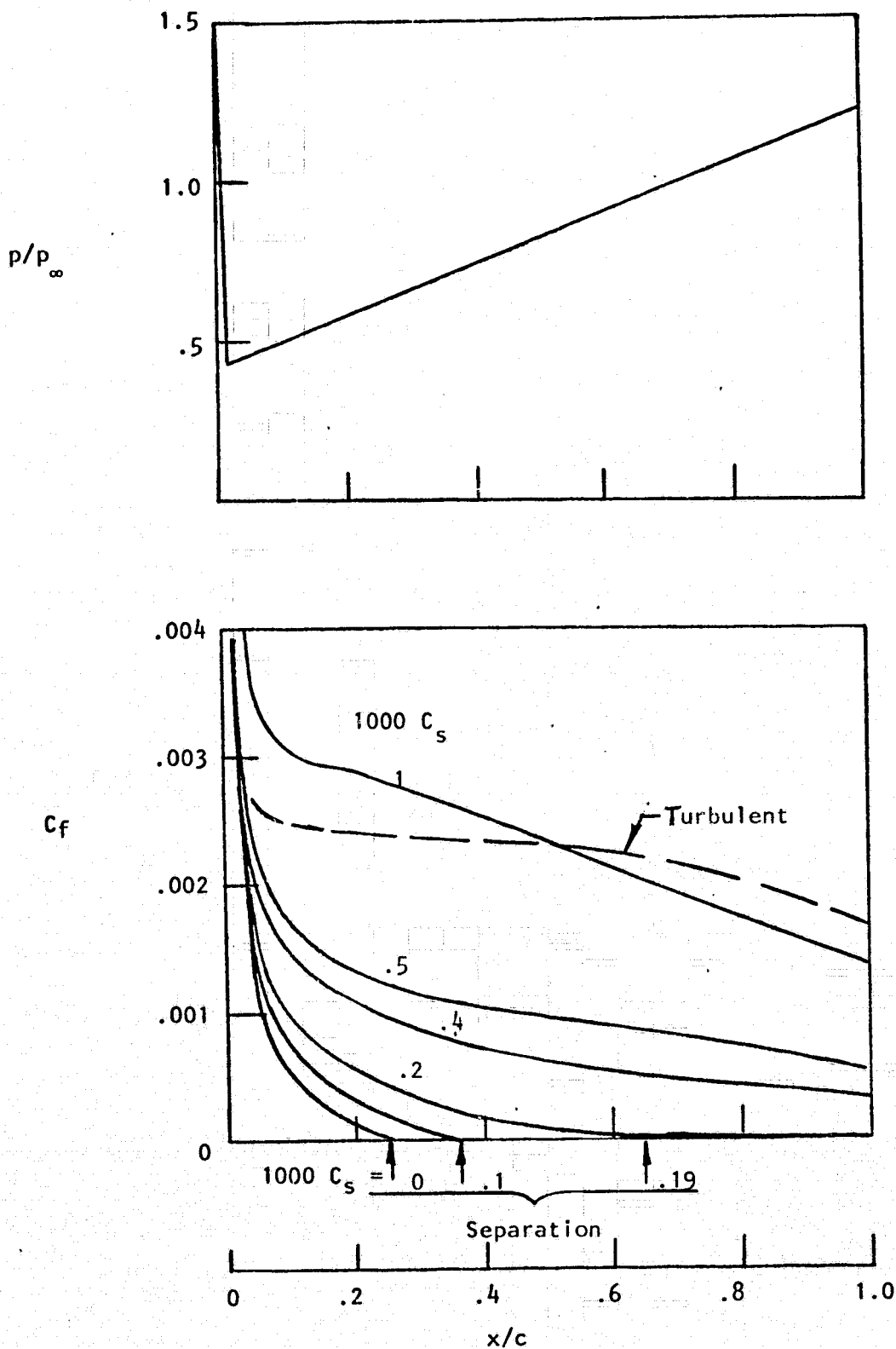
FIGURE A-1.   CHORDWISE VARIATION OF LOCAL SKIN FRICTION
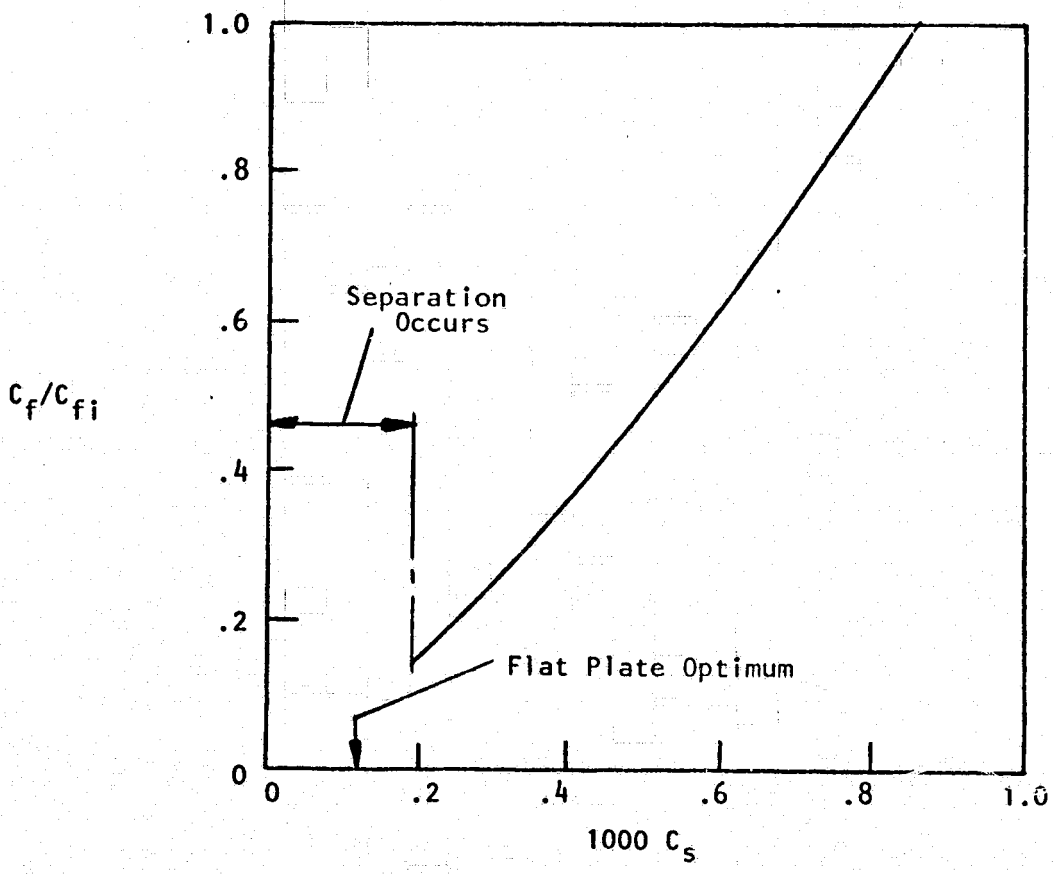AND SEPARATION ON AN AIRFOIL WITH UNIFORM SUCTION

FIGURE A-2. NET REDUCTION IN AVERAGE SKIN FRICTION DRAG
AS A FUNCTION OF SUCTION PARAMETER

where

$$P_1 \equiv -6$$

$$P_2 \equiv -1.28 + 1.52 \, V_o \, T_o$$

and the subscript o denotes values at the stagnation point.

A computer code was developed for numerical solution of Equations (A-6) and (A-7) by standard integration techniques. Some representative results obtained with this scheme are presented in Figure (A-1). Here the variation of skin friction coefficient over an airfoil surface with the indicated pressure distribution for various uniform rates of suction are presented. The selected pressure distribution is nominal but corresponds roughly to that encountered on a symmetric airfoil at a free stream Mach number of $M_\infty = .75$ (Reference 19). As can be seen, for suction rates moderately greater than the optimum value separation is suppressed with substantial reduction in skin friction relative to the turbulent estimates which are also shown. These results are summarized in Figure (A-2) in terms of net reduction in average skin friction as a function of the suction flow coefficient.

APPENDIX B
LIFT AUGMENTATION DUE TO WING SUCTION

According to Reference (9), the section lift coefficient corresponding to the inviscid pressure distribution shown in Figure (2) is 1.084. Further it is indicated that if viscous effects are taken into account the lift coefficient is reduced to a value .779. The pressure drag coefficient is .00266.

For the purpose of the present estimate it is assumed that the higher value of C_L can be attained when suction is applied in accordance with the distribution shown in Figure (6). In the absence of suction the lower value prevails.

It is now assumed that the two-dimensional pressure drag varies as the square of the lift, similar to the variation of the nominal drag polar which has the form $C_D = C_{D_O} + k\, C_L^2$. In this form, the factor k is considered to be the sum of the three-dimensional induced drag factor and the two-dimensional pressure drag factor. Without improved lift, the k-factor due to pressure drag is given by

$$k_1 = c_{D_p} / c_{L_1}^2$$

where c_{D_p} is the pressure drag coefficient and c_{L_1} is the smaller of the stated lift coefficients.

Assuming that the change in pressure drag is small, the k-factor with improved lift is

$$k_2 = c_{D_p} / c_{L_2}^2$$

The improved maximum L/D is then given by

$$\frac{(L/D)_2}{(L/D)_1} = \frac{k_i + k_1}{k_i + k_2}$$

where k_i is the three-dimensional induced drag factor.

To evaluate the improvement, the value of k_i is taken as

$$k_i = \frac{1}{\pi \times \text{Aspect Ratio}} = \frac{1}{\pi \times 7} = .045$$

Substitution of the numerical data yields

$$\frac{(L/D)_2}{(L/D)_1} = \frac{.045 + .0044}{.045 + .0023} \cong 1.02$$